



저작자표시-비영리-변경금지 2.0 대한민국

이용자는 아래의 조건을 따르는 경우에 한하여 자유롭게

- 이 저작물을 복제, 배포, 전송, 전시, 공연 및 방송할 수 있습니다.

다음과 같은 조건을 따라야 합니다:



저작자표시. 귀하는 원저작자를 표시하여야 합니다.



비영리. 귀하는 이 저작물을 영리 목적으로 이용할 수 없습니다.



변경금지. 귀하는 이 저작물을 개작, 변형 또는 가공할 수 없습니다.

- 귀하는, 이 저작물의 재이용이나 배포의 경우, 이 저작물에 적용된 이용허락조건을 명확하게 나타내어야 합니다.
- 저작권자로부터 별도의 허가를 받으면 이러한 조건들은 적용되지 않습니다.

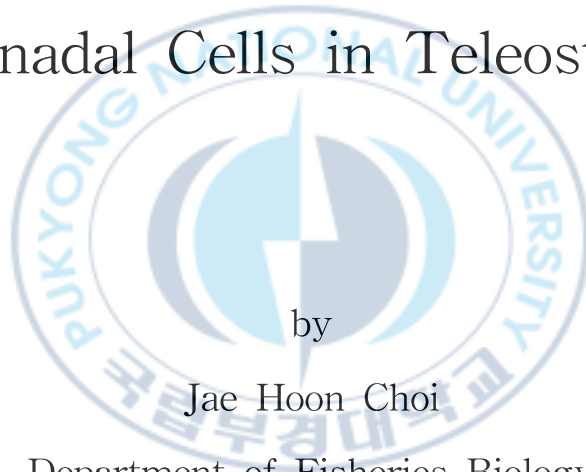
저작권법에 따른 이용자의 권리는 위의 내용에 의하여 영향을 받지 않습니다.

이것은 [이용허락규약\(Legal Code\)](#)을 이해하기 쉽게 요약한 것입니다.

[Disclaimer](#)

Thesis for the Degree of Doctor of Philosophy

Studies on the Development of
3D *In Vitro* Culture Systems
for Gonadal Cells in Teleost Fishes



Jae Hoon Choi

Department of Fisheries Biology

The Graduate School

Pukyong National University

August, 2025

Studies on the Development of
3D *In Vitro* Culture Systems
for Gonadal Cells in Teleost Fishes
경골어류 생식소 세포의
3차원 체외 배양 시스템 개발에 관한 연구

Advisor: Prof. Seung Pyo Gong

by
Jae Hoon Choi

A thesis submitted in partial fulfillment of the requirements
for the degree of

Doctor of Philosophy

in Department of Fisheries Biology, The Graduate School,
Pukyong National University

Agust, 2025

Studies on the Development of 3D *In Vitro* Culture Systems
for Gonadal Cells in Teleost Fishes

A dissertation

by

Jae Hoon Choi

Approved by:

(Chairman) Yoon Kwon Nam

(Member) Chan-Hee Kim

(Member) Jung Ha Kang

(Member) Jae Hyun Im

(Member) Seung Pyo Gong

August 22, 2025

Contents

Contents	i
List of Figures	iii
List of Tables	vi
Abstract (Korean)	vii
CHAPTER 1. General Introduction	1
CHAPTER 2. General Materials and Methods	6
CHAPTER 3. Establishment and Characterization of Testicular Aggregate Culture Systems in Marine Medaka (<i>Oryzias dancena</i>)	14
I. Introduction	15
II. Materials and methods	18
III. Results	24
IV. Discussion	45
CHAPTER 4. Establishment and Characterization of Ovarian Aggregate Culture Systems in Marine Medaka (<i>Oryzias dancena</i>)	50
I. Introduction	51

II. Materials and methods	54
III. Results	58
IV. Discussion	70
CHAPTER 5. 3D Aggregate Culture of Testicular Cells by Inclusion of a Testis-Derived Somatic Cell Line in Olive Flounder (<i>Paralichthys olivaceus</i>)	73
I. Introduction	74
II. Materials and methods	76
III. Results	85
IV. Discussion	99
CHAPTER 6. General Discussion and Conclusion	103
References	107
Acknowledgement (Korean)	126

List of Figures

Fig. 1. Investigation of the optimal concentration of trypsin-EDTA for digesting marine medaka (<i>Oryzias dancena</i>) testes	25
Fig. 2. Sperm removal using Percoll density gradient centrifugation (PDGC)	26
Fig. 3. Evaluation of the formation of testicular aggregates by Matrigel suspension culture	29
Fig. 4. Evaluation of the formation of testicular aggregates by a three-layer gradient system (3-LGS)	30
Fig. 5. Evaluation of the formation of testicular aggregates in ultra-low attachment 96 well plate (ULA)	31
Fig. 6. Comparison of the morphological traits from testicular aggregates depending on kinds of culture media	34
Fig. 7. Comparison of the morphologies from testicular aggregates depending on protein supplements in mESM2	35
Fig. 8. Evaluation of the number and the size of testicular aggregates depending on protein supplements in mESM2	36
Fig. 9. Evaluation of the effects of fish serum (FS), basic fibroblast growth factor (bFGF), and embryo extract (EE) on the viability of the cells composing testicular aggregates	38
Fig. 10. Evaluation of the effects of FS, bFGF, and EE on the gene expression levels from testicular aggregates	39
Fig. 11. Evaluation of the number and the size of testicular aggregates	

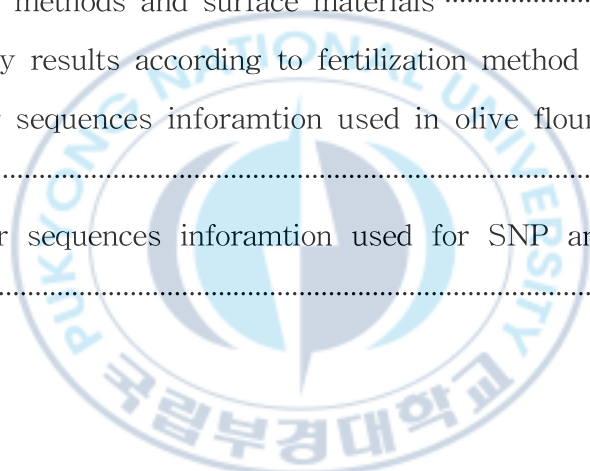
depending on non-protein series supplements in mESM2	41
Fig. 12. Representative pictures of <i>O. dancena</i> embryos obtained through natural fertilization, or through artificial fertilization using either fresh sperm or sperm derived from testicular aggregates	43
Fig. 13. Comparison for the morphologies of ovarian aggregates depending on ovarian cell population separated by PGDC	60
Fig. 14. Characterization of ovarian aggregates depending on ovarian cell population separated by PDGC	61
Fig. 15. Evaluation of the effects of FS, bFGF, and EE on the morphology of ovarian aggregates	63
Fig. 16. Evaluation of the effects of FS, bFGF, and EE on the viability and the size of ovarian aggregates	64
Fig. 17. Evaluation of the effects of FS, bFGF, and EE on relative mRNA expression levels from ovarian aggregates	65
Fig. 18. Evaluation of the effects of bFGF and GDNF on relative mRNA expression levels from ovarian aggregates	67
Fig. 19. Evaluation of the effects of hFSH on germ cell maintenance and 17 β -estradiol secretion from ovarian aggregates	69
Fig. 20. Establishment and characterization of testicular cell line from olive flounder (<i>Paralichthys olivaceus</i>) testis (OFT)	86
Fig. 21. Validation of species from OFT	87
Fig. 22. Sequence alignment analysis of <i>COI</i> and <i>16s rRNA</i> from OFT ..	88
Fig. 23. Karyotype analysis from OFT	90
Fig. 24. Validation of genetical sex from OFT	91
Fig. 25. Electroporation of green fluorescent protein expression vector into OFT	93
Fig. 26. Effects of sex hormones and growth factors, and inclusion with	

OFT on testicular aggregate formation in *P. olivaceus* 94
Fig. 27. Evaluation of sex hormones and growth factors on the viability of
the cells composing 3D co-cultured testicular aggregates 70
Fig. 28. Evaluation of sex hormones and growth factors on the gene
expression levels from 3D co-cultured testicular aggregates 71



List of Tables

Table 1. Comparison of 2D and 3D culture systems for germ cell culture	5
Table 2. Primer sequences information used in marine medaka (<i>Oryzias dancena</i>) for qRT-PCR analysis	23
Table 3. Aggregate formation from <i>O. dancena</i> dispersed testicular cells by different culture methods and surface materials	32
Table 4. Fertility results according to fertilization method	44
Table 5. Primer sequences information used in olive flounder (<i>Paralichthys olivaceus</i>)	83
Table 6. Primer sequences information used for SNP analysis to identify genetic sex	84



경골어류 생식소 세포의 3차원 체외 배양 시스템 개발에 관한 연구

최 재 훈

부 경 대 학 교 대 학 원 수 산 생 물 학 과

요 약

어류의 생식선줄기세포는 유전정보를 다음 세대로 전달하는 중요한 세포로 종 보존, 형질 전환 어류 생산, 양식품종 개량 등에 핵심적인 역할로 활용될 수 있다. 현재까지 어류에서 생식선줄기세포는 2차원 배양으로 진행되었으나, 이러한 방식은 생식소의 세포 미세환경을 재현하기 어려워 생식세포의 분화 및 기능 유지에 한계가 있다. 이러한 한계를 극복하기 위해 최근에는 세포 기반 3차원 응집체 배양이 주목받고 있으며, 생식세포와 체세포 간 상호작용을 구조적으로 모사하고 기능을 유지할 수 있는 모델로 평가되고 있다. 그러나 어류에서 이러한 연구는 아직 초기 단계에 머물러 있으며, 응집체 유도 방법, 적절한 배지 조성, 기능적 평가 지표 등에 대한 연구가 부족한 실정이다. 따라서 본 연구에서는 생물학적 모델 어류인 바다송사리(*Oryzias dancena*)와 국내 양식어종인 넙치(*Paralichthys olivaceus*)의 3차원 응집체 유도 및 배양조건에 대해 조사하였다.

먼저, 어류에서 정소 응집체를 유도하기 위해서 Matrigel suspension, 3-layer gradient system, 그리고 ultra-low attachment 96 well plate (ULA)를 활용해 정소 응집체 형성을 평가하였다. 그 결과, ULA에 배양하는 것이 응집체 형성에 효율적이라는 것을 확인하였다. 이 후, basic medium (BM)과 modified ESM2 (mESM2)가 정소 응집체의 형태, 생존율, 기능 유전자 발현에 미치는 영향을 비교하였다. 그 결과 온전한 mESM2 배지가 조밀하고 생존율이 높은 응집체 형성, 생식세포 및 체세포 유전자 발현 증가, 응집체 수 및 크기 유지에 필수적인 요인임을 확인하였다. 최종적으로 확립된 배양조건을 통해 배양된 정소 응집체로부터 유도된 정자는 수정능이 있음을 확인하였다.

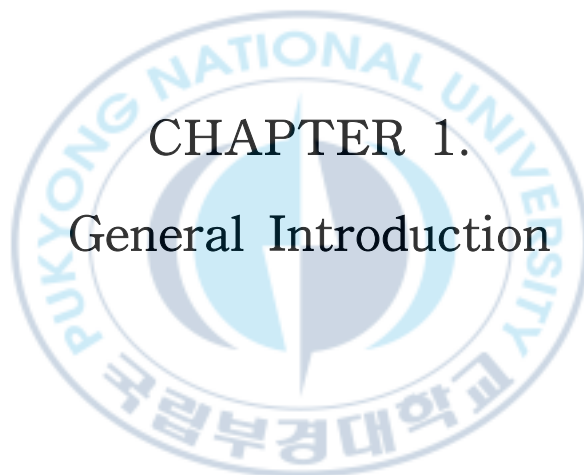
바다송사리 난소 응집체를 유도하기 위해서 Percoll 밀도기울기차 원심분리법으로 분리한 두 종류의 세포 균집을(총 6개 Percoll 층에서, 1-4층 및 2-3층에서 각각 회수된 난소세포 균집) ULA에 배양하고 성장인자 및 첨가물 4종(bFGF, GDNF, FS, EE), 이 그리고 FSH가 난소 응집체 배양에 미치는 영향을 평가하였다. 그 결과, 1-4층에서 회수된 난소세포 균집이 재현성 있게 단일 응집체로 형성이 되었으며, bFGF, FS, EE는 *scp3* 유전자 발현을 유의적으로 높여준다는 것을 확인하였다. 한편, bFGF와 GDNF를 단일 혹은 복합으로 처리하였을 때, *nanos2* 유전자 발현이 유의적으로 증가함을 확인하였다. 그러나, GDNF는 *scp3* 유전자를 유의적으로 억제하는 것을 확인하였다. 또한, hFSH를 첨가여부와 상관없이 유도된 난소 응집체는 22일간 난모세포를 유지함과 동시에 E_2 를 생산하고 있음을 확인하였다.

넙치의 정소 유래 세포를 사용하여 3차원 공배양을 통해 정소 응집체를 유도하기 위해서, 정소 유래 OFT

세포주의 확립과 특성분석을 진행하였고, 확립된 세포주와 성호르몬 및 성장인자가 응집체에 미치는 영향을 확인하였다. 그 결과, OFT는 넙치 수컷의 Sertoli 세포에서 유래된 세포주로 확인되었으며, 안정적으로 배양되고 있음을 확인하였다. 확립된 세포주는 정소 세포가 24시간 내에 응집체를 형성하는데 중요한 역할을 하였으며, 성호르몬 및 성장인자 처리는 생존율에는 영향을 미치지 않았으나, *plzf*와 *scp3* 유전자 발현의 유의적인 증가를 유도하였다.

본 연구 결과들은 어류 생식선 줄기세포의 배양 및 분화를 위한 기초연구의 기반이 될 수 있을 것으로 생각하며, 향후 어류 번식생물학, 생식세포 공학 및 대리모 기술 개발에 기여할 수 있을 것으로 기대한다.





CHAPTER 1.
General Introduction

Germline stem cells (GSCs) maintain the undifferentiated germ cell pool within the gonads through mitotic division enabled by their self-renewal capacity, and ultimately transmit their genetic information through differentiation into sperm and eggs (Matsuoka et al., 2014; Cao et al., 2019; Kleppe et al., 2025). In aquaculture research, GSCs have been considered as key resources for species conservation, transgenic fish production, and mitigating reproductive barriers (Ruy and Gong, 2020; Xie et al., 2020).

Indeed, transplantation of *in vitro* cultured germ cells into teleost fishes, including rainbow trout (*Oncorhynchus mykiss*; Iwasaki-Takahashi et al., 2020), and zebrafish (*Danio rerio*; Kawasaki et al., 2012; Wong et al., 2013) produced functional donor-derived gametes, demonstrating that fish GSCs can be used for surrogate production. Also, induction of fertilizable sperms from *in vitro* cultured spermatogonia were reported from honmoroko (*Gnathopogon caerulescens*; Higaki et al., 2017) and four-eyed sleepers (*Bostrychus sinensis*; Zhang et al., 2022), suggesting expanded possibilities for applications in aquaculture. However, since GSCs occupy small portion in the gonads (Iwasaki-Takahashi et al., 2020), the development of *in vitro* culture system is essential for efficient utilization.

In mammals, pluripotent stem cells such as embryonic stem cells (ESCs) and induced pluripotent stem cells (iPSCs) can be differentiated into germ cell lineages (Bradley et al., 1984; Okita et al., 2007; Hayashi et al., 2012). In teleost fish, ESC cell lines or ESC-like cell lines were established from various species including medaka (Hong et al., 1996), zebrafish (Ho et al., 2014), olive flounder (Nie et al., 2023), Nile tilapia (Fan et al., 2017), and red drum (Walsh et al., 2024). Also, iPSCs were cultured in zebrafish (Roselló et al., 2013; Peng et al., 2019). Although those cell lines showed

pluripotency, differentiation into germ cells from cultured ESCs or iPSCs has not been reported. A key reason is that teleost fish specify their primordial germ cells very early by maternally inherited germ plasm (Knaut et al., 2000; Li et al., 2014). Thus, unlike in mammals, ESCs and iPSCs are not suitable for fish reproductive biotechnology.

To date, *in vitro* GSCs culture have been performed by two-dimensional (2D) culture method and three-dimensional (3D) culture method. In the 2D culture method, GSCs were cultured on the mitotically inactivated feeder cells (Wong et al., 2013; Hamidabadi and Bojnordi, 2017; Iwasaki-Takahashi et al., 2019). Although 2D culture method can provide high reproducibility, this method places cells in a non-natural environment without extracellular matrix (ECM), which hinders the recapitulation of the complexity of the *in vivo* cellular microenvironment (Suarez-Martinez et al., 2022). Also, since cultured cells grow as a monolayer on a flat surface, cell signaling is restricted to a single direction (Suarez-Martinez et al., 2022). On the other hands, 3D culture method have been used by various methods including organ culture (Miura and Miura, 2001; Wang et al., 2022; Celiz et al., 2023), soft agar culture systems (SACS; Jabari et al., 2020) and methylcellulose culture systems (MCS; Huleihel et al., 2015). The 3D culture methods allow cell signaling with multi-directions, this methods support long-term male GSCs culture and stemness, comparing 2D culture method (Lee et al., 2019; Wu et al., 2023). Moreover, *in vitro* induced fertile sperm were produced by testicular organ culture (Sato et al., 2011). Likewise, adipose matrix or hydrogel culture of ovarian follicles preserve spherical architecture so that signals between granulosa and oocyte circulate in and out of the follicle, whereas 2D attachment causes follicle to flatten and

disrupt cell signaling (Brito et al., 2024). A summary of the comparison between 2D and 3D culture method is presented in Table 1.

On the other hands, organ culture, SACS, MCS, and ECM-embedded gonadal cell cultures are not suitable for continuous culture, as they do not allow subculturing. To overcome this limitation, organoids, which formed through self-organization of dissociated primary cells, have emerged as a promising alternative (Alves-Lopes et al., 2017; Sakib et al., 2019). Indeed, several studies have demonstrated that organoids can be successfully subcultured, indicating potential as a continuous culture system (Fan et al., 2022; Lim et al., 2025). In mammals, testicular and ovarian organoids have been used not only to recapitulate gonadal architecture (Lee et al., 2006; Cham et al., 2021), but also to produce functional gametes and offspring *in vitro* (Li et al., 2021; Nanki et al., 2020). Despite their potential, studies about fish gonadal organoids remain limited. To date, only two studies have reported the induction of testicular aggregates capable of producing fertilizable sperm *in vitro*, which successfully led to offspring production through artificial fertilization (Higaki et al., 2017; Zhang et al., 2022). Although both studies successfully generated offsprings through artificial fertilization using *in vitro* induced sperm, appropriate induction methods and culture conditions for the formation of fish gonadal aggregates have no yet been investigated.

For this reason, the present study aimed to evaluate appropriate methods and culture conditions for inducing gonadal aggregates using the experimental model fish marine medaka (*Oryzias dancena*). In addition, I established a testicular cell line from the commercially important aquaculture species, olive flounder (*Paralichthys olivaceus*), and developed and characterized the 3D co-culture testicular aggregate system.

Table 1. Comparison of 2D and 3D culture systems for germ cell culture

	2D culture	3D culture
Culture structure	Grow as a monolayer on a flat surface	Grow in scaffolds, spheroid or organoid
Stemness maintenance	Risk of spontaneous differentiation or cell death	More suitable for maintaining undifferentiation due to niche-like microenvironment
Differentiation	Require strong external induction signals	Efficient differentiation due to cell-cell interaction
Niche reconstruction	Very limited or absent	Possible to mimic germ cell niche
Cell-cell interactions	Planar contact	Multidirectional interactions
Ease of observation	Easy to observe	More difficult due to structural complexity
Application suitability	Suitable for basic studies and short-term cultures	Suitable for long-term cultures, physiological modeling, and transplantation studies



CHAPTER 2.
General Materials and Methods

1. Fish

Adult marine medaka (*Oryzias dancena*) were bred in the Laboratory of Cell Biotechnology, Pukyong National University (Busan, Republic of Korea). They were fed 5 times a day with a commercial diet for flounder larvae (EWHA, Busan, Republic of Korea) and brine shrimp larvae (*Artemia nauplius*). Water temperature and water salinity were adjusted to 26°C and 5 psu, respectively. Photoperiod was adjusted at light for 14 hours and darkness for 10 hours. In the case of the males, whose total length were 3.2 to 3.5 cm, were separated from females 3 days before inducing testicular aggregates. However, the females, whose total length were 3.2 to 3.5 cm, were separated from males a day before inducing ovarian aggregates. All procedures dealing with animals complied with the guidelines provided by Pukong National University approved our research proposal (approval No. PKNUIACUC-2021-31)

Olive flounder (*Paralichthys olivaceus*) used in this study were reared at the National Institute of Fisheries Science (NIFS; Busan, Republic of Korea). The fish were maintained in 1-ton flow through tanks adjusted to $19 \pm 0.3^\circ\text{C}$, following a natural photoperiod regulated by an electronic timer and illuminated with fluorescent lights. They were fed commercial extruded pellets (Daebong LS Co., Ltd., Jeju, Korea) twice daily. All procedures were conducted in accordance with the Animal Protection Act enforced by the Ministry of Agriculture, Food, and Rural Affairs of the Republic of Korea, and the protocols were approved by the Institutional Animal Care and Use Committee of NIFS (approval No. 2024-NIFS-IACUC-47).

2. Gonadal cell isolation for inducing gonadal aggregates

2.1 Gonads extraction

Adult *O. dancena* individuals were used for testicular and ovarian cell isolation. Male and female fish were anesthetized by immersion in cold water (4°C) for 5 minutes and disinfected in 70% (v/v) ethanol for 10 seconds to prevent microbial contamination (Graziano et al., 2013). Testes and ovaries were surgically extracted under sterile conditions and washed three times with Dulbecco's phosphate-buffered saline (DPBS; Gibco, Grand Island, NY, USA) containing 1% (v/v) penicillin-streptomycin (P/S; Gibco). The isolated testes and ovaries were transferred to 35 mm Petri dishes (SPL Life Science, Pocheon, Republic of Korea) and mechanically dispersed using sterile surgical blades (No. 20; FEATHER Safety Razor, Osaka, Japan) prior to enzymatic digestion.

To extract testes from *P. olivaceus*, a similar process was performed. Males were anesthetized in seawater containing 0.1% (v/v) 2-phenoxy ethanol (Sigma-Aldrich, ST. Louis, MO, USA) for 10 minutes and disinfected in 70% (v/v) ethanol for 10 seconds. The surgically extracted testes were washed 3 times with DPBS. And finally 0.5 g of testicular fragments were moved into 100 mm Petri dishes (Corning, Corning, NY, USA), respectively. Finally, they were dissected with sterile surgical blades (No. 10; Paragon, Sheffield, UK) before enzymatic digestion.

2.2 Enzymatic digestion

For testicular and ovarian tissues digestion from *O. dancena*, they were digested by 2 mL of 0.05% (v/v) trypsin-EDTA (Gibco) with gentle pipetting every 10 minutes for 1 hour to aid tissue digestions. The activities of trypsin-EDTA were terminated by adding an equal volume of culture medium composing Dulbecco's Modified Eagle Medium (DMEM; Gibco) supplemented with 10% (v/v) fetal bovine serum (FBS; Gibco) and 1% (v/v) P/S. Subsequently, digested testicular or ovarian cells were filtered through 40 µm cell strainers (Falcon, Corning, NY, USA), and the testicular or ovarian cells were harvested by centrifugation (400 × g, 5 minutes).

In the case of enzymatic digestion from *P. olivaceus* testes, dissected testes were digested by 10 mL of 0.25% (v/v) trypsin-EDTA with gentle pipetting every 10 minutes for 2 hours. Inactivations of trypsin-EDTA were performed same way with *O. dancena*. After that, testicular cells were filtered sequentially through 100 µm and 40 µm cell strainers (Falcon). Finally, *P. olivaceus* testicular cells were harvested by centrifugation with same condition with *O. dancena*.

2.3 Gonadal cell isolation via Percoll density gradient centrifugation (PDGC)

To remove excess differentiated germ cells such as sperms and spermatids from harvested *O. dancena* testicular cells, PDGC was performed. Harvested testicular cells were resuspended by 300 µL culture medium and were carefully layered onto the top of a discontinuous 5-step

Percoll solution (20%, 30%, 40%, 50%, and 60%; 1 mL each; Sigma-Aldrich) in 15 mL conical tubes (Falcon). They were centrifuged at $800 \times g$ for 30 minutes. The layers were collected separately, and the morphology of the cells from each layer was examined using an inverted microscope (Eclipse TS100; Nikon, Tokyo, Japan). Also, the each Percoll layer was named follow as: top to 20% Percoll solution is 1st layer, 20% to 30% Percoll solution is 2nd layer, 30% to 40% Percoll solution is 3rd layer, 40% to 50% Percoll solution is 4th layer, 50% to 60% Percoll solution is 5th layer, and 50% to bottom Percoll solution is 6th layer, respectively. Harvested cells from 1st layer to 4th layer were used for the formation of testicular aggregates.

To evaluate the formation of ovarian aggregates according to ovarian cell populations from *O. dancena*, two different cell populations were isolated as follows; 1. ovarian cell populations harvested from 2nd layer to 3rd layer and 2. ovarian cell populations harvested from 1st layer to 4th layer. On the other hands, testicular cell populations harvested from 1st layer to 4th layers were utilized for establishing a somatic cell line derived from *P. olivaceus* testis and assessing its role in the formation of 3D co-cultured testicular aggregates.

3. Composition of cell culture medium

Two types of cell culture media were used depending on the purpose of the experiment: basic medium (BM) and modified embryonic stem cell medium 2 (mESM2). BM consisted of Leibovitz's L-15 Medium (L15; Gibco) supplemented with 10% (v/v) KnockOut™ serum replacement (KSR;

Gibco) and 1% P/S. mESM2 was adapted from the previously established ESM2 formulation for fish embryonic stem cell culture, with modifications in the embryo extract (EE) and fish serum (FS) components depending on the cell type and species. The base composition of mESM2 was as follows: DMEM, 15% (v/v) FBS, 20 mM hydroxyethyl piperazine ethane sulfonic acid (HEPES; Thermo Fisher Scientific, Waltham, MA, USA), 1 mM non-essential amino acids (NEAA; Gibco), 1 mM sodium pyruvate (SP; Gibco), 2 nM sodium selenite (SS; Sigma-Aldrich), 100 μ M β -mercaptoethanol (BME; Gibco), 10 ng/mL human basic fibroblast growth factor (bFGF; Gibco), 1% (v/v) FS derived from rainbow trouts (*Oncorhynchus mykiss*) or *P. olivaceus*, 50 μ g/mL EE prepared from *O. dancena* or *P. olivaceus* embryos, and 1% (v/v) P/S. For culturing testicular aggregates and ovarian aggregates derived from *O. dancena*, commercial products of *O. mykiss* serum (Caisson Laboratories, Inc., North Logan, UT, USA) were used. The preparation of *P. olivaceus* serum or EE derived from *O. dancena* or *P. olivaceus* was performed following previously described protocols (Kim et al., 2009; Ryu and Gong, 2017).

4. Analysis of cell viability

To evaluate cell viability, gonadal aggregates were transferred into 1.5 mL microcentrifuge tubes (Corning) and enzymatically dissociated using 500 μ L of 0.05% (v/v) trypsin-EDTA for 30 minutes. During the incubation, gentle pipetting was performed every 10 minutes. Subsequently, an equal volume of DMEM supplemented with 10% (v/v) FBS and 1% (v/v) P/S was added to inactivate trypsin-EDTA. The cell suspensions were collected by centrifugation at $400 \times g$ for 5 minutes, and the pellet

was resuspended in 500 μ L of DPBS. Cell viabilities were then determined using the trypan blue (Gibco).

In addition, localization of live and dead cells within the gonadal aggregates was determined using the Live/Dead Viability/Cytotoxicity Kit (Molecular Probes, Eugene, OR, USA), according to the manufacturer's protocol. Aggregates were stained with fluorescent indicators: 2 μ M calcein AM to identify live cells and 4 μ M ethidium homodimer-1 to identify dead cells. After staining, samples were observed under a fluorescence microscope (Olympus, Hamburg, Germany) to visualize the localization of live and dead cells within the three-dimensional structures. For the negative controls, aggregates were treated with 70% ethanol for one hour prior to staining to ensure complete loss of viability.

5. Analysis of gene expression

To characterize the olive flounder testicular cell line (OFT), reversed transcription polymerase chain reaction (RT-PCR) were performed. And, to evaluate gene expression levels depending on supplements from gonadal aggregates, quantitative reverse transcription polymerase chain reaction (qRT-PCR) were performed. At first, total RNA from gonadal aggregates or OFT was extracted using RNeasy Plus Micro Kit (Qiagen, Valencia, CA, USA), following the manufacturer's instructions. The cDNA was synthesized by GoScript TM reverse transcription system (Promega, Madison, WI, USA). Finally, cDNA was subjected to RT-PCR or qRT-PCR depending on purpose. The detail conditions for RT-PCR and qRT-PCR were described in Chapter 3, Chapter 4, and Chapter 5 materials and methods.

6. Statistical analysis

All data are presented as mean \pm standard deviation (SD), with a minimum of three replicates. Statistical analyses were performed using SPSS software (version 19.0; SPSS Inc., Chicago, IL, USA). Differences between groups were assessed using one-way analysis of variance (ANOVA) or *t*-test, followed by a Duncan's method. Significant differences were determined when *p* values were less than 0.05.



CHAPTER 3.

Establishment and Characterization of Testicular Aggregate Culture systems in Marine Medaka (*Oryzias dancena*)

I . Introduction

In teleost testis, spermatogenesis is proceeded through complex interactions between germ cells and their surrounding somatic cells (Ibtisham and Honaramoo, 2020). Throughout this process, diploid spermatogonia undergo asymmetric division to produce haploid spermatozoa that transmit genetic material to the next generation (Shivdasarni et al., 2003). Hence, the development of a reliable *in vitro* testicular culture system that can recapitulate spermatogenesis holds great potential for studies on male infertility and the advancement of reproductive biotechnology in aquaculture.

To date, considerable efforts have been made to reproduce spermatogenesis *in vitro* using both two-dimensional (2D) and three-dimensional (3D) culture strategies (Iwanami et al., 2006; Sato et al., 2011; Stukenborg et al., 2008). However, 2D systems have failed to support complete spermatogenesis, because of their inability to replicate the spatial architecture and cellular interactions required between germ and somatic cells (Reuter et al., 2014; Alves-Lopes et al., 2017). In contrast, testis organ culture, a 3D culture method, has shown success in generating functional sperm *in vitro* (Sato et al., 2011). Nonetheless, this method poses limitations in its inability to support long-term subculture, which is crucial for reducing animal use and enabling sustainable experimentation. Taken together, an ideal *in vitro* model for testicular function should provide both appropriate cell - cell interactions and long-term culture viability.

Testicular organoids, which mimic the native structure and functionality of the testis, have emerged as promising candidates to meet these requirements. These organoids can preserve germ - somatic cell interactions *in vitro* and potentially be maintained through repeated subculturing under optimized conditions. In mammalian systems, several approaches have been explored to generate such structures. For instance, embedding primary testicular cells from 18-day-old rats into a collagen and Matrigel matrix led to the formation of cyst-like aggregates and an increased yield of haploid cells compared to 2D cultures (Lee et al., 2006). The application of a three-layer gradient system (3-LGS) promoted the reorganization of dissociated rat testicular cells into spherical and tubular organoid structures that retained germ cell populations for up to three weeks (Alves-Lopes et al., 2017). In pigs, highly biomimetic testicular organoids have been produced by initially forming spheroids in ultra-low attachment (ULA) 96-well plates, followed by culture on an air - liquid interface (Cham et al., 2021).

Despite these promising outcomes in mammals, the establishment of testicular organoids in teleost species remains largely underexplored. A few studies in species such as honmoroko (*Gnathopogon caerulescens*; Higaki et al., 2017) and four-eyed sleeper (*Bostrychus sinensis*; Zhang et al., 2022) have demonstrated *in vitro* generation of sperm from testicular aggregates, yet the culture conditions and formation strategies for such aggregates have not been thoroughly characterized.

Therefore, the present study aimed to establish foundational culture conditions for the generation of testicular aggregates in marine medaka (*Oryzias dancena*). As an initial step toward developing a stable and

reproducible testicular organoid system for fish, the effects of different culture methods and media compositions were evaluated for the formation of testicular aggregates. To accomplish this, the dissociation protocol was optimized to obtain primary testicular cells devoid of mature sperm. Then, I investigated their ability to self-assemble into aggregates using three culture approaches: (1) Matrigel suspension, (2) the 3-LGS method, and (3) ultra-low attachment (ULA) culture. Subsequently, I compared the effects of various media formulations on the number and size of the resulting aggregates to determine optimal culture conditions. Finally, I evaluated whether the established conditions could support the production of fertilizable sperm from *in vitro* cultured aggregates.



II. Materials and methods

1. Investigation of the optimal concentration of trypsin-EDTA

To optimize the concentration of trypsin-EDTA for isolating cells from testicular tissues, testes were enzymatically dissociated using varying concentrations of trypsin-EDTA, and the resulting cell yield and viability were evaluated. The testes were excised from adult male marine medaka (*Oryzias dancena*). Subsequently, they were rinsed three times in DPBS supplemented with 1% penicillin-streptomycin (P/S), and transferred into 35 mm Petri dishes. Tissues were minced using a surgical blade and digested for 1 hour with different concentrations of trypsin-EDTA including 0.025% (v/v), 0.05% (v/v), 0.1% (v/v), and 0.2% (v/v).

To terminate the enzymatic reaction, an equal volume of culture medium containing 10% FBS and 1% P/S was added. The resulting cell suspension was passed through a 40 μ m cell strainer to remove tissue debris, and cells were collected by centrifugation at $400 \times g$ for 5 minutes. The cell pellet was then resuspended in 300 μ L of culture medium (10% FBS, 1% P/S), and total cell count was performed using a hemocytometer (Marienfeld-Superior, Lauda-Königshofen, Germany). Cell viabilities were determined by trypan blue exclusion assay (Gibco), with non-stained (live) and blue-stained (dead) cells counted to calculate the percentage of viable cells.

2. Induction of testicular cell aggregates

2.1. Matrigel suspension

For Matrigel suspension culture, Matrigel was diluted by 1:1 ratio with L-15. Subsequently, testicular cells were suspended in 5 μL of diluted Matrigel at three different final cell concentrations: 1.25×10^5 , 2.5×10^5 , and 3.75×10^5 cells/ μL . The 5 μL Matrigel containing testicular cells was carefully deposited as a single drop onto either 35 mm cell culture dishes or Petri dishes and allowed to solidify for 20 minutes at 28°C. When gelation was complete, 2 mL of basic medium (BM) was gently added to each dish to begin the culture.

2.2. Three-layer gradient system (3-LGS)

For 3-LGS culture, three successive layers of Matrigel were constructed on the center of the membrane in 24-well hanging cell inserts (Corning), which were first placed upside down during layering. First, 5 μL of diluted Matrigel was applied directly onto the center of the insert membrane and incubated at 28°C for 20 minutes for gelation. Then, a second 3 μL Matrigel layer containing isolated testicular cells was gently layered onto the first, followed by another 20 minutes gelation step. Finally, an 8 μL layer of Matrigel was added to cover the previous two layers, and the gel was allowed to solidify for an additional 20 minutes. After all three layers were established, the insert was inverted back and placed into a 24-well plate containing 600 μL of BM, and the cells were cultured.

2.3. Ultra-low attachment (ULA) plate method

In the ULA method, isolated testicular cells were suspended in either 5 μL of Matrigel or 150 μL of BM, and seeded into ULA plates (Corning), which feature hydrophilic hydrogel coatings to prevent cell attachment. For the Matrigel-based condition, cells were suspended in 5 μL of Matrigel (final concentration: 2.5×10^5 cells/ μL), placed in the well, and allowed to gel for 20 minutes at 28°C before adding 150 μL of BM. In the medium-only suspension, the same cell concentration was maintained by directly seeding cells in 150 μL of BM without Matrigel.

3. Evaluation of testicular aggregate number, size, and cell viability

Testicular aggregates formed in ULA plates were collected and gently washed with 2 mL of DPBS in a 35 mm Petri dish. The washed aggregates were transferred to 96-well plates (Thermo Fisher Scientific), and images of all aggregates were captured using a light microscope to analyze their number and size. The total number of aggregates was counted manually based on the captured images, and their size was measured using TSVIEW7 software (Version 7; Fuzhou Xintu Photonics Co., Ltd., Fuzhou, China). Size was defined as the average of the measured width and height in each image and expressed in micrometers. Between 30 to 60 aggregates per group were analyzed depending on the experiment.

To determine the cell viability within aggregates, collected aggregates

were dispersed by 0.05% (v/v) trypsin-EDTA. The cell viability was measured by trypan blue staining. Additionally, the spatial distribution of live and dead cells within aggregates was investigated using the Live/Dead Viability/Cytotoxicity Kit (Molecular Probes). Aggregates were stained according to the manufacturer's protocol.

4. Quantitative reverse transcription polymerase chain reaction (qRT-PCR)

For each sample, 100 ng of total RNA was treated with DNase I (Sigma-Aldrich) to eliminate genomic DNA contamination. Complementary DNA (cDNA) synthesis was carried out using the GoScript™ reverse transcription system (Promega, Madison, WI, USA). Subsequently, 1 ng of synthesized cDNA was used for qRT-PCR analysis using the LightCycler® 480 SYBR Green Master Mix (Roche Diagnostics, Mannheim, Germany). The reaction conditions were as follows: initial denaturation at 94°C for 3 minutes, followed by 40 amplification cycles (denaturation at 94°C for 30 seconds, annealing at 60°C for 30 seconds, and elongation at 72°C for 30 seconds). Primer sequences for each target gene are listed in Table 2. Relative gene expression was determined using the $2^{-\Delta\Delta C_t}$ method. The ΔC_t was calculated by subtracting the C_t value of the internal reference gene (*18s rRNA*) from the C_t of the target gene, and the $\Delta\Delta C_t$ was obtained by comparing the ΔC_t values between experimental and control samples (Livak and Schmittgen, 2001).

5. Artificial Fertilization

To perform artificial fertilization, mature *O. dancena* females were separated from males 24 hours before the procedure. Females were anesthetized by brief immersion in ice water for 10 seconds, then placed on aluminum foil. Excess water on the body surface was removed using sterile wipers (KIMTECH, Seoul, Republic of Korea) to prevent unintended activation of the eggs. Unfertilized eggs were collected by gently pressing the abdomen and transferred (30 - 50 eggs per trial) to 1.5 mL microtubes (Corning).

For fertilization, testicular aggregates harvested from three wells of a ULA plate (total suspension volume: 450 μ L) were directly added to the tube containing the eggs. After incubation at room temperature for 10 minutes, the eggs were transferred to 60 mm Petri dishes filled with 5 mL of sterile breeding water and incubated at 28°C. Embryos that reached the two-cell stage were transferred individually into 24-well plates to avoid interference from unfertilized or deteriorating eggs.

For negative control, unfertilized eggs were incubated in 450 μ L of mESM2 medium for 10 minutes and cultured under identical conditions. As a positive control using fresh sperm, testes were dissected and finely minced on an IVF dish (SPL Life Sciences) using a surgical blade (No. 20). The spermatozoa were then suspended in 450 μ L of mESM2 and used immediately for fertilization. Additionally, embryos from natural mating were collected directly from the gonopore of fertilized females and cultured under the same conditions. Embryonic development across all groups was monitored using a stereomicroscope (SMZ745T; Nikon).

Table 2. Primer sequences information used in marine medaka (*Oryziasdancena*) for qRT-PCR analysis

Genes	Primer sequences (5'>3')	Product size (bp)	Accession number
<i>nanos2</i>	Forward : AAACCTACACCTGTCCCATCTG Reverse : AACTTGTAGGAGGGCAGCATC	111	XM_036217407.1
<i>scp3</i>	Forward : CAGCTGCTAGCTTTGAGGAA Reverse : CTGAGAGAAGTCTGCTGCATTG	224	XM_024295185.2
<i>sox9a</i>	Forward : GGAGAAGTGTCACCTCCGACG Reverse : TTGTAGTCCGGACCCCTGAT	138	XM_024272555.2
<i>18s</i> <i>rRNA</i>	Forward : TCCAGCTCCAATAGCGATTCCAC Reverse : AGAACCGGAGTCCTATTCCA	253	HM347347.1

III. Results

1. Testicular cell isolation and removal of sperm

To identify the most effective concentration of trypsin-EDTA for dissociating testicular cells from adult *Oryzias dancena*, testes were enzymatically digested using various concentrations of trypsin-EDTA, followed by evaluation of the total cell yield and viability. The results revealed that 0.05% and 0.1% trypsin-EDTA significantly increased the number of isolated cells compared to 0.025% and 0.2% treatments (Figure 1; $3.02 - 3.19 \times 10^5$ cells/mg vs. $1.70 - 2.02 \times 10^5$ cells/mg, $p < 0.05$). Despite differences in yield, cell viability remained consistently high (>89.9%) across all groups, with no statistically significant variation (Figure 1). Based on these results, 0.05% trypsin-EDTA was selected as the optimal condition for testicular cell dissociation.

To eliminate sperm cells from the isolated testicular cell population, the dissociated cells were subjected to discontinuous five-step Percoll density gradient centrifugation (Figure 2A). Morphological assessment of each layer revealed that spermatozoa, both motile and immotile, were predominantly found in the 5th layer and 6th layer (Figure 2B), whereas the 1st layer to 4th layer were largely free of sperm contamination. Consequently, testicular cells harvested from the 1st layer to 4th layer were used for subsequent experiments.

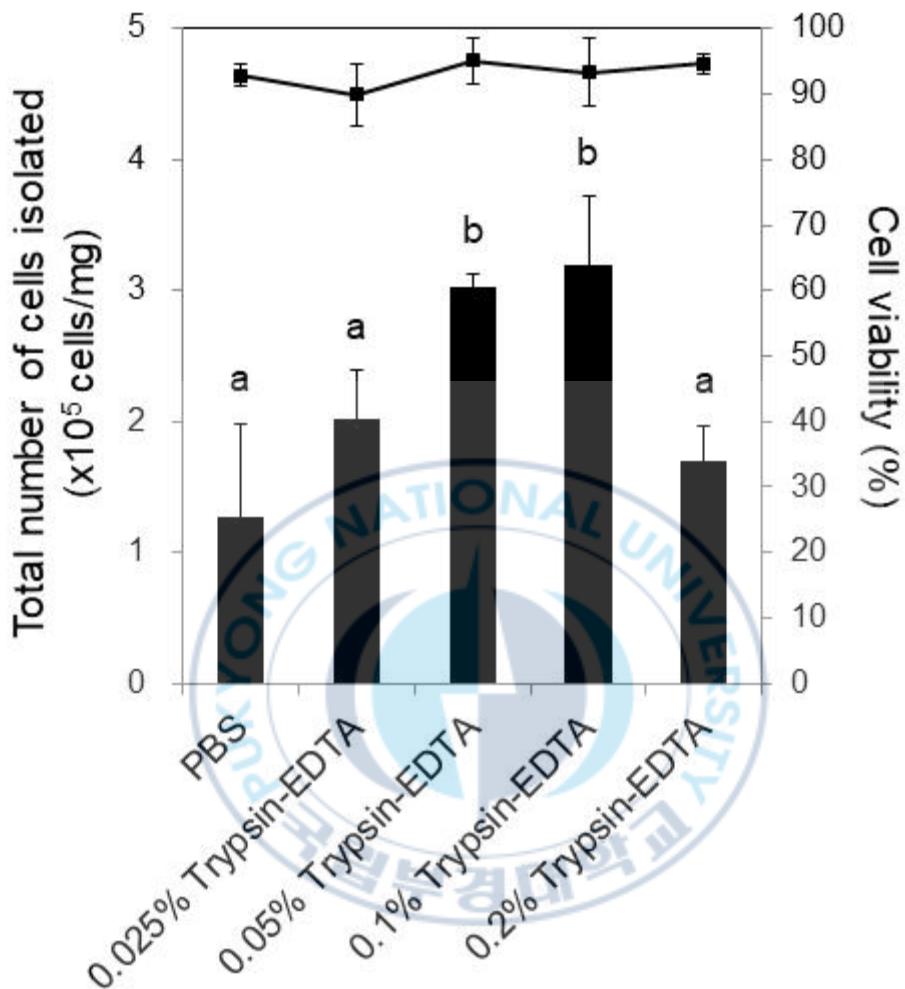


Figure 1. Investigation of the optimal concentration of trypsin-EDTA for digesting marine medaka (*Oryzias dancena*) testes. Various concentrations of trypsin-EDTA were used for isolating total number of cells from *O. dancena* testes. In 0.05% and 0.1% trypsin-EDTA, total testicular cells were harvested more effectively than in the others. Significant difference was not detected in cell viability with groups. All values are expressed as mean \pm standard deviation of three independent experiments. ^{ab}Different letters indicate significant differences ($p < 0.05$).

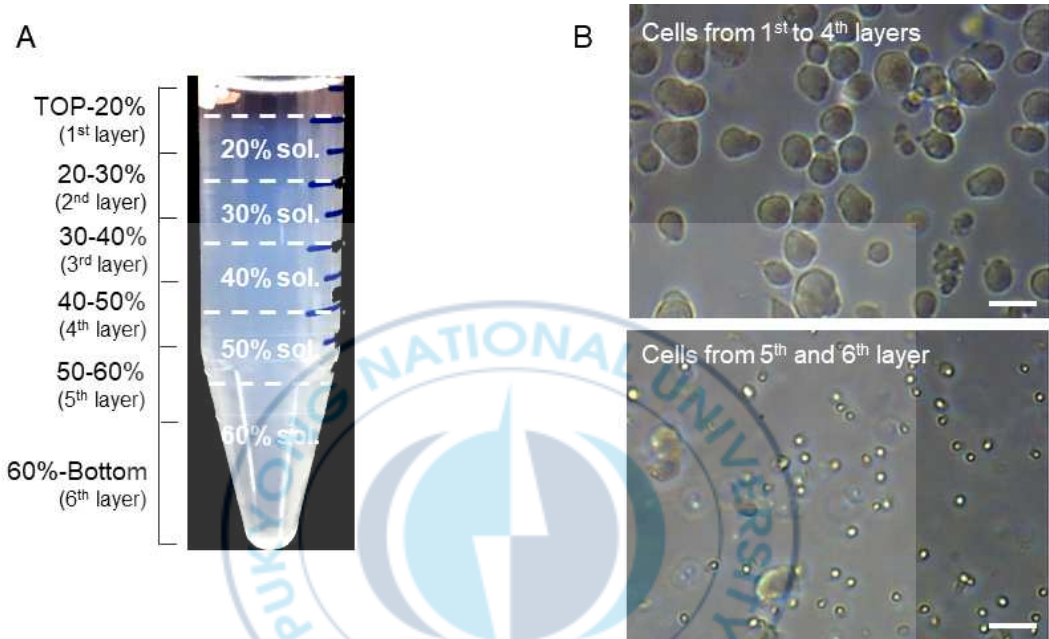


Figure 2. Sperm removal using Percoll density gradient centrifugation (PDGC). Digested testicular cells were separated to 6 different layers by PDGC. Separated testicular cell populations in each fraction were observed with a microscope. (A) A picture taken after PDGC. (B) Pictures of testicular cells isolated from 1st to 4th layers or 5th to 6th layers. Sperms, spermatids and red blood cells were observed in the 5th and 6th layers. Scale bar = 20 μm.

2. Effects of culture methods on the formation of testicular aggregates

To establish an effective 3D culture strategy for promoting the self-aggregation of testicular cells, various culture methods were tested. In the Matrigel suspension method, testicular cells at three different densities (1.25 , 2.5 , and 3.75×10^5 cells/ μL) were suspended in Matrigel droplets and placed onto three types of culture surfaces: tissue-culture-treated polystyrene, and standard Petri dishes. The cultures were maintained for 14 days, and the formation of cell aggregates was assessed.

On both types of polystyrene surfaces, the testicular cells began to cluster into small spots at day 1. At day 14, spherical aggregates had formed across all tested surfaces (Figure 3). While the Matrigel droplets began to degrade starting from day 3, complete degradation was not observed by day 14. This degradation process occurred more rapidly at higher cell densities. Despite this, aggregate formation was successfully achieved in 80 - 100% of samples across all cell concentrations by day 14 (Table 3). Typically, small multiple aggregates were formed, but at 2.5×10^5 cells/ μL and 3.75×10^5 cells/ μL in Petri dishes—large single aggregates were also observed (Figure 3 and Table 3).

Using the 3-layer gradient system (3-LGS), small multiple aggregates were induced only in a single trial at the highest concentration group (3.75×10^5 cells/ μL), indicating limited effectiveness (Figure 4 and Table 3).

In another approach, ultra-low attachment (ULA) culture was tested without Matrigel. In this condition, 1.25×10^6 testicular cells began forming aggregates by day 7, and by day 14, small multiple aggregates had

consistently formed in all replicates, achieving a 100% success rate. Interestingly, when Matrigel was included in the ULA system, a similar aggregate morphology was observed, but the overall efficiency of aggregate formation dropped significantly to 37.5% (Figure 5 and Table 3).

2. Effects of Media types on the number and size of testicular aggregates

To determine a more suitable culture medium for promoting testicular aggregate formation, I compared the effects of mESM2 and BM media using ULA culture for 14 days. Following the culture period, aggregate morphology, count, and size were investigated.

Two distinct morphological types of aggregates, hollow and compacted types, were consistently observed in both media conditions (Figure 6A). Hollow-type aggregates displayed a spherical appearance but contained either an empty core or only a few testicular cells within. In contrast, compacted-type aggregates were densely filled with closely packed testicular cells and lacked hollow regions.

The proportion of compacted-type aggregates varied significantly between the two media. In BM medium, compacted aggregates accounted for $43.7 \pm 14.4\%$ on day 7 and $47.3 \pm 4.4\%$ on day 14. However, when cultured in mESM2, the proportion markedly increased to $96.1 \pm 4.4\%$ on day 7 and $99.2 \pm 1.5\%$ on day 14, indicating that mESM2 promotes the formation of more compact aggregates (Figure 6B).

The total number of aggregates formed did not differ significantly between

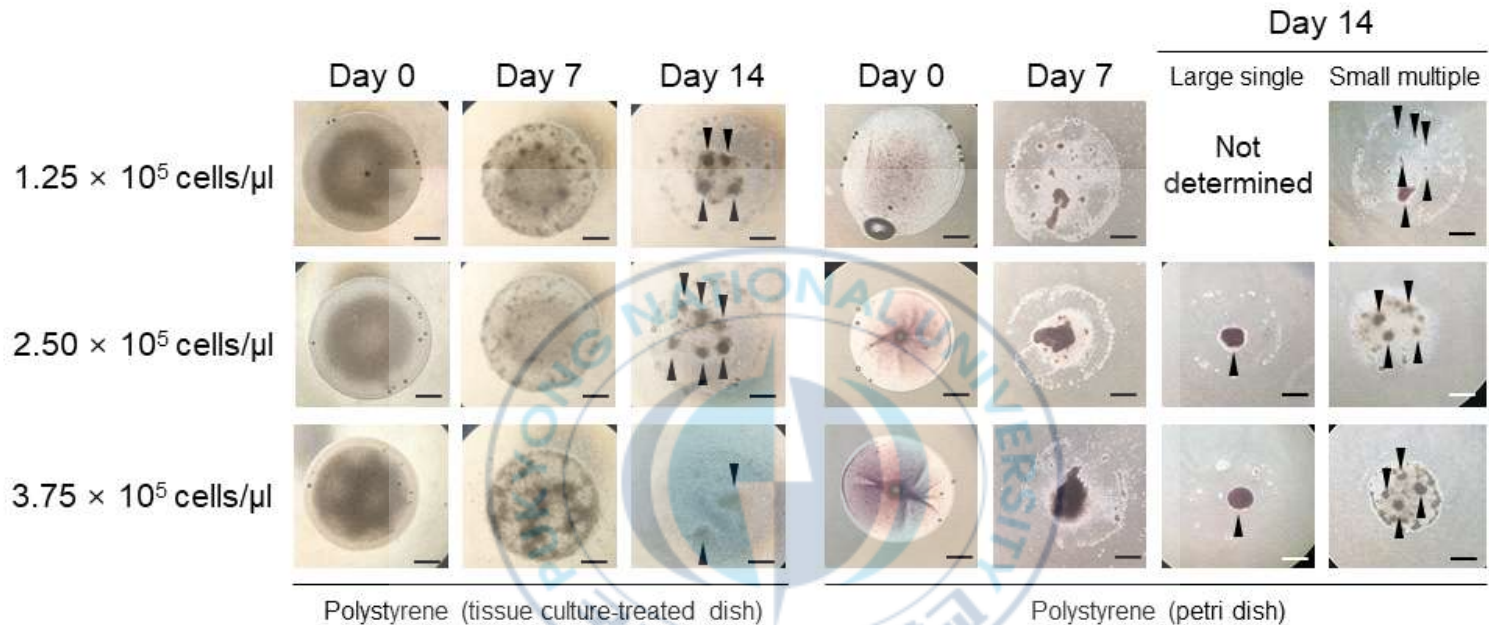


Figure 3. Evaluation of the formation of testicular aggregates by Matrigel suspension culture. Matrigel drops containing three different concentration of *O. dancena* testicular cells were formed on tissue-culture-treated dishes and Petri dishes, respectively. The pictures of testicular cells cultured by Matrigel suspension were taken at day 0, day 7, and day 14. When Matrigel drops were formed on tissue culture-treated dishes, small multiple type of aggregates were observed. Also, attached cells were observed on dishes. But, Matrigel drops, formed on Petri-dishes, large single and small multiple type of aggregates were observed. Arrow heads indicate induced testicular aggregates. Scale bar = 500 μ m.

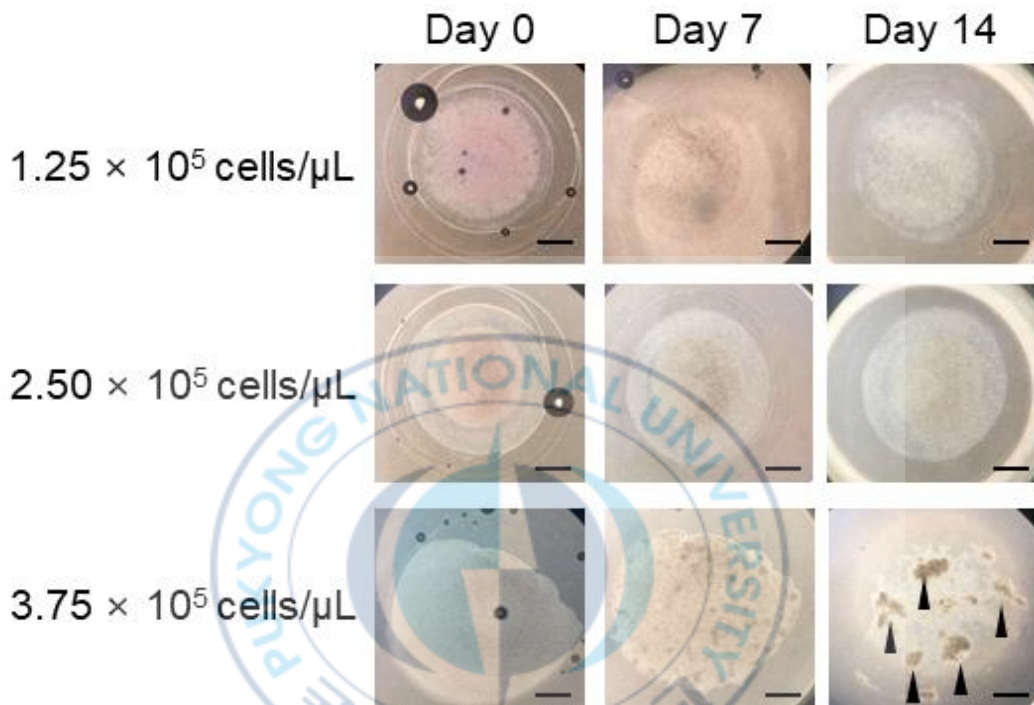


Figure 4. Evaluation of the formation of testicular aggregates by a three-layer gradient system (3-LGS). Three different concentration of *O. dancena* testicular cells were induced to aggregates using 3-LGS. The pictures of testicular cells cultured by 3-LGS were taken at day 0, day 7, and day 14. Arrow heads indicate induced testicular aggregates. Only when 3.75×10^5 cells/ μ L concentration of testicular cells were cultured by 3-LGS, aggregation was observed. Scale bar = 500 μ m.

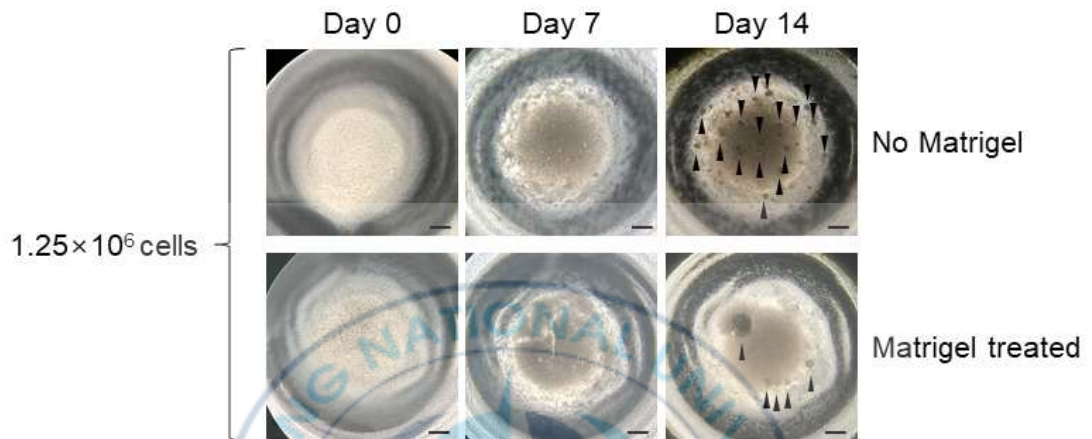


Figure 5. Evaluation of the formation of testicular aggregates in ultra-low attachment 96 well plate (ULA). 1.25×10^6 cells of *O. dancena* testicular cells were induced to aggregates in ULA. Testicular cells were cultured in ULA with or without Matrigel. Pictures of testicular cells cultured in ULA were taken at day 0, day 7, and day 14. The small multiple aggregates were observed regardless of the presence of Matrigel. Arrow heads indicate induced testicular aggregates. Scale bar = 500 μ m.

Table 3. Aggregate formation from *O. dancena* dispersed testicular cells by different culture methods and surface materials

Culture methods	Surface materials	Matrigel +cell drop volume (μl)	Suspended cell Concentration (cells/μL)	Final no. of cell seeded (cells)	No. of trials	No. (%) ^a of aggregate formation	No. (%) ^b of aggregate type	
							Large single	Small multiple
Matrigel suspension	Polystyrene (tissue culture-treated dish)	5	1.25 x 10 ⁵	6.25 x 10 ⁵	5	4 (80)	0 (0)	4 (80)
			2.50 x 10 ⁵	1.25 x 10 ⁶	3	3 (100)	0 (0)	3 (100)
			3.75 x 10 ⁵	1.875 x 10 ⁶	3	3 (100)	0 (0)	3 (100)
Matrigel suspension	Polystyrene (petri dish)	5	1.25 x 10 ⁵	6.25 x 10 ⁵	5	5 (100)	0 (0)	5 (100)
			2.50 x 10 ⁵	1.25 x 10 ⁶	10	10 (100)	2 (20)	8 (80)
			3.75 x 10 ⁵	1.875 x 10 ⁶	5	5 (100)	2 (40)	3 (60)
3-layer gradient system	Matrigel	3	1.25 x 10 ⁵	3.75 x 10 ⁵	4	0 (0)	0 (0)	0 (0)
			2.50 x 10 ⁵	7.5 x 10 ⁵	4	0 (0)	0 (0)	0 (0)
			3.75 x 10 ⁵	1.125 x 10 ⁶	3	1 (33.3)	0 (0)	1 (33.3)
Ultra-low attachment 96 well plate	Hydrophilic gel	-	-	1.25 x 10 ⁶	5	5 (100)	0 (0)	5 (100)
		5	2.50 x 10 ⁵	1.25 x 10 ⁶	8	3 (37.5)	0 (0)	3 (37.5)

^aPercentage of number of trials. ^bPercentage of number of aggregate formation

the two media on either day 7 or day 14 (Figure 6C). Regarding aggregate size, those cultured in mESM2 were significantly larger than those in BM on day 7, although this difference was not maintained by day 14. Regardless of medium type, the aggregate size increased significantly from day 7 to day 14 (Figure 6D).

3. Effects of the composition of mESM2 on the culture of testicular aggregates: protein series supplements

mESM2 consists of various supplements, which were classified in this study into two groups: protein-based components (FBS, FS, bFGF, and EE) and non-protein components (BME, NEAA, Ss, and Sp). To examine how protein-based supplements affect the formation of testicular aggregates, I cultured testicular cells in ULA conditions for 14 days using nine different media. These included the original mESM2 (used as the control) and eight modified versions in which one or more protein-containing components were selectively removed.

Among the tested groups, only the media lacking FBS failed to support the formation of testicular aggregates, while the others successfully promoted aggregation. As shown in Figure 7, compacted-type aggregates were generally formed in all media capable of supporting aggregation, and fusion between multiple aggregates was occasionally observed, regardless of media composition.

There were no significant differences in the number of aggregates among the eight groups that retained FBS but lacked FS, bFGF, and/or EE (Figure 8A). Similarly, aggregate sizes remained comparable among these groups, showing no statistical differences (Figure 8B).

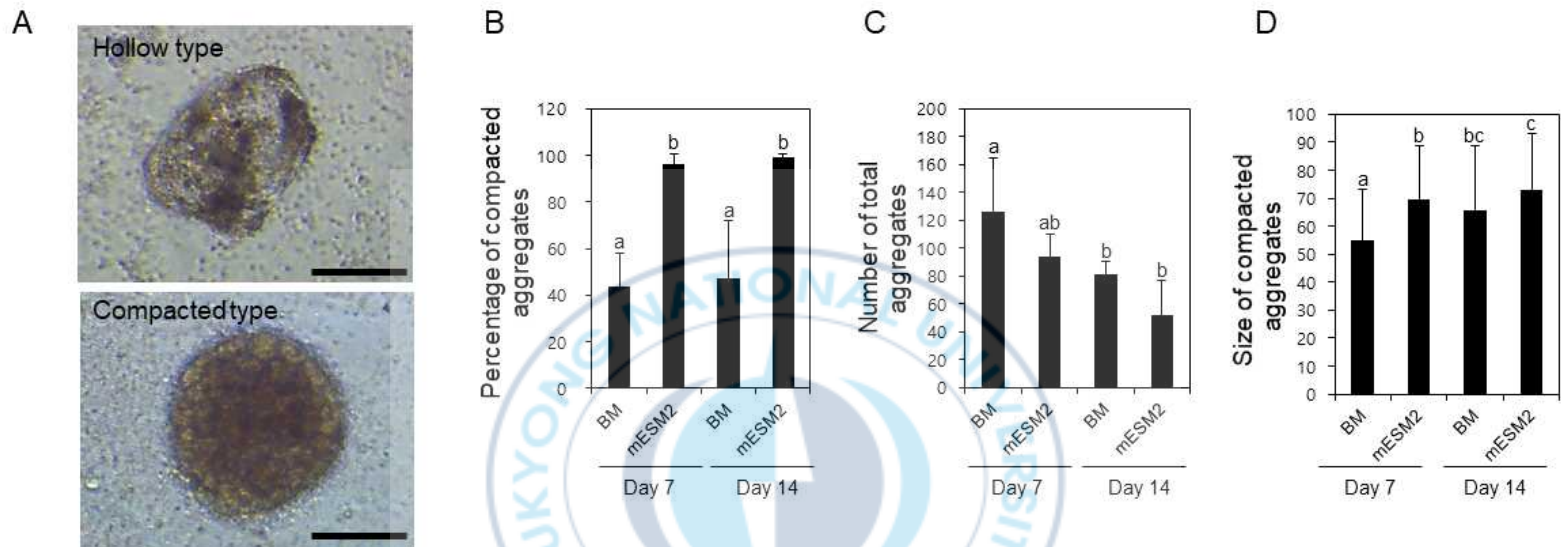


Figure 6. Comparison of morphological traits from testicular aggregates depending on kinds of culture media. Harvested testicular cells were seeded in ULA and cultured in basic medium (BM) or modified ESM2 (mESM2). (A) Representative pictures of testicular aggregates of hollow type or compacted type. Scale bar = 100 μm . (B) Comparison of the percentages of compacted testicular aggregates at 7 days and 14 days depending on BM or mESM2. (C) Comparison of the numbers of induced testicular aggregates at 7 days and 14 days depending on BM or mESM2. (D) Comparison of the sizes of induced testicular aggregates at 7 days and 14 days depending on BM or mESM2. All values are expressed as mean \pm standard deviation of three or four independent experiments. ^{abc}Different letters indicate significant differences ($p < 0.05$).

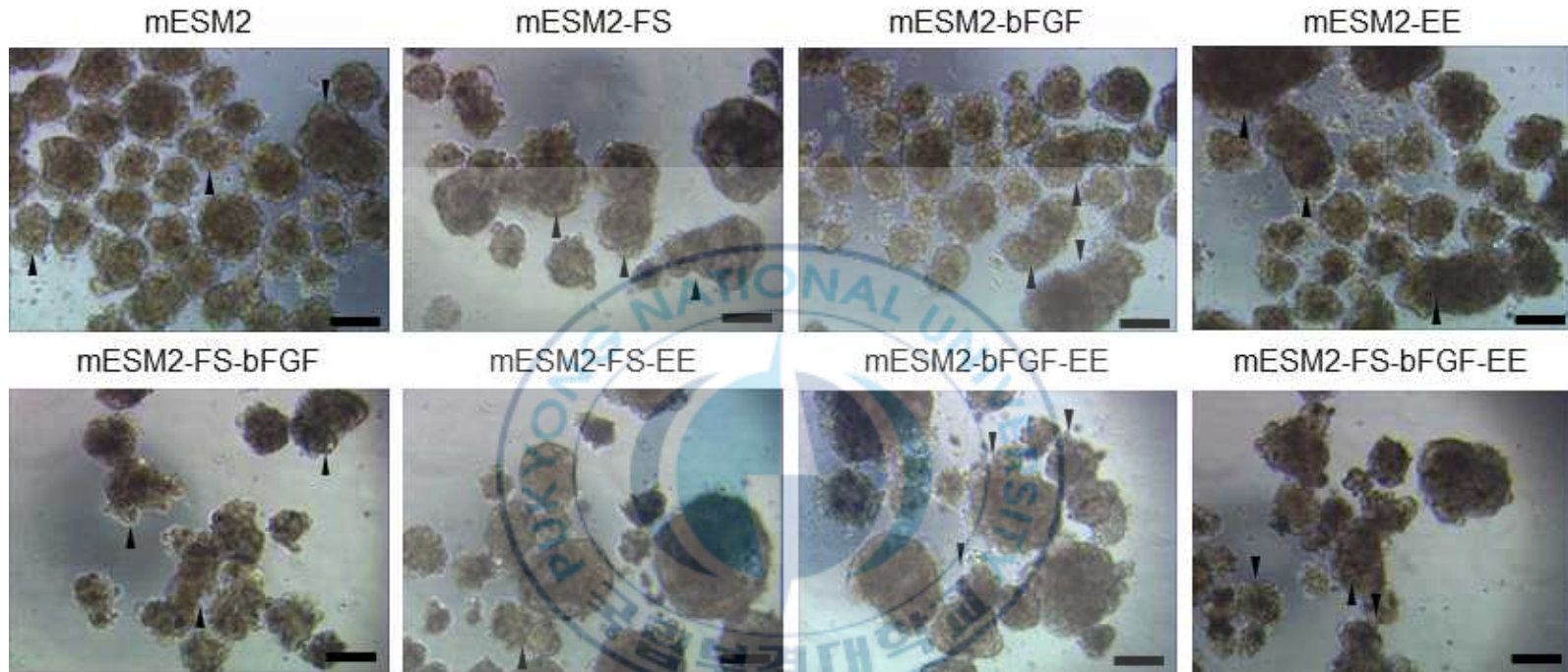
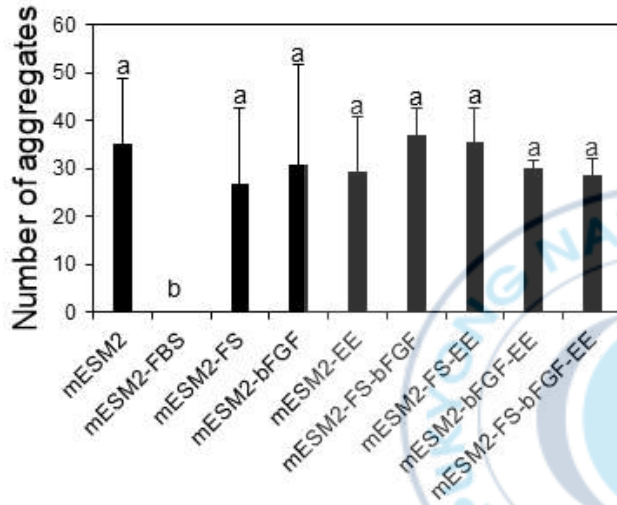


Figure 7. Comparison of the morphologies from testicular aggregates depending on protein supplements in **mESM2**. The testicular aggregates were induced in mESM2-based ULA conditions with various combinations of protein supplements omitted. Each testicular aggregate at day 14 was transferred to a 35 mm Petri dish containing DPBS, and pictures were taken. Arrow heads indicate that two or more aggregates stick together. Scale bar = 100 μ m. FS: fish serum; bFGF: basic fibroblast growth factor; EE: embryo extract.

A



B

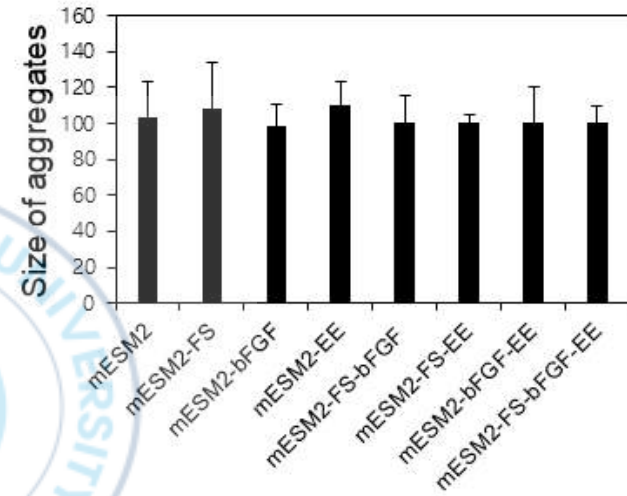


Figure 8. Evaluation of the number and the size of testicular aggregates depending on protein supplements in mESM2. The testicular aggregates were induced in mESM2-based ULA conditions with various protein supplements omitted. The number and the size of testicular aggregates were measured from each testicular picture. (A) Measurement of the number of testicular aggregates cultured in each medium. (B) Measurement of the size of testicular aggregates cultured in each medium. FBS; fetal bovine serum. All values are expressed as mean \pm standard deviation of three independent experiments at least. ^{ab}Different letters indicate significant differences ($p < 0.05$).

To further investigate the specific effects of FS, bFGF, and EE on testicular aggregate culture, I cultured isolated testicular cells for 14 days in either full mESM2 medium or a modified version lacking FS, bFGF, and EE (mESM2 - FS - bFGF - EE). Cell viability and gene expression levels within the resulting aggregates were then assessed and compared.

As depicted in Figure 9A, most cells in both media groups were viable, showing strong green fluorescence, while only a few dead cells (red) were detected, typically located internally. Trypan blue staining also confirmed high cell viability in both conditions, with no significant difference between the groups (Figure 9B; $90.66 \pm 0.63\%$ in mESM2 vs. $91.08 \pm 1.12\%$ in mESM2 - FS - bFGF - EE).

To evaluate potential functional differences, testicular aggregates were analyzed by qRT-PCR for the expression of *nanos2* (a marker for spermatogonia), *scp3* (a mid-meiotic germ cell marker), and *sox9a* (a marker for testicular somatic cells). While *nanos2* expression was comparable between the two groups (Figure 10A), significantly higher levels of *scp3* and *sox9a* were detected in aggregates cultured with the complete mESM2 medium (Figure 10B and Figure 10C), with 2.68- and 2.14-fold increases, respectively.

These findings suggest that although FS, bFGF, and EE are not critical for aggregate formation or cell viability, they do enhance germ cell differentiation and promote somatic cell function within the testicular aggregates.

4. Effects of the composition of mESM2 on the culture of testicular aggregates: non-protein series supplements

To evaluate the contribution of non-protein components in mESM2 to the

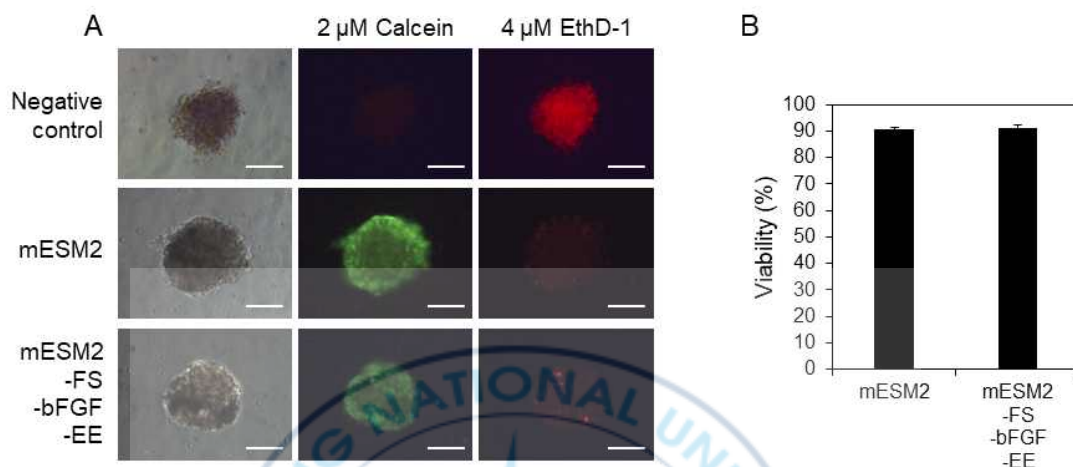


Figure 9. Evaluation of the effects of fish serum (FS), basic fibroblast growth factor (bFGF), and embryo extract (EE) on the viability of the cells composing testicular aggregates. Testicular aggregates were cultured in ULA containing mESM2 or mESM2 without FS, bFGF, EE for 14 days. Subsequently, their viabilities were compared by live/dead cell staining and trypan blue staining (A) Pictures taken after live/dead cells staining. Live cells were stained by 2 μ M calcein and dead cells were stained by 4 μ M EthD-1. Negative control were immersed in 70% ethanol for 1 hour before live/dead cell staining. Scale bar = 100 μ m. (B) Comparison of the viability of cells composing testicular aggregates cultured in each media. The result was determined by trypan blue staining. All values are expressed as mean \pm standard deviation of three independent experiments at least.

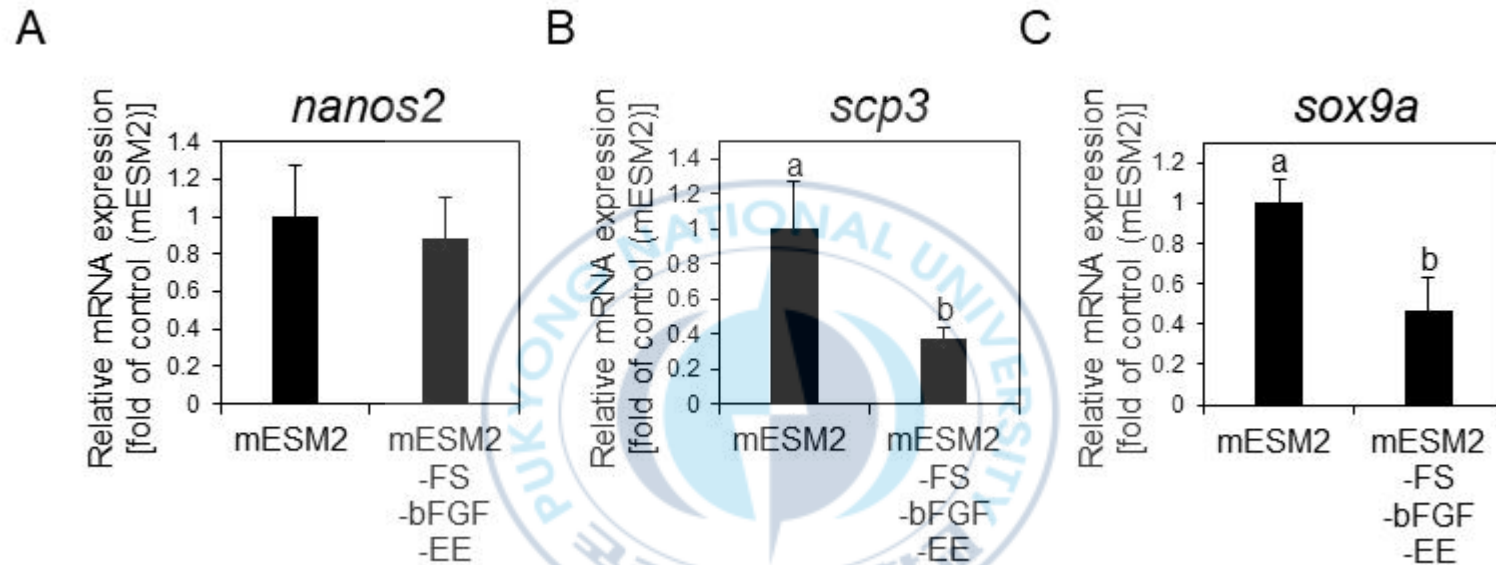


Figure 10. Evaluation of the effects of FS, bFGF, EE on the gene expression levels from testicular aggregates. Testicular aggregates cultured in each medium were harvested at day 14. Subsequently, they were analyzed by qRT-PCR to compare three genes expression levels. (A) Relative mRNA expression of *nanos2* (spermatogonia marker). (B) Relative mRNA expression of *scp3* (meiosis marker). (C) Relative mRNA expression of *sox9a* (Sertoli cell marker). All values are expressed as mean \pm standard deviation of three independent experiments at least. ^{ab} Different letters indicate significant differences ($p < 0.05$).

formation of testicular aggregates, I prepared 15 different culture media by selectively removing one or more non-protein supplements from the original mESM2 formulation. Isolated testicular cells were cultured in each of these modified media, and the resulting aggregates were evaluated in terms of number and size.

Across all experimental conditions, compact spherical aggregates were formed, occasionally showing adhesion between them. However, as shown in Figure 11A, the number of aggregates significantly declined in all modified media compared to the full mESM2 control group. Notably, the fewest aggregates were observed when all non-protein supplements were excluded, suggesting that each component plays a role in promoting aggregate formation.

Regarding aggregate size, several media lacking specific combinations of supplements, including BME, NEAA, Sp, and Ss, resulted in significantly smaller aggregates compared to the control (Figure 11B). In particular, the exclusion of BME, whether alone or in combination with other supplements, consistently led to a reduction in aggregate size. Interestingly, BME alone was not sufficient to restore normal aggregate size, whereas co-treatment with NEAA, Sp, or Ss was necessary to observe a recovery effect.

These findings indicate that non-protein supplements in mESM2, especially BME, contribute not only to the quantity but also to the dimensional growth of testicular aggregates, likely through synergistic interactions with other components.

5. Evaluation of fertility of the sperms derived from testicular aggregates

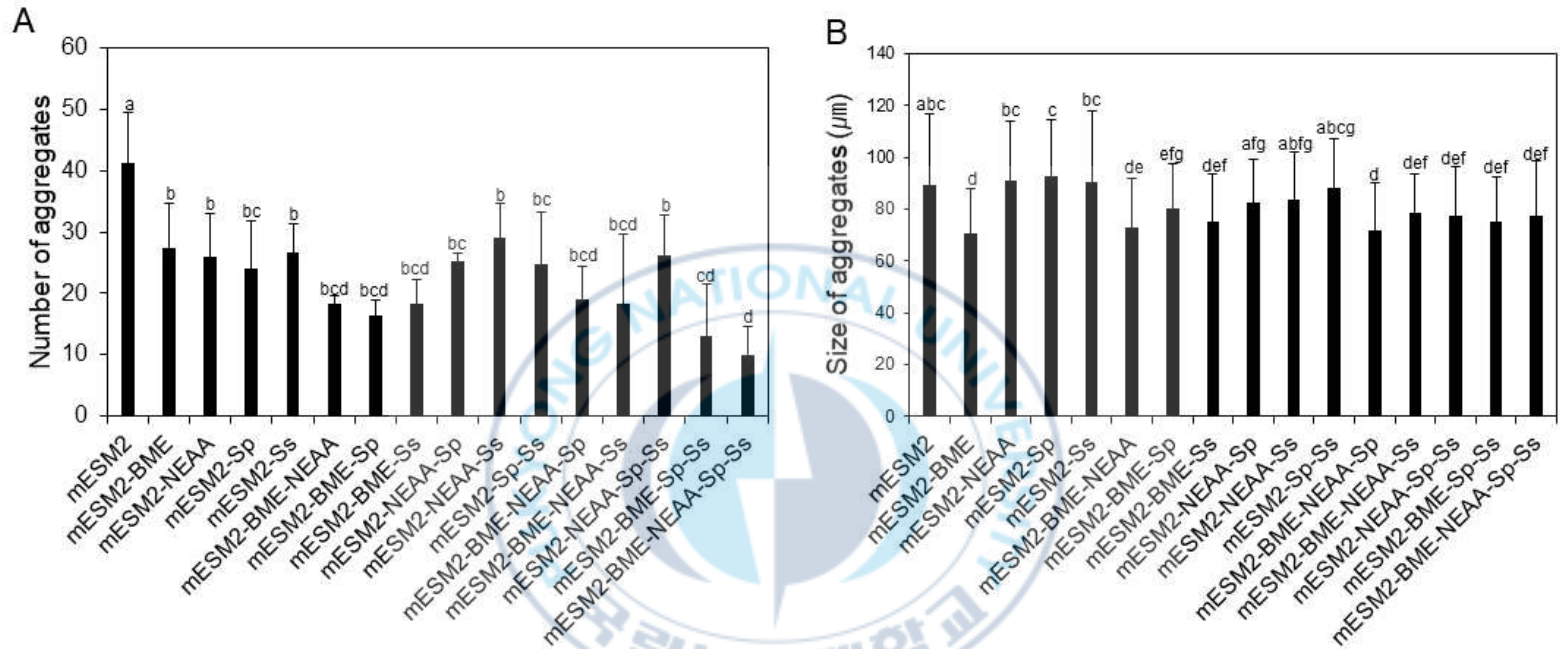
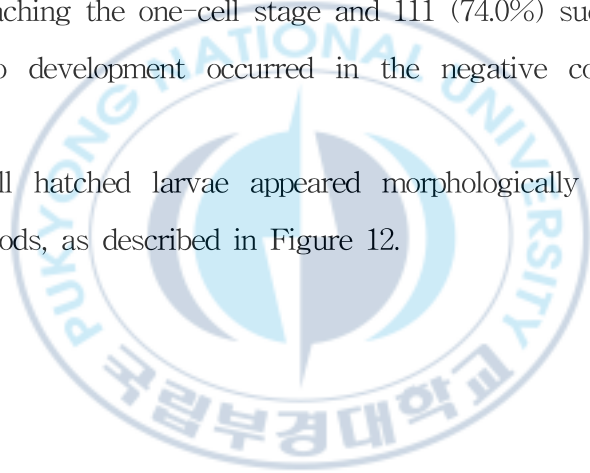


Figure 11. Evaluation of the number and the size of testicular aggregates of non-protein series supplements in mESM2. The testicular aggregates were induced in mESM2-based ULA condition with various combinations of non-protein supplements omitted. The number and the size of testicular aggregates were measured from each testicular picture. (A) Comparison of the number of aggregates cultured in each medium. (B) Comparison of the size of aggregates cultured in each medium. All values are expressed as mean \pm standard deviation of three independent experiments at least. ^{abcdef}Different letters indicate significant differences ($p < 0.05$).

After 14 days of culture, numerous motile spermatozoa were observed in the vicinity of the testicular aggregates. To evaluate their fertilizing ability, *in vitro* fertilization (IVF) was carried out using these sperm. As shown in Table 4, IVF with sperm derived from the testicular aggregates resulted in the development of 122 one-cell-stage embryos out of 276 eggs (44.2%), while only four of these embryos progressed to the hatchling stage (1.4%).

In comparison, fertilization using freshly isolated sperm led to 107 one-cell-stage embryos from 180 eggs (59.4%), with 78 hatchlings produced (43.3%). Natural fertilization yielded the highest efficiency, with 124 out of 150 eggs (82.7%) reaching the one-cell stage and 111 (74.0%) successfully hatching. As expected, no development occurred in the negative control group using unfertilized eggs.

Importantly, all hatched larvae appeared morphologically normal across all fertilization methods, as described in Figure 12.



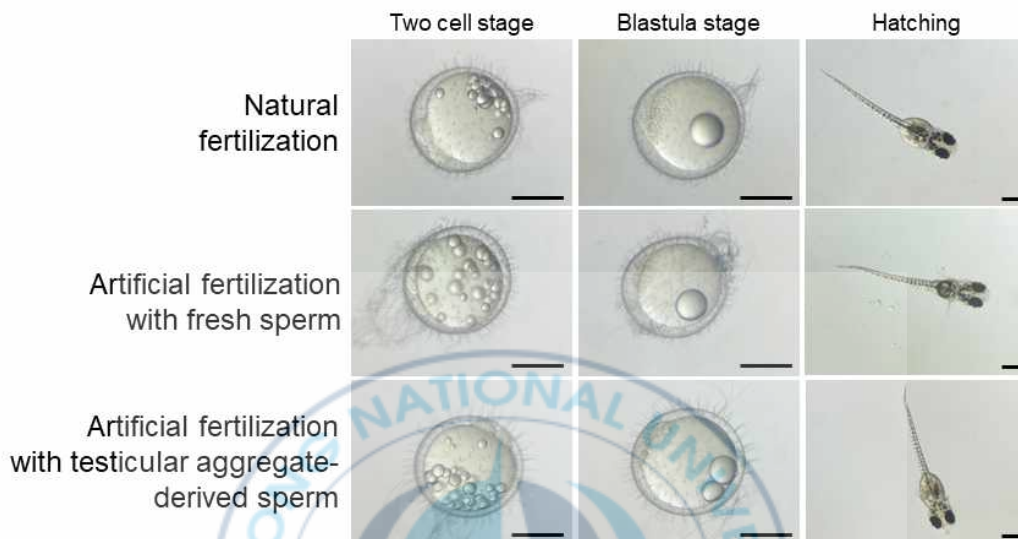


Figure 12. Representative pictures of *O. dancena* embryos obtained through natural fertilization, or through artificial fertilization using either fresh sperm or sperm derived from testicular aggregates. Naturally fertilized eggs were harvested right after mating. For artificial fertilization, unfertilized eggs were collected by pushing on abdomens. 30–50 of unfertilized eggs were fertilized in 1.5 mL tubes with fresh sperm or *in vitro* differentiated sperm. The fertilized eggs of *O. dancena* reached to the two cell stage and the early blastula stage at 2 hours and 6 hours post-fertilization, respectively. Hatching was occurred at 11 days post-fertilization. Scale bar = 500 μ m.

Table 4. Fertility results according to fertilization method

	No. of eggs	No. (%) ^a of one cell stage embryos	No. (%) ^a of two cell stage embryos	No. (%) ^a of blastula stage embryos	No. (%) ^a of hatched fish larvae
Natural fertilization by mating	150	124 (82.7)	124 (82.7)	114 (76)	111 (74)
Artificial fertilization with fresh sperm	180	107 (59.4)	81 (45)	80 (44.4)	78 (43.3)
Artificial fertilization with aggregate-derived sperm	276	122 (44.2)	6 (2.2)	4 (1.5)	4 (1.5)
NC	103	51 (49.5)	0 (0)	0 (0)	0 (0)

^aPercentage of number of trials

IV. Discussion

In this study, I evaluated the effects of culture methods and media compositions on the formation of testicular aggregates in marine medaka (*Oryzias dancena*) to determine optimal culture conditions.

Previous studies on mammalian testicular organoid cultures have shown that testicular cells from immature testes can self-organize into organoids (Alves-Lopes et al., 2017; Cham et al., 2021; Edmonds and Woodruff, 2020). According to Alves-Lopes et al. this may be due to the high proportion of Sertoli cells present in immature testes (Alves-Lopes et al., 2017). Likewise, it has been reported that testicular cells from adult mice can form spheroids when mixed with immature somatic cells (Edmonds and Woodruff, 2020). A similar phenomenon was observed in a teleost species, honmoroko (*Gnathopogon caeruleus*), where testicular aggregates were successfully generated from testicular cells derived from immature or non-spawning individuals, which have a higher Sertoli cell-to-germ cell ratio (Higaki et al., 2017).

O. dancena is a useful experimental model due to its ease of breeding in laboratory conditions, short generation time, and relatively small genome (Song et al., 2009). Additionally, as a euryhaline species, it is suitable for studies in marine ecotoxicology (Song et al., 2009). Based on these advantages, this species has been employed in various culture studies, including the establishment of embryonic stem cells (Lee et al., 2015; Choi and Gong, 2018; Song and Gong, 2022) and whole testis organ culture (Kang et al., 2019; Lee et al., 2021). However, despite its general utility as

a model organism, *O. dancena* presents limitations for testicular aggregate studies (Dong et al., 2014). One of the main challenges is the technical difficulty in isolating immature testes due to their small size. The first spawning occurs around 9 weeks post-hatching, at which point the fish reach an average body length of 22.58 ± 2.73 mm (Song et al., 2009), making early testis isolation difficult. Furthermore, as a species that spawns daily, *O. dancena* does not have a defined non-spawning season.

To address these limitations, I utilized Percoll density gradient centrifugation to enrich Sertoli cells by removing sperm and spermatids from adult testicular cell populations. This method has previously been used in mammals to separate testicular cell types (de Barros et al., 2012; Goel et al., 2007; Heidari et al., 2014) and in fish to isolate spermatogonia or somatic cells (Zhang et al., 2022; Linhartová et al., 2014; Lacerda et al., 2008). In our results, sperm and spermatids were successfully separated, leading to an increased Sertoli-to-germ cell ratio. Importantly, cell populations containing sperm and spermatids did not form aggregates in culture, suggesting that the removal of these cells was critical for successful aggregate formation.

Next, I investigated the influence of various culture methods on aggregate formation. Previous research has shown that testicular organoids can form in the presence or absence of Matrigel in mammalian models such as rats (Alves-Lopes et al., 2017), humans (Strange et al., 2018), pigs (Cham et al., 2021), and bovines (Cortez et al., 2022) In our study, I evaluated three Matrigel-based methods—Matrigel suspension, 3-LGS, and ULA with Matrigel—as well as a Matrigel-free method using ULA alone. The 3-LGS did not support aggregate formation in *O. dancena*, in contrast

to results in rat (Alves-Lopes et al., 2017), indicating that the 3-LGS method was not optimal in *O. dancena*.

In contrast, Matrigel suspension on polystyrene allowed aggregates to form with a high frequency (80 - 100%), regardless of tissue culture treatment. However, this method also presented issues. Many testicular cells adhered to the dish surface during culture. Since testicular somatic cells adhere more strongly to substrates than germline stem cells (Ryu and Gong, 2020), this likely reduced the number of somatic cells available for aggregation. Additionally, I observed rapid Matrigel degradation beginning on day 3, with floating Matrigel fragments containing cells in the medium, which likely further interfered with aggregate formation.

Interestingly, the form of aggregates, either large single or small multiple, appeared to vary depending on the surface properties of the culture dish. On tissue-culture-treated dishes, more somatic cells adhered, leading to fewer contributing to aggregates, while on Petri dishes, less adherence allowed more somatic cells to participate. To improve upon the limitations of Matrigel suspension methods, I used ultra-low attachment (ULA) plates, which promote cell aggregation by concentrating cells at the bottom of round wells. This method enabled consistent aggregate formation (100%) by day 7, with significant growth observed by day 14, even without Matrigel. This suggests that ULA culture is the most effective method tested for *O. dancena* testicular aggregate formation.

I also compared basal medium (BM) with modified ESM2 (mESM2), which has been used in fish embryonic stem cell and spermatogonial stem cell culture (Hong and Schartl, 1996; Fan et al., 2017; Ho et al., 2014; Hong et al., 2004). Aggregates cultured in mESM2 were mostly compact,

whereas those in BM were often hollow. Although the mechanism behind hollow aggregate formation in BM remains unclear, mESM2 appeared more suitable for *O. dancena*. Removal of FS, bFGF, and EE from mESM2 did not significantly affect aggregate number or size but did reduce expression of *scp3* and *sox9a*, markers of meiotic germ cells and Sertoli cells, respectively (Lee et al., 2021; Nakamura et al., 2017). These results imply that FS, bFGF, and EE are essential for germ cell differentiation and maintenance of testicular somatic cell function. Among them, bFGF is known to play a significant role in promoting the growth and differentiation of spermatogonial stem cells (Kubota et al., 2004; Mizapour et al., 2012; Masaki et al., 2018) and Sertoli cells (Guo et al., 2015). Thus, the specific function of bFGF warrants further investigation in this context.

Regarding non-protein supplements, exclusion of BME from mESM2 led to a significant reduction in aggregate size, either alone or in combination with other factors. BME enhances cell survival and growth by mitigating oxidative stress and supporting cytokine uptake (Bui-Marinos et al., 2022). It has been shown to stimulate proliferation of leukemia and lymphoma cells in mice (Hewlett et al., 1977), as well as spleen cells (Burger et al., 1980). In fish, BME has been used to support long-term culture of testicular and ovarian cells (Higaki et al., 2013). Although BME alone did not restore aggregate size, its combination with other non-protein supplements had a synergistic effect, suggesting that oxidative stress management is important and that BME functions best with co-factors.

Finally, I confirmed that motile sperm were produced from aggregates cultured for 14 days. Considering the short motility period of fish sperm, 30 seconds to 5 minutes depending on species (Yang and Tiersch, 2009),

the presence of motile sperm after 14 days strongly suggests they originated from the aggregates. However, the hatching rate after artificial fertilization was only 1.4% (4/276 eggs), indicating that the culture conditions were not sufficient to support complete functional maturation. In other studies using adult *Bostrychus sinensis* and *Gnathopogon caerulescens*, where sex hormones were supplemented in the media, fertilization rates reached $26.9 \pm 4.1\%$ and $21.7 \pm 12.8\%$, respectively (Higaki et al., 2017; Zhang et al., 2022). Among the hormones used, 11-ketotestosterone (11-KT) has been identified as essential for spermatogonial differentiation in several species (Miura and Miura, 2011; Cavaco et al., 2001; Leal et al., 2009), and FSH has also been shown to promote germline development (Nóbrega et al., 2015). Because 11-KT synthesis is regulated by FSH, further studies incorporating these hormones into *O. dancena* testicular aggregate culture may improve sperm quality and functionality, contributing to both basic research and applications in fish reproductive biotechnology.

CHAPTER 4.

Establishment and Characterization of Ovarian Aggregate Culture Systems in Marine Medaka (*Oryzias dancena*)

I . Introduction

Understanding how female germline stem cells (GSCs) in teleosts proliferate and differentiate is crucial for advancing fields such as developmental biology, transgenic fish technology, and the conservation of endangered species (Okutsu et al., 2006; Wong et al., 2013; Iwasaki-Takahashi et al., 2020). While numerous studies have made significant contributions to elucidating these biological processes (Okutsu et al., 2006; Spradling et al., 2011; Lacerda et al., 2014), there is still a need for more advanced *in vitro* systems that enable detailed exploration of the underlying cellular and molecular mechanisms involved in female GSC development.

In vitro systems provide a controlled environment, which is particularly advantageous for dissecting cell behavior and gene expression dynamics at both cellular and molecular levels. This level of precision and experimental reproducibility is often difficult to achieve *in vivo* (Xu et al., 2021). However, conventional two-dimensional (2D) culture systems have limitations in replicating the complex architecture and cellular heterogeneity of the ovarian microenvironment. Interactions among various gonadal cell types within highly organized tissue structures play essential roles in maintaining GSC populations and regulating their proliferation and differentiation (Reuter et al., 2014; Alves-Lopes et al., 2017). The absence of such spatial organization in 2D systems limits their utility for detail studies of female GSC biology.

To address these limitations, organoid technology presents a promising alternative. Ovarian organoids, in particular, are capable of mimicking the three-dimensional architecture and physiological functions of ovaries *in vitro*. Previous research in mammals has demonstrated successful generation of ovarian organoids. For instance, in mice, organoids were formed in ultra-low attachment (ULA) 96-well plates and then cultured at an air-liquid interface, which allowed the transdifferentiation of spermatogonia into fertilizable oocytes (Luo et al., 2021). Similarly, in humans, organoids derived from ovarian cancer cells have been cultured using a modified Matrigel bilayer system to assess responses to chemotherapeutic agents (Maru et al., 2019). These findings suggest that organoid technology is sufficiently developed to support the establishment of ovarian organoids and further imply its potential application in teleost species.

Despite its advantages, to the best of our knowledge, no study has yet reported the successful development of ovarian organoids in teleost fish. This underscores the need for a stable and reproducible culture system specifically tailored for fish ovarian tissues.

In the present study, I aimed to establish ovarian aggregate culture system using the marine medaka (*Oryzias dancena*) as a model species. As an initial approach, I sought to induce the formation of ovarian cell aggregates and assess their potential as precursors to organoid structures. To this end, I first evaluated which ovarian cell populations were most effective in forming aggregates by separating dispersed ovarian cells via Percoll density gradient centrifugation and culturing the different fractions under suspension conditions. Subsequently, I investigated the influence of

various media supplements on aggregate formation and maintenance. Finally, I assessed whether these aggregates were capable of maintaining ovarian functionality, particularly in terms of germ cell preservation and the synthesis of 17β -estradiol, during *in vitro* culture.



II. Materials and methods

1. Induction of ovarian cell aggregates

To induce ovarian cell aggregates, 1.25×10^6 cells from each of two distinct ovarian cell populations (1. harvested ovarian cells from 2nd layer and 3rd layer vs 2. harvested ovarian cells from 1st layer to 4th layer) were mixed in 150 μL of culture medium and seeded into individual wells of a 96-well ultra-low attachment (ULA) plate. Cultures were maintained at 28°C in an incubator, and unless otherwise specified, medium was changed every three days by replacing half (75 μL) of the total volume. For cultures extending beyond 7 days, the full 150 μL volume was replaced every third day.

To examine the influence of specific growth factors on gene expression, 10 ng/mL of basic fibroblast growth factor (bFGF) and/or 10 ng/mL of glial cell-derived neurotrophic factor (GDNF; PeproTech, Hamburg, Germany) were added to a modified culture medium lacking FS, bFGF, and EE. These conditions were maintained throughout the culture period.

For determining the optimal concentration of human follicle-stimulating hormone (hFSH; Thermo Fisher Scientific) for inducing *cyp19a1* expression, hFSH was added to the medium at final concentrations of 50 ng/mL, 100 ng/mL, or 150 ng/mL. Stock solutions of hFSH were prepared in distilled water. Cultures were maintained for 7 days with half volume medium replacement every three days. The concentration range was selected based

on a previous report involving FSH induced 17β -estradiol (E2) synthesis in Russian sturgeon (Yom-Din et al., 2016). On day 7, ovarian aggregates were collected for histological analysis and *cyp19a1* expression assessment.

2. Hematoxylin and eosin staining

Ovarian cell aggregates cultured *in vitro* were first transferred into 35 mm Petri dishes containing 2 mL of DPBS to wash off residual media. For fixation, the aggregates were placed into 15 mL conical tubes and incubated overnight at 4°C in 1 mL of Bouin's solution (CliniSciences, Montrouge, France). After fixation, Bouin's solution was carefully removed, and the aggregates were dehydrated through a graded ethanol series as follows: 70% (1 h), 80% (1 h), 90% (1 h), 95% (1 h), 99% (1 h), followed by a second step in 99% ethanol for 1 h.

The dehydrated samples were embedded in Paraplast® (Leica Biosystems, St. Louis, USA) and sectioned into 5 μ m-thick slices. For deparaffinization, tissue sections were immersed twice in xylene (Duksan) for 2 minutes each. Rehydration was then performed by sequential immersion in decreasing concentrations of ethanol (reverse of the dehydration series), each for 30 seconds.

Rehydrated tissue sections were stained with hematoxylin (Leica Biosystems) for 2 minutes, followed by eosin (Biognost, Zagreb, Croatia) for 1 minute.

3. Reverse transcription polymerase chain reaction

(RT-PCR) and quantitative RT-PCR (qRT-PCR)

100 ng of total RNA was treated with DNase I (Sigma-Aldrich) to remove potential genomic DNA contamination, following the manufacturer's protocol. Complementary DNA (cDNA) was then synthesized using the GoScript™ Reverse Transcription System (Promega, Madison, WI, USA) in accordance with the manufacturer's instructions.

Conventional RT-PCR was performed under the following thermal cycling conditions: an initial denaturation at 94°C for 3 minutes, followed by 35 cycles of amplification consisting of denaturation at 94°C for 30 seconds, annealing at 60°C for 30 seconds, and extension at 72°C for 30 seconds. PCR products were separated by electrophoresis on a 1.2% agarose gel (Lonza, Rockland, ME, USA) and visualized under UV light.

For quantitative real-time PCR (qRT-PCR), cDNA synthesized as described above was used. The qRT-PCR thermal profile consisted of an initial denaturation at 94°C for 3 minutes, followed by 40 amplification cycles (94°C for 30 seconds, 60°C for 30 seconds, and 72°C for 30 seconds). Gene expression levels were calculated using the $2^{-\Delta\Delta Ct}$ method, where $\Delta Ct = Ct_{\text{target}} - Ct_{\text{reference}}$ (*18S rRNA*), and $\Delta\Delta Ct = \Delta Ct_{\text{sample}} - \Delta Ct_{\text{calibrator}}$ (Livak and Schmittgen, 2001). Primer sequences utilized in this study are listed in Table 3.

4. Measurement of size and viability of ovarian aggregates

For size measurement, aggregates cultured for 7 days were retrieved from ULA plates and washed with 2 mL DPBS in 35 mm Petri dishes.

The aggregates were subsequently transferred into 96-well plates (Thermo Fisher Scientific), and images of 20 individual aggregates were captured. Aggregate size was quantified using TSVIEW7 software (Version 7) and defined as the average of the measured width and height in each image.

To evaluate the viability of cells within ovarian cell aggregates, collected aggregates were dispersed by 0.05% (v/v) trypsin-EDTA. The cell viability was measured by trypan blue staining. Additionally, the spatial distribution of live and dead cells within aggregates was investigated using the Live/Dead Viability/Cytotoxicity Kit (Molecular Probes). Aggregates were stained according to the manufacturer's protocol.

5. Measurement of 17β -estradiol (E_2) concentration

To assess E_2 production during ovarian cell aggregate culture, 150 μ L of culture supernatant was collected on days 7, 10, 13, 16, 19, and 22. The collected media were immediately stored at -70°C in a deep freezer until further analysis. E_2 levels were quantified using an Estradiol ELISA Kit (Cayman Chemical Company, MI, USA) according to the manufacturer's instructions. Fresh mESM2 medium was used as the blank control for baseline comparison.

III. Results

1. Determination of the optimal cell populations for ovarian cell aggregate formation

To identify the optimal cell population for generating structured ovarian cell aggregates, enzymatically dissociated ovarian cells from *Oryzias dancena* were subjected to discontinuous Percoll density gradient centrifugation with five distinct layers. Two specific cell fractions were collected: one from the 2nd layer and 3rd layer and the other from 1st layer to 4th layer. Each fraction was separately cultured in ultra-low attachment (ULA) plates, and aggregate formation was assessed after 7 days (Figure 13A). Two distinct aggregation patterns were observed, the formation of either a large, singular aggregate or multiple smaller aggregates (Figure 13B). Notably, cells from the 20 - 40% layers predominantly formed multiple small aggregates in 90% of cases (9/10), while 10% produced a single large aggregate. In contrast, cells from the top to 50% layers consistently formed a single large aggregate in all trials (9/9) (Figure 13C).

To compare the cellular characteristics of these aggregates, histological and gene expression analyses were performed. Histological sections revealed the presence of pre-vitellogenic oocytes exclusively in aggregates derived from 1st layer to 4th layer (Figure 14A). RT-PCR showed that both aggregate types expressed germ cell markers (*nanos2*, *scp3*) and ovarian somatic cell markers (*lshr*, *foxl2*). However, expression of *lhr*, a gene associated with more differentiated somatic cells, was detected only in aggregates from 1st layer to 4th layer fraction (Figure 14B).

Taken together, these findings suggest that cells collected from 1st layer to 4th layer are more suitable for forming functionally relevant ovarian cell aggregates, and thus were selected for subsequent experiments.

2. Effects of media supplements on the culture of ovarian cell aggregates

To evaluate the role of specific media components in supporting ovarian cell aggregate formation, the effects of FS, bFGF, and EE were examined. Ovarian cells isolated from 1st layer to 4th layer using Percoll density gradient centrifugation were cultured for 7 days in either standard mESM2 or a modified version lacking FS, bFGF, and EE. The resulting aggregates from both groups were then compared.

In both media conditions, all samples consistently produced large, singular ovarian cell aggregates, with no discernible morphological differences between the two groups (Fig. 15). Live/dead cell staining revealed that the majority of cells within the aggregates remained viable, emitting green fluorescence indicative of live cells and showing negligible red fluorescence associated with cell death, regardless of media formulation (Fig. 16A). Trypan blue staining assays supported these findings, showing similarly high cell viability across both groups (Fig. 16B; $92.58 \pm 2.14\%$ in mESM2 vs. $92.61 \pm 1.82\%$ in mESM2 without FS, bFGF, and EE).

In terms of aggregate size, no significant differences were observed between the two conditions (Figure 16C; $876.46 \pm 88.69 \mu\text{m}$ in mESM2 vs. $852.12 \pm 194.23 \mu\text{m}$ in mESM2 without FS, bFGF, and EE). However, gene

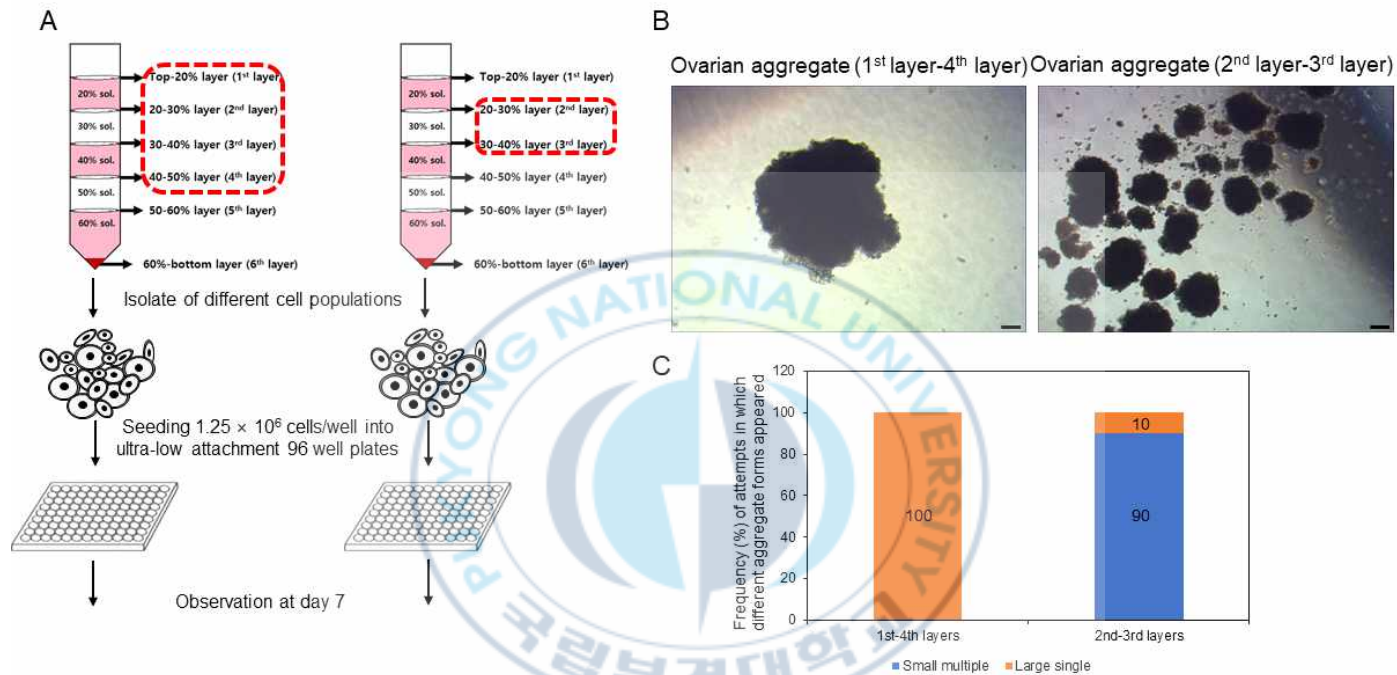
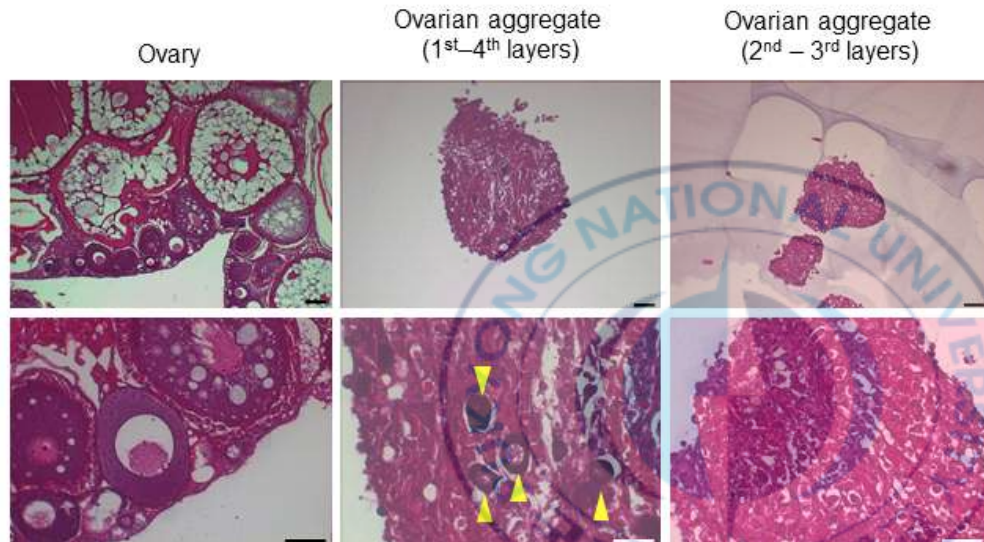


Figure 13. Comparison for the morphologies of ovarian aggregates depending on ovarian cell population. The two different *O. dancena* ovarian cell populations were isolated by PDGC, and 1.25×10^6 cells were induced aggregates in ULA for 7 days. (A) The schematic diagram of experiment process. (B) Representative pictures of two different morphologies of ovarian aggregates. Scale bar = 100 μ m. (C) The results about frequencies of two different morphology according to ovarian cell population.

A



B

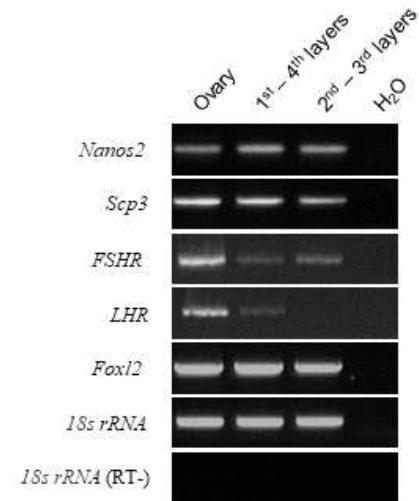


Figure 14. Characterization of ovarian aggregates depending on ovarian cell population separated by PDGC. At day 7, two different ovarian aggregates examined by hematoxylin and eosin staining and RT-PCR. (A) Pictures of histological assay. Among two different ovarian aggregates, pre-vitellogenic oocytes (yellow arrow heads) were only observed in ovarian aggregates which were composed ovarian cells separated from 1st to 4th layers. Scale bar = 100 μ m. (B) Validation of mRNA expression from each ovarian aggregate. The expression of germ cell specific (*nanos2*, *scp3*) and somatic cell specific (*fshr*, *lhr*, *foxl2*) markers was analyzed by RT-PCR assay.

expression analysis yielded a notable result: while expression of *nanos2*, a marker for oogonia, remained unchanged, the expression of *scp3*, which is specific to meiotic germ cells, was significantly reduced in the absence of FS, bFGF, and EE (Figure 17A and Figure 17B).

These results demonstrated that although the removal of FS, bFGF, and EE does not affect aggregate morphology, viability, or size, these components may play a role in promoting meiotic progression within ovarian germ cells.

3. Effects of bFGF and GDNF on *nanos2* and *scp3* expression

The above findings on *scp3* expression suggest that the three components including FS, bFGF, and EE, either individually or in combination, play a pivotal role in promoting germ cell differentiation under ovarian aggregate culture conditions. Among these, bFGF was selected for further investigation due to its well-documented involvement in germ cell development, including the induction of spermatogonial differentiation (Masaki et al., 2018) and stimulation of *scp3* expression (Aflatoonian et al., 2009). To further clarify the role of bFGF, I also evaluated the influence of GDNF, a factor known to function differently from bFGF in germ cell differentiation (Masaki et al., 2018).

Ovarian cells were cultured for 7 days in media lacking FS, bFGF, and EE, with the addition of bFGF, GDNF, or both. Following culture, expression levels of *nanos2* and *scp3* were assessed via qRT-PCR. As shown in Figure 18, both genes exhibited significantly increased expression after 7 days of culture even in the absence of both bFGF and GDNF, with 1.97 ± 0.24 fold and 1.45 ± 0.2 fold increases for *nanos2* (Figure 18A) and *scp3* (Figure 18B), respectively, compared to pre-culture levels.

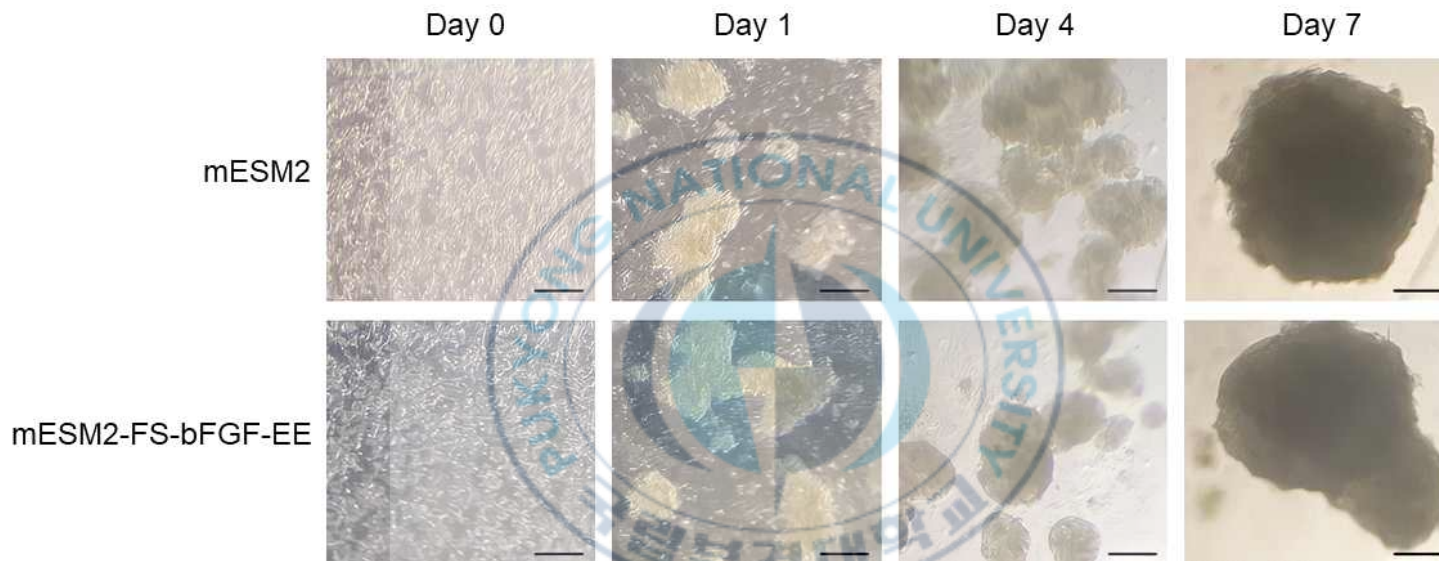


Figure 15. Evaluation of the effects of FS, bFGF and EE on the morphology of ovarian aggregates. Ovarian aggregates were induced in ULA containing mESM2 or mESM2 without FS, bFGF and EE for 7 days. Representative images were taken at day 0, day 1, day 4, and day 7. Over time, ovarian cells were induced to aggregates as a single mass. However, significant difference was not observed in morphologies between two groups. Scale bar = 250 μ m.

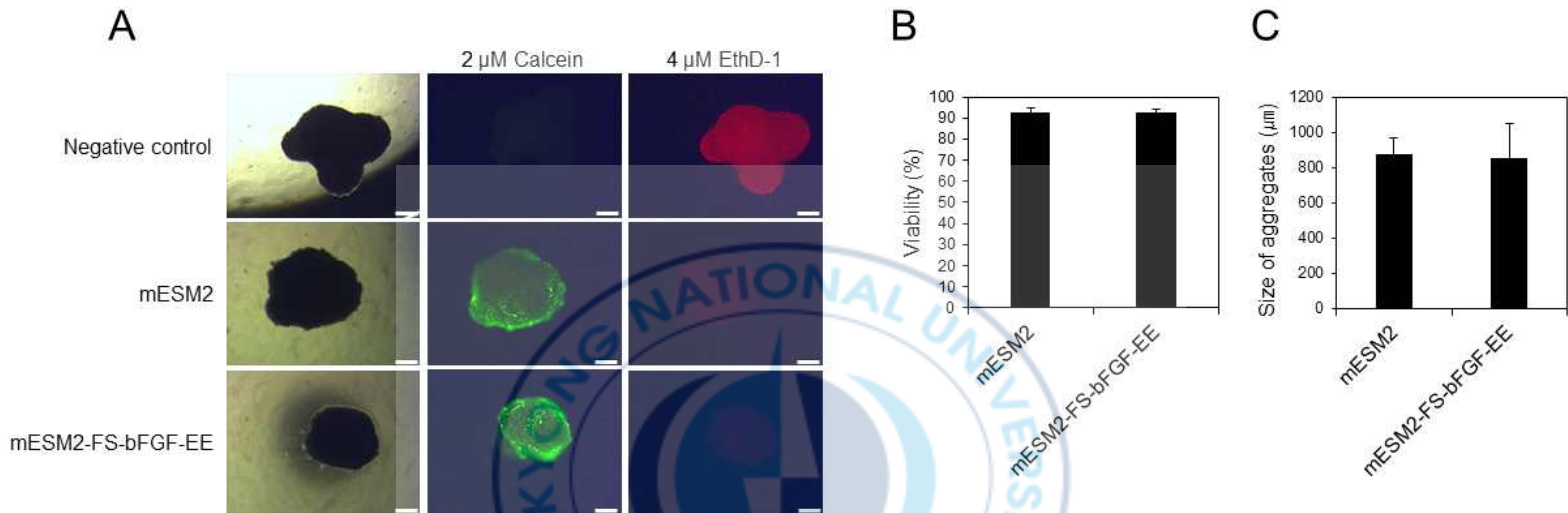


Figure 16. Evaluation of the effects of FS, bFGF and EE on the viability and the size of ovarian aggregates. Ovarian aggregates were induced in ULA containing mESM2 or mESM2 without FS, bFGF and EE for 7 days. Subsequently, their viabilities and sizes were compared. (A) Pictures taken after live/dead cells staining. Live cells were stained by 2 μ M calcein and dead cells were stained by 4 μ M EthD-1. Negative control were immersed in 70% ethanol for 1 hour before live/dead cell staining. Scale bar = 200 μ m. (B) Comparison of the viabilities of cells composing ovarian aggregates cultured in each medium. The viabilities were quantified by trypan blue staining. (C) Comparison of the size of ovarian aggregates. Significant differences were not observed on the viability and the size between two groups. All values are expressed as mean \pm standard deviation of three independent experiments at least.

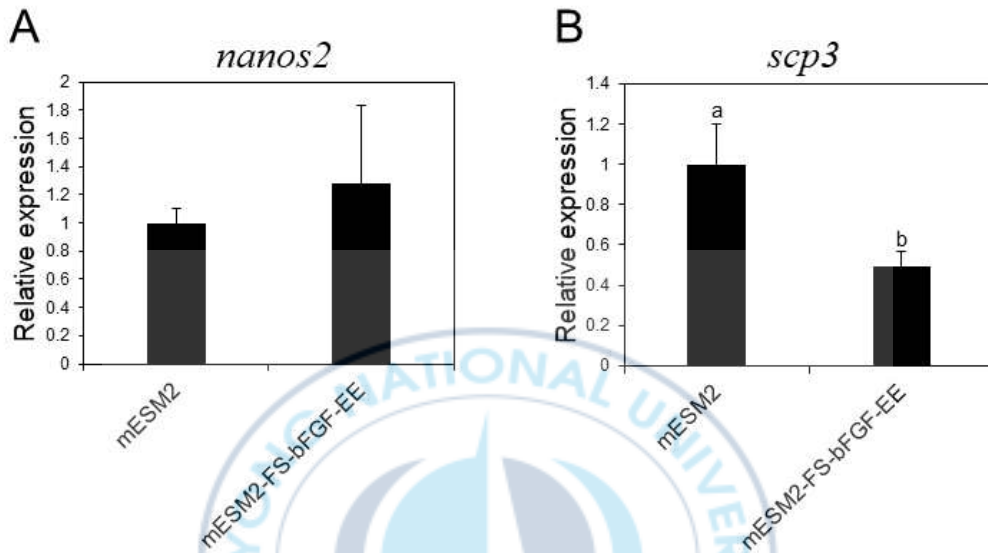


Figure 17. Evaluation of the effects of FS, bFGF and EE on relative mRNA expression levels from ovarian aggregates. Ovarian aggregates cultured for 7 days were analyzed by qRT-PCR analysis to compare genes expression levels of specific genes. (A) Relative mRNA expression of *nanos2* (oogonial stem cell marker). (B) Relative mRNA expression of *scp3* (meiosis marker). Significant difference was not observed in *nanos2* but in *scp3*. All values are expressed as mean \pm standard deviation of three independent experiments at least. ^{ab}Different letters indicate significant differences ($p < 0.05$).

When bFGF alone was supplemented, a pronounced enhancement in the expression of both genes was observed, showing 5.19 ± 1.11 fold increase for *nanos2* (Figure 18A) and 5.29 ± 0.76 fold for *scp3* (Figure 18B). In contrast, treatment with GDNF alone led to a similar increase in *nanos2* expression as seen in the bFGF group but resulted in significantly lower *scp3* expression. Co-treatment with both bFGF and GDNF maintained elevated *nanos2* expression at a level comparable to single treatments, while *scp3* expression was greater than that observed in the GDNF-only group but remained lower than in the bFGF-only group.

These observations collectively highlight the critical role of bFGF in regulating *scp3* expression during ovarian cell aggregate culture, underscoring its importance in promoting meiotic progression of germ cells under these conditions.

3. Evaluation of germ cell maintenance and E₂ synthesis of ovarian cell aggregates

To determine whether ovarian cell aggregates could maintain ovarian functions following culture, I investigated the effects of human follicle-stimulating hormone (hFSH) on germ cell maintenance and estradiol (E₂) synthesis. Ovarian cell aggregates derived from top to 50% Percoll layers were cultured in mESM2 media with or without hFSH supplementation, and subsequent analyses were performed, including histological evaluation, *cyp19a1* expression assessment, and E₂ measurement.

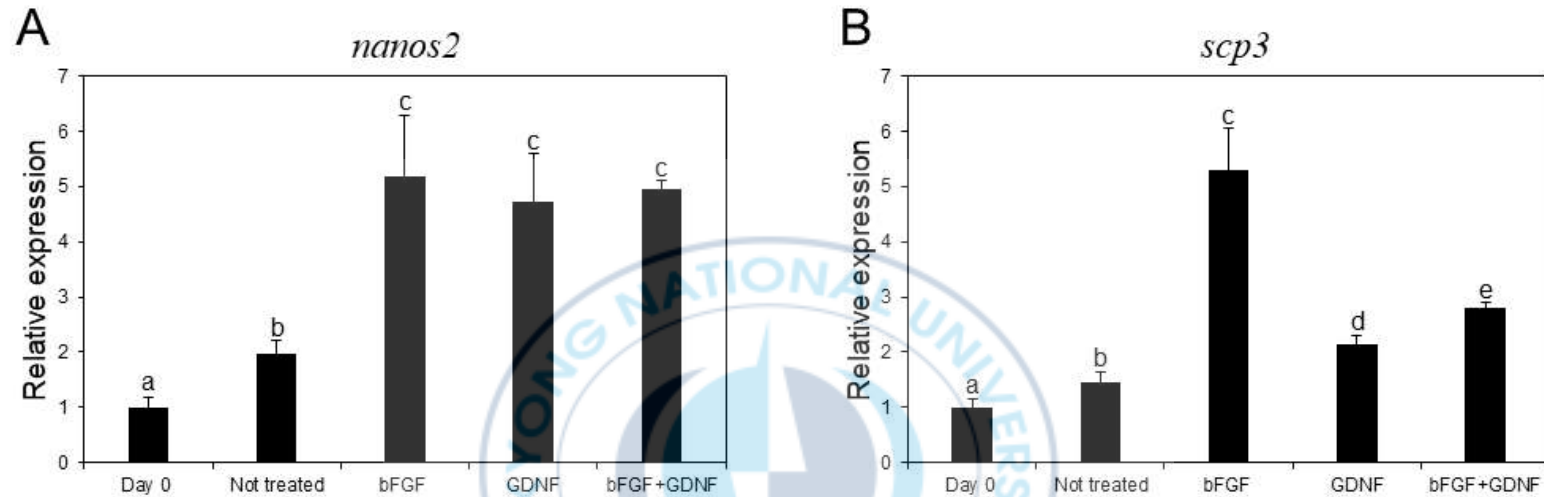


Figure 18. Evaluation of the effects of bFGF and Glial cell line-derived neurotrophic factor (GDNF) on relative mRNA expression levels from ovarian aggregates. bFGF and GDNF were supplemented alone or together in mESM2 without FF, bFGF, and EE. Ovarian aggregates were cultured with each culture media for 7 days and were analyzed by qRT-PCR assay. (A) Relative mRNA expression of *nanos2*. (B) Relative mRNA expression of *scp3*. Two factors increased *nanos2* mRNA expression. In *scp3*, when only bFGF was added, the highest expression level was observed. All values are expressed as mean \pm standard deviation of three independent experiments at least. ^{abcde}Different letters indicate significant differences ($p < 0.05$).

After 7 days of culture, histological examination revealed the presence of a small number of pre-vitellogenic oocytes within the aggregates regardless of hFSH treatment (50 ng/mL), suggesting that the cultured ovarian aggregates inherently maintained germ cell populations without the need for specific hormonal stimulation (Figure 19A).

When examining the effect of hFSH concentration on *cyp19a1* expression, no statistically significant difference was observed between treated and untreated groups (Figure 19B, $p = 0.2794$). However, given that the 50 ng/mL hFSH treatment group exhibited a 1.86 ± 0.42 fold increase in *cyp19a1* expression compared to the control, the impact of hFSH on E_2 production was analyzed.

Measurement of E_2 concentrations in the culture media from days 7 to 22 showed that although E_2 levels were lower after day 7, they were maintained throughout the later culture period. No significant effect of hFSH treatment on E_2 levels was detected at any time point (Figure 19C; p -values were 0.1993, 0.0937, 0.0620, 0.0999, 0.6828, and 0.6774 for days 7, 10, 13, 16, 19, and 22, respectively).

Taken together, these results suggest that although the ovarian cell aggregates did not exhibit a marked response to hFSH, they retained a minimal but sustained ability for E_2 synthesis during the culture period.

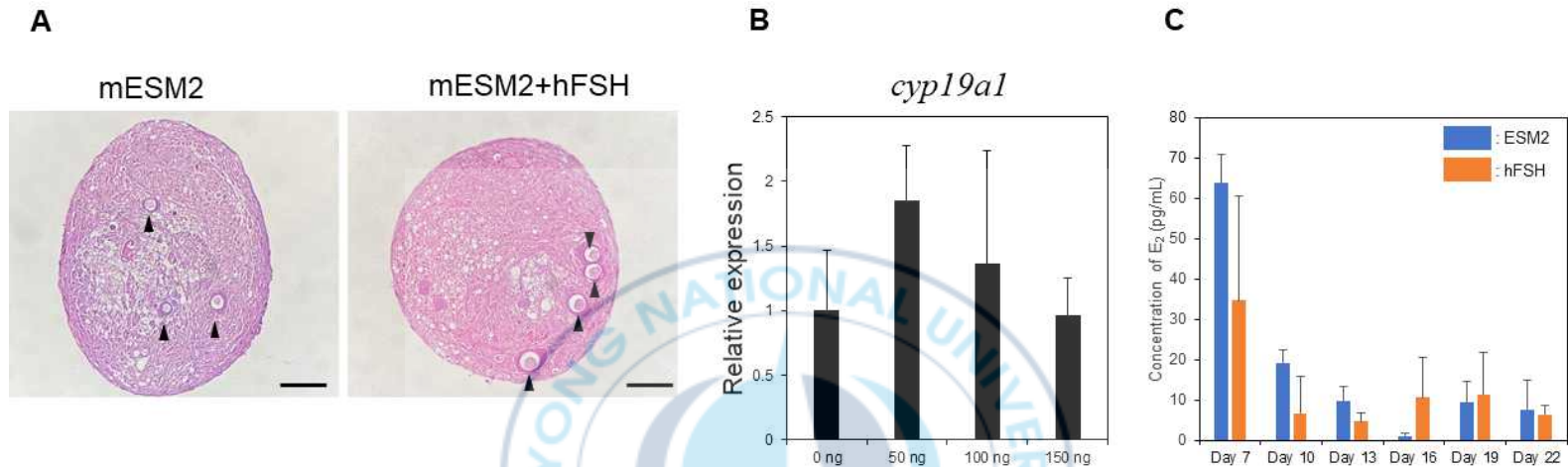


Figure 19. Evaluation of the effects of hFSH on germ cell maintenance and 17β-estradiol secretion from ovarian aggregates. Ovarian aggregates were cultured in mESM2 with or without 50 ng/mL hFSH for 22 days. (A) Pictures of histological analysis. A small number of pre-vitellogenicoocytes (arrow heads) were observed in all groups, regardless of hFSH treatment. Scale bar = 200 μm. (B) Relative mRNA expression levels of *cyp19a1* in ovarian aggregates treated with different concentrations of hFSH. No significant differences were detected among the groups. (C) Concentration of 17β-estradiol secreted by ovarian aggregates cultured with or without hFSH. The 17β-estradiol quantities in the medium were harvested, and measured at day 7, day 10, day 13, day 16, day 19, and day 22. No significant differences in 17β-estradiol quantities were observed between groups. Additionally, from day 10 to day 22, estradiol levels remained lower compared to those on day 7. All values are expressed as mean ± standard deviation of three independent experiments at least.

IV. Discussion

Establishing an *in vitro* model for studying germline stem cells (GSCs) is a crucial objective in reproductive biology (Ge et al., 2015). In fish species, *in vitro* GSC culture has been reported in various species including zebrafish, medaka, rainbow trout, and dogfish (Xie et al., 2020). However, these studies have predominantly focused on male GSCs, with relatively fewer efforts directed toward female GSCs. For example, Wong et al. (2013) succeeded in culturing female GSCs from zebrafish for over six weeks, and demonstrated the production of offspring through germ cell transplantation. Similarly, Jeong et al. showed that short-term (10-day) cultured female GSCs from medaka retained colonization ability upon transplantation, suggesting their potential as functional germ cells.

These findings highlight the current lack of a robust *in vitro* system tailored for female GSC research and underscore the necessity for its development. Notably, all existing female GSC culture models in fish have relied on 2D culture systems that required germ cell transplantation for further differentiation into functional gametes (Wong et al., 2013; Iwasaki-Takahashi et al., 2020). This limitation suggests that conventional 2D culture platforms fail to mimic the complex cellular interactions present *in vivo*, which are essential for GSC differentiation. Accordingly, adopting a 3D culture approach may offer a more physiologically relevant environment to support female GSC development.

Indeed, several studies on male fish GSCs have demonstrated successful *in vitro* spermatogenesis solely through 3D aggregation culture, bypassing

the need for transplantation techniques (Higaki et al., 2017; Zhang et al., 2022; Choi et al., 2023). Such findings support the idea that 3D systems more effectively recapitulate the native microenvironment, and that ovarian organoids derived from 3D cultures could serve as valuable models for studying female GSCs.

In the present study, I observed the formation of two distinct aggregate morphologies, large single aggregates and smaller multiple aggregates, depending on the cell population used. When cells isolated from the 1st to 4th layer of Percoll gradient were cultured, 100% of samples formed large, singular aggregates. In contrast, cells from the 2nd to 3rd layer predominantly (90%) generated smaller, multiple aggregates. Morphologically, the large single aggregates more closely resembled previously reported mouse ovarian organoids (Li et al., 2021), suggesting that cells from the upper 50% layer are more suitable for aggregate formation in *Oryzias dancena*.

Additionally, only the aggregates derived from the upper 50% layer exhibited pre-vitellogenic oocytes, implying greater functional potential. This observation is consistent with our previous findings in medaka, where female GSCs were enriched under similar conditions (Ryu and Gong, 2020). I also noted higher expression of *lhr*, a somatic cell marker essential for oocyte maturation (Ogiwara et al., 2013; Kitano et al., 2022), exclusively in these aggregates. The presence of this marker suggests enhanced somatic-germ cell communication, further supporting the functional superiority of aggregates formed from 1st to 4th layer. These collective results indicate that the 1st to 4th layer fraction following Percoll gradient centrifugation is optimal for forming functional ovarian cell aggregates in *O. dancena*.

Basic fibroblast growth factor (bFGF) and glial cell-derived neurotrophic factor (GDNF) are widely recognized as crucial regulators of GSC proliferation in mammals, including mouse (Kanatsu-Shinohara et al., 2003), hamster (Kanatsu-Shinohara et al., 2008), rat (Wu et al., 2009), bovine (Suyatno et al., 2018), and human (Sadri-Ardekani et al., 2009). These growth factors have also been employed in teleost GSC cultures, such as in swamp eel (Sun et al., 2022), rohu (Panda et al., 2011), zebrafish (Kawasaki et al., 2012), and dogfish (Gautier et al., 2014). In this study, I found that treatment with bFGF alone upregulated *scp3* expression in ovarian cell aggregates, suggesting promotion of meiotic differentiation. However, when GDNF was administered in combination with bFGF, *scp3* expression was downregulated, indicating an inhibitory interaction.

While GDNF is generally associated with promoting GSC proliferation while maintaining undifferentiated states (Meng et al., 2000; Masaki et al., 2018), bFGF has been shown to enhance spermatogonial differentiation by modifying the germline niche in mouse (Masaki et al., 2018), and also to induce *scp3* expression in human embryonic stem cells (Aflatoonian et al., 2009). Taken together, our findings imply that bFGF may exert a similar role in *O. dancena* ovarian cultures, fostering differentiation. Therefore, inclusion of bFGF may be critical for advancing the differentiation of ovarian cell aggregates in this species.

CHAPTER 5.

3D Co-Cultured testicular aggregates by
Inclusion of a Testis-Derived Somatic Cell
Line in Olive Flounder (*Paralichthys olivaceus*)

I . Introduction

Germline stem cells (GSCs) transmit their genetic information to the next generation through complex interactions with somatic cells (Lubzens et al., 2010; Choi and Gong, 2023). Utilizing this unique capability, surrogate broodstock technology, which involves producing donor-derived gametes in recipient organisms by transplanting donor GSCs has emerged as a promising tool in aquaculture for the production of superior offspring, preservation of valuable genetic resources, and enhancement of aquaculture productivity (Yoshizaki and Yazawa, 2019). However, the limited number of GSCs available from donor individuals presents a significant challenge to the practical application of this technology (Iwasaki-Takahashi et al., 2020). Thus, establishing efficient *in vitro* culture systems for GSCs is essential.

Several studies have reported the *in vitro* culture of GSCs from various teleost species. The first male GSC line, SG3, was established from medaka (*Oryzias latipes*) and maintained for over two years without feeder cells while retaining the expression of germ cell-specific markers (Hong et al., 2004). Other studies have reported similar achievements in species such as swamp eel (*Monopterus albus*; Sun et al., 2022), Chinese hook snout carp (*Opsariichthys bidens*; Chen et al., 2022), orange-spotted grouper (*Epinephelus coioides*; Zhong et al., 2022), and tiger puffer fish (*Takifugu rubripes*; Tan et al., 2023). Nevertheless, the successful production of fertile gametes directly from GSCs cultured without somatic support remains largely unattained. In contrast, studies using co-cultures of GSCs with testicular somatic cells have demonstrated that maintaining close germ cell

- somatic cell interactions is critical for supporting GSC survival, proliferation, and differentiation, as seen in zebrafish (*Danio rerio*; Kawasaki et al., 2012; Wong et al., 2013) and rainbow trout (*Oncorhynchus mykiss*; Iwasaki-Takahashi et al., 2020).

The olive flounder (*Paralichthys olivaceus*) is a commercially important aquaculture species in East Asia, especially in Korea, Japan, and China (Cho et al., 2012). Various efforts, including selective breeding (Park et al., 2021), triploid induction (Hwa and Sum, 1994; Ko et al., 2016), and genome editing using CRISPR/Cas9 (Kim et al., 2019), have been made to improve its aquaculture traits. However, *in vitro* culture systems for *P. olivaceus* GSCs have not yet been developed.

In a previous study, olive flounder testicular somatic cell (OFT) line was used to serve as a supporting cell source for male *P. olivaceus* GSCs culture (Jo et al., 2025). However, conventional two-dimensional (2D) culture systems often fail to culture spermatogonial stem cell over 7 days. To better mimic the *in vivo* niche and improve GSC support, 3D co-culture models have been proposed as a promising strategy.

Therefore, in this study, I aimed to induce 3D testicular aggregates by co-culturing primary dispersed testicular cells from *P. olivaceus* with the established OFT cell line. Furthermore, I evaluated the effects of sex hormones and growth factors on the morphology, viability, and expression of germ cell markers within the aggregates. This approach is expected to provide fundamental insights for the development of functional *in vitro* GSC culture systems in *P. olivaceus* and contribute to advancing reproductive biotechnology in aquaculture species.

II. Materials and methods

1. Primary culture and subculture

To establish olive flounder testicular cell (OFT) line, surgically extracted testis dispersed by 0.25% (v/v) trypsin-EDTA. 4.5×10^5 cells of total digested cells were seeded into 0.2% gelatin (Sigma-Aldrich) coated 6 well plates. Primary testicular cells were cultured in an incubator adjusted to 20°C. The cell culture medium, mESM2 without EE, was changed every 3days. When the attachment cells reached over 90 % confluence, they were subcultured at 1:2 ratio.

2. Characterization of olive flounder testicular cell (OFT) line

2.1. Reverse transcription polymerase chain reaction (RT-PCR)

To identify the cell types present in the OFT cell line, the expression profiles of genes specific to germ cells (*vasa*, *nanos2*, *scp3*) and gonadal somatic cells (*wt1*, *gsdf*, *fgl2*) were evaluated. 100 ng of total RNA was isolated from OFT cells at passage 30, and subjected to cDNA synthesis using the SuperScript™ IV VILO™ Master Mix with ezDNase (Invitrogen, Vilnius, Lithuania), in accordance with the supplier's instructions. PCR amplification was carried out using AccuPower PCR Master Mix (Bioneer, Daejeon, Republic of Korea). The specific primer sequences employed are

listed in Table 5. The RT-PCR procedure involved an initial denaturation at 95°C for 5 minutes, followed by 35 amplification cycles of 95°C for 30 seconds, 60°C for 30 seconds, and 72°C for 30 seconds, with a final extension step at 72°C for 5 minutes.

2.2. Cell origin analysis

Mitochondrial DNA was isolated from OFT cell line, as well as from fin tissue of *P. olivaceus*, using the QIAamp Micro Kit (Qiagen) following the manufacturer's protocol. Conventional PCR was then performed using a 2× premix (SolGent, Daejeon, Republic of Korea) with primers targeting cytochrome c oxidase subunit 1 (*COI*) and *16S rRNA* (primer sequences are provided in Table 1). The PCR protocol included an initial denaturation at 95°C for 10 minutes, followed by 35 cycles of 95°C for 50 seconds, 50°C for 50 seconds, and 72°C for 50 seconds, concluding with a final extension at 72°C for 7 minutes. PCR products were separated by electrophoresis on 1.5% (w/v) agarose gels (Biosesang, Yongin, Republic of Korea) and visualized using a gel documentation system (Uvitec, Cambridge, UK). Subsequently, the amplified products were sequenced using an ABI 3730XL DNA Analyzer (Applied Biosystems, Foster City, CA, USA) and the resulting sequences were compared with those in GenBank using the NCBI BLAST tool.

2.3. Karyotype analysis

To analyze the chromosomal composition of the established cell lines,

OFT at passage 30 were subjected to karyotype analysis. Cells were seeded into 25 cm² culture flasks and incubated for 24 hours at 20°C. Following incubation, 3 µg/mL colchicine (Sigma-Aldrich) was added to the cultures for 2 hours and 30 minutes at 20°C to arrest cells in metaphase. After removing the medium, cells were washed with 1 mL DPBS and detached using 2 mL of 0.25% trypsin-EDTA. Trypsinization was stopped by adding 2 mL of mESM2 without EE, and the cells were collected by centrifugation at 400 × g for 5 minutes at room temperature. The pellet was gently resuspended in 3 mL of 0.075 M KCl (Shinyo Pure Chemical, Osaka, Japan) and incubated for 20 minutes at room temperature to induce hypotonic swelling. Cells were again centrifuged under the same conditions and fixed in 3 mL of Carnoy's solution (methanol:acetic acid, 3:1; Daejung, Seoul, Republic of Korea) at room temperature for 1 hour, with the fixative being refreshed every 30 minutes. After a final centrifugation, the cells were resuspended in 200 µL of Carnoy's solution. Drops of 20 µL cell suspension were placed onto microscope slides, which were subsequently immersed in 100% (v/v) acetic acid (Daejung) for one day, air-dried, and stained with 8% (v/v) Giemsa solution (Gibco) prepared in Gurr's buffer (Gibco) for 8 minutes. The stained slides were rinsed with distilled water and dried at room temperature. Chromosomal spreads were examined using a microscope (Zeiss, Jena, Germany; Merck, Darmstadt, Germany) at 1000× magnification. For each cell line, karyotypic normality was determined by analyzing 63 metaphase spreads, and the normality percentage was calculated as: (number of normal metaphase spreads/total number of metaphase spreads analyzed) × 100 (Choi et al., 2020).

2.4. Sex analysis

Genomic DNA was extracted from OFT and OFO cells using the QIAamp Micro Kit (Qiagen, Hilden, Germany) following the manufacturer's protocol. SNP genotyping analysis was performed using a QuantStudio 5 Real-Time PCR System (Applied Biosystems, Foster City, CA, USA) under the following cycling conditions: initial denaturation at 95°C for 5 minutes, followed by 35 cycles of 95°C for 15 seconds and 60°C for 1 minute. The reactions were carried out in a total volume of 20 μ L using 2 \times Real-Time PCR Master Mix (Attoplex, Gyeonggi-do, Republic of Korea), with each primer added at a final concentration of 0.5 μ M and each probe primer at 0.25 μ M. The specific SNP primer sets used in this study are listed in Table 6. For positive controls, genomic DNA was extracted from the fins of male and female *P. olivaceus* individuals maintained by the National Institute of Fisheries Science (NIFS).

2.5. Transfection of foreign gene

Aliquots containing 1×10^6 OFT cells were harvested by centrifugation at $400 \times g$ for 5 minutes. The cell pellets were then resuspended in 100 μ L of Opti-MEM (Gibco) supplemented with 10 μ g of the green fluorescent protein (GFP) expression vector pEGFP-C1. The cell suspensions were transferred into 2 mm gap electroporation cuvettes (NEPA Electroporation Cuvettes; Nepa Gene Co. Ltd., Chiba, Japan) and subjected to electroporation at 160 V using a NEPA21 Super Electroporator (NEPA GENE Co., Ltd., Chiba, Japan). Immediately following electroporation, 1 mL of mESM2

medium was added to stabilize the cells, and they were subsequently transferred into 6-well plates (Corning) and cultured at 20°C. After 48 hours, GFP expression was assessed under a fluorescence microscope (Axio Vert A1; Zeiss, Jena, Germany). Transfection efficiency was determined by ImageJ software (version 1.51k; National Institutes of Health, Bethesda, MD, USA).

3. Effects of sex hormones and growth factors on culture of 3D co-cultured aggregates

3.1. Induction of 3D co-cultured testicular aggregates

To evaluate the effects of OFT on the formation of aggregates, 5×10^5 cells of isolated testicular cells and 5×10^5 OFT cells were seeded into ULA plates. They were cultured for 14 days with culture medium exchanged every 2 days. For control, 1×10^6 cells of isolated testicular cells were seeded into ULA plates. Basically, mESM2 was used for culturing aggregates, but mESM2 supplemented with 10 ng/ μ L of 11-ketotestosterone (11-KT), 10 ng/ μ L of 17 β -estradiol (E₂), 10 ng/ μ L of 17 α , 20 β -dihydroxy-4-pregnen-3-one (DHP), 10 ng/ μ L of human chorionic gonadotropin (hCG), 10 ng/ μ L of epidermal growth factor (EGF), and 10 ng/ μ L of insulin-like growth factor 1 (IGF-1) also used to evaluate the effect of those supplements on the morphology, viability, and levels of germ cell specific genes.

3.2. Effects of sex hormones and growth factors on morphology

To evaluate the effects of sex hormones and growth factors on the morphology of aggregates, cultured 3D co-cultured testicular aggregates, which cultured with or without supplements, were taken pictured at day 1, day 7, and day 14 using a microscope.

3.2. Effects of sex hormones and growth factors on viability

To determine the cell viability within aggregates, collected aggregates were dispersed by 0.25% (v/v) trypsin-EDTA. The cell viability was measured by trypan blue staining. Additionally, the spatial distribution of live and dead cells within aggregates was investigated using the Live/Dead Viability/Cytotoxicity Kit (Molecular Probes). Aggregates were stained according to the manufacturer's protocol.

3.3. Quantitative reverse transcription polymerase chain reaction (qRT-PCR)

The synthesized cDNA from each culture condition of aggregates, was used for qRT-PCR analysis using the LightCycler® 480 SYBR Green Master Mix (Roche Diagnostics, Mannheim, Germany). The reaction conditions were as follows: initial denaturation at 94°C for 3 minutes, followed by 40 amplification cycles (denaturation at 94°C for 30 seconds, annealing at 60°C for 30 seconds, and elongation at 72°C for 30 seconds). Primer sequences

for each target gene are listed in Table 5. Relative gene expression was determined using the $2^{-\Delta\Delta Ct}$ method. The ΔCt was calculated by subtracting the Ct value of the internal reference gene (*18s rRNA*) from the Ct of the target gene, and the $\Delta\Delta Ct$ was obtained by comparing the ΔCt values between experimental and control samples (Livak and Schmittgen, 2001).



Table 5. Primer sequences information used in olive flounder (*Paralichthys olivaceus*)

Genes		Primer sequence (5'>3')	Size (bp)	Purpose	Accession No.
<i>vasa</i>	Forward	CAGGACAGCACAGCGAAGAG	141	RT-PCR & qRT-PCR	JQ070418.1
	Reverse	GCAACAAGCTAAACAGCAAATAAGAG			
<i>nanos2</i>	Forward	CGGACCACTGTCGCTTCTG	159	RT-PCR & qRT-PCR	XM_020087405.1
	Reverse	ACCGGCGTGTGTGTGCTT			
<i>scp3</i>	Forward	TGGCTACCGTCCGCAAGT	154	RT-PCR & qRT-PCR	XM_020090502.1
	Reverse	CGATATGAACACGAACCAAATTAAGT			
<i>wt1</i>	Forward	TGTTTGGTTGCCACAATCCTT	101	RT-PCR	XM_020098636.1
	Reverse	CAGCTGAGATGCCATTTGGTATAC			
<i>gsdf</i>	Forward	CCTGAGATGAACACTGTGCAATG	151	RT-PCR	KY123266.1
	Reverse	GCACGGAGGAAATGATGACTGT			
<i>fgl2</i>	Forward	AAGACAAAGAAGAAGATGTGAAGACAGA	200	RT-PCR	XM_020105694.1
	Reverse	AAGGCACCTGGCTGCAGTT			
<i>18s rRNA</i>	Forward	ATGGCCGTTCTTAGTTGGTG	218	RT-PCR & qRT-PCR	EF126037.1
	Reverse	CACACGCTGATCCAGTCAGT			
<i>COI</i>	Forward	TGTA AAAACGACGGCCAGTCAACCAACCACAAAGACATTGGCAC	650	Species identification	NC_082846.1
	Reverse	CAGGAAACAGCTATGACACTTCAGGGTGACCGAAGAATCAGAA			
<i>16s rRNA</i>	Forward	CCGGTCTGAACTCAGATCACGT	542	Species identification	NC_082846.1
	Reverse	CGCCTGTTTATCAAAAACAT			

Table 6. Primer sequences information used for SNP analysis to identify of genetic sex

Primer name	Primer Sequence ('5-3')	Size (bp)
5227A	TCAAATGGCATAGATGGACA	116
5227T	TCAAATGGCATAGATGGACT	
5227	TCATGCGGTAATTGCTTTGTA	
5227-FAM	FAM-ATGCGGACGAGTAGTTCATTCGAA-EBQ	
8483C	AGTCCACATTTACGAGAGTTC	170
8483T	AGTCCACATTTACGAGAGTTT	
8483	GATGAACGAGAAATTAGATTTCCCCG	
8483-JOE	JOE-GCTTACGGAGGGCAGCTAGCAACGA-EBQ	
5512C	ATGGCCTGGATTGCATCAAC	154
5512T	ATGGCCTGGATTGCATCAAT	
5512	CTTAGCATAAGGAACCCACGTC	
5512-CY5	CY5-TTCCGACGCGTTGTACACGGGCAA-EBQ	

III. Results

1. Primary cell culture and gene expression Analysis

The olive flounder testicular cell (OFT) line was derived from the testes of *P. olivaceus* through primary culture followed by subculturing. At passage 5, OFT were predominantly composed of fibroblast-like and epithelial-like cells (Figure 20A). In contrast, OFT were predominantly composed of cobblestone-like and fibroblast-like cells at passage 20 (Figure 20A). At passage 30, RT-PCR analysis was performed to characterize the established cell line. Specifically, the expression levels of germ cell markers (*vasa*, *nanos2*, and *scp3*) and testicular somatic cell markers (*wt1*, *gsdf*, and *fgl2*) were evaluated. Strong expression of *wt1* and *fgl2* was detected in OFT cells (Figure 20B). Although testicular tissues exhibited expression of *vasa*, *nanos2*, *scp3*, and *gsdf*, these germ cell markers were not detected in the OFT.

2. Species identification

To confirm the species origin of OFT, PCR amplification targeting the cytochrome c oxidase subunit 1 (*COI*) gene and the *16s rRNA* gene was performed. As shown in Figure 21, PCR products for *COI* (650 bp) and *16s rRNA* (542 bp) were successfully amplified in both OFT, matching the sizes observed in the positive controls. Furthermore, sequencing analysis revealed that the amplified

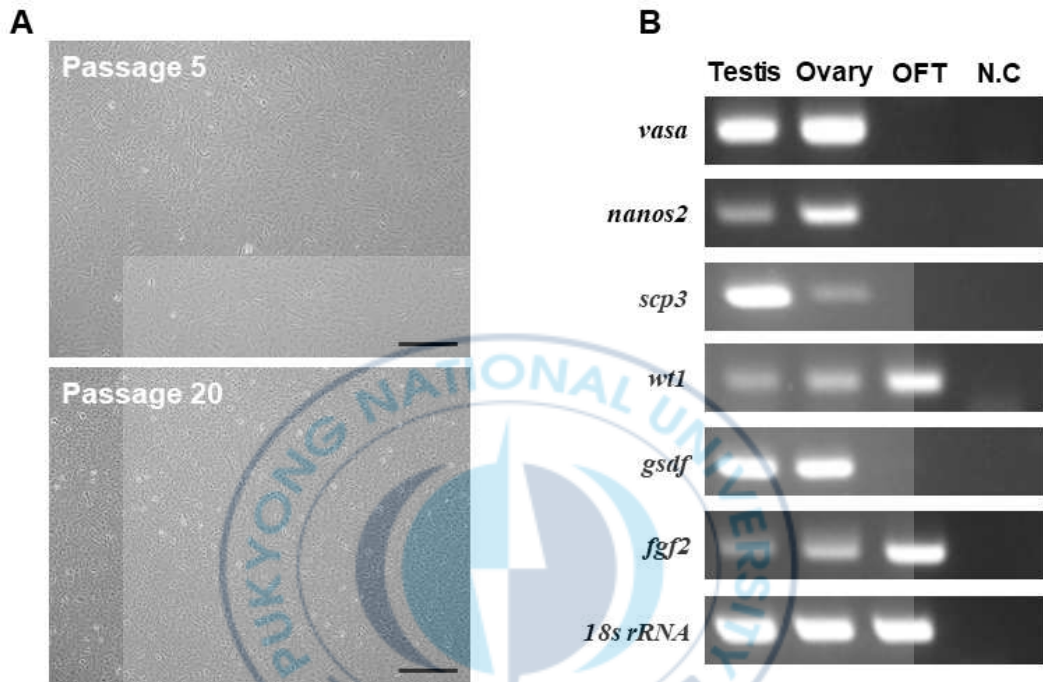


Figure 20. Establishment and characterization of testicular cell line from olive flounder (*Paralichthysolivaceus*) testis (OFT). Primary testicular cells were seeded in 6 well gelatin coated plates and were sub-cultured over 30 times stably.(A) The representative images of OFT at passage 5 and passage 20. In passage 5, epithelial-like and fibroblast-like cells were dominant. In passage 20, cobblestone-like and fibroblast-like cells were dominant. Scale bar = 400 μ m. (B) The RT-PCR results from OFT at passage 30. In OFT, the expressions of germ cell specific markers including *vasa*, *nanos2*, *scp3* were not detected, but the expressions of somatic cell markers including *wt1* and *fgf2* were observed.

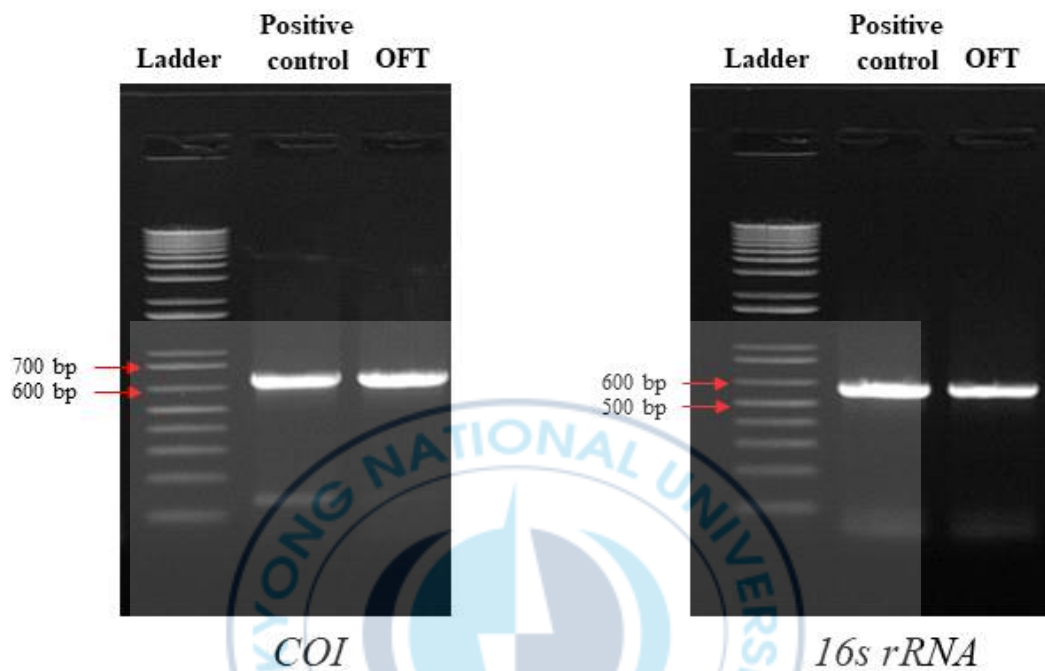


Figure 21. Validation of species from OFT. Amplification of *COI* and *16s rRNA* regions from OFT. The amplified *COI* region was detected at 650 bp and the amplified *16s rRNA* was 542 bp. For the positive controls, genomic DNA isolated from *P. olivaceus* fin tissue was used. Amplified PCR products were observed at the same size as the positive control. Arrows indicate ladder sizes.

16s rRNA

Paralichthys olivaceus x Verasper variegatus mitochondrion, complete genome
 Sequence ID: NC_082846.1 Length: 16946 Number of Matches: 1
 Range 1: 2062 to 2603

Score	Expect	Identities	Gaps	Strand	Frame
1002 bits(542)	0.0()	542/542(100%)	0/542(0%)	Plus/Minus	
Query 1	CGAACCCTTAATAGCGGCTGCACCAATTAGGATGTCCTGATCCAACATCGAGGTCGTAAAC	60			
Sbjct 2603	CGAACCCTTAATAGCGGCTGCACCAATTAGGATGTCCTGATCCAACATCGAGGTCGTAAAC	2544			
Query 61	CCCCTTGTCGATATGGGCTCTAAAAGGGGATTCGCGCTGTTATCCCTAGGGTAACTTGGTT	120			
Sbjct 2548	CCCCTTGTCGATATGGGCTCTAAAAGGGGATTCGCGCTGTTATCCCTAGGGTAACTTGGTT	2484			
Query 121	CGTTGATCGGCGTTGCCGGATCAGTTTGGTCAGAAATTTCTGCTGATAGAGCTGTCGCTC	180			
Sbjct 2483	CGTTGATCGGCGTTGCCGGATCAGTTTGGTCAGAAATTTCTGCTGATAGAGCTGTCGCTC	2424			
Query 181	TAGCTTGTAGGAGGAGGAAATGTAGGGGTGACTCCCTTTCCACGTTGGGGTTTTGTGT	240			
Sbjct 2423	TAGCTTGTAGGAGGAGGAAATGTAGGGGTGACTCCCTTTCCACGTTGGGGTTTTGTGT	2364			
Query 241	TCCCCATGGTCGCCCCAACCGAAGACATCAAGGCTGGTTTCATTTAGTTCAGGGCCCTTA	300			
Sbjct 2363	TCCCCATGGTCGCCCCAACCGAAGACATCAAGGCTGGTTTCATTTAGTTCAGGGCCCTTA	2304			
Query 301	GCTGGGTGTATTTGACATGATCTGCCCTTGCCTCTAAAGCTCCATAGGGCTTCTCTGCT	360			
Sbjct 2308	GCTGGGTGTATTTGACATGATCTGCCCTTGCCTCTAAAGCTCCATAGGGCTTCTCTGCT	2244			
Query 361	TATGAGCTTATCCCCGCTTCTGCACGGGAGATCAATTTTCACTGCGGGAAAGAGAC	420			
Sbjct 2243	TATGAGCTTATCCCCGCTTCTGCACGGGAGATCAATTTTCACTGCGGGAAAGAGAC	2184			
Query 421	AGCTAAGCCCTCGTTATGCCATCATACGGGTCTTCAATTAAGACAAAGTGAATACGCT	480			
Sbjct 2183	AGCTAAGCCCTCGTTATGCCATCATACGGGTCTTCAATTAAGACAAAGTGAATACGCT	2124			
Query 481	ACCTTTGCACGGTCAAAATACCGCGCCGTTGAACATGATGTCACTGGGCGAGGCGGAC	540			
Sbjct 2123	ACCTTTGCACGGTCAAAATACCGCGCCGTTGAACATGATGTCACTGGGCGAGGCGGAC	2064			
Query 541	CT 542				
Sbjct 2063	CT 2062				

COI

Paralichthys olivaceus x Verasper variegatus mitochondrion, complete genome
 Sequence ID: NC_082846.1 Length: 16946 Number of Matches: 1
 Range 1: 5552 to 6201

Score	Expect	Identities	Gaps	Strand	Frame
1201 bits(650)	0.0()	650/650(100%)	0/650(0%)	Plus/Plus	
Query 1	TCTATCTCGTATTTGGTGCCTGAGCCGGAATAGTGGGACAGCCCTAAGCCTCCTCATTC	60			
Sbjct 5552	TCTATCTCGTATTTGGTGCCTGAGCCGGAATAGTGGGACAGCCCTAAGCCTCCTCATTC	5611			
Query 61	GGGCAGAACTCAGCCAACTGGTCTCTCCTAGGGGACGACCAAGATTTATAAGTAATCG	120			
Sbjct 5612	GGGCAGAACTCAGCCAACTGGTCTCTCCTAGGGGACGACCAAGATTTATAAGTAATCG	5671			
Query 121	TTAACCACACGCTTTGTAATAATCTTTTTCATAGTTATACCAATTATGATGGAGGCT	180			
Sbjct 5672	TTAACCACACGCTTTGTAATAATCTTTTTCATAGTTATACCAATTATGATGGAGGCT	5731			
Query 181	TTGGCAACTGACTTATCCCCCTGATAATCGTGCCCGACAGACATAGCATTCCCTGGAATAA	240			
Sbjct 5732	TTGGCAACTGACTTATCCCCCTGATAATCGTGCCCGACAGACATAGCATTCCCTGGAATAA	5791			
Query 241	ATAACATAAGCTTCTGACTTCTACCCCTTCATTCCTCTCTCCTGGCTTCTTCAGGTG	300			
Sbjct 5792	ATAACATAAGCTTCTGACTTCTACCCCTTCATTCCTCTCTCCTGGCTTCTTCAGGTG	5851			
Query 301	TGAAAGCTGGTGGCGGTACCGGGTGGACTGTCTACCTCCCTAGCTAGCAACCTGGCCC	360			
Sbjct 5852	TGAAAGCTGGTGGCGGTACCGGGTGGACTGTCTACCTCCCTAGCTAGCAACCTGGCCC	5911			
Query 361	ATGCTGGAGCCTCAGTAGACTTAACCATCTTTCACCTGACCTTGCAGGATTTTCATCAA	420			
Sbjct 5912	ATGCTGGAGCCTCAGTAGACTTAACCATCTTTCACCTGACCTTGCAGGATTTTCATCAA	5971			
Query 421	TTCTGGGAGCTATCAACTTCACTACCATTATAACATGAAACCCCAACTGTCACAA	480			
Sbjct 5972	TTCTGGGAGCTATCAACTTCACTACCATTATAACATGAAACCCCAACTGTCACAA	6031			
Query 481	TATACCAAATCCCGTGTGTCTGAGCCGCTTAATACGGCTGTCTGCTGCTCT	540			
Sbjct 6032	TATACCAAATCCCGTGTGTCTGAGCCGCTTAATACGGCTGTCTGCTGCTCT	6091			
Query 541	CGCTGCCAGTTTTAGCCGCGGTATTACAATACTGCTTACAGACCGAAACCTTAATACAA	600			
Sbjct 6092	CGCTGCCAGTTTTAGCCGCGGTATTACAATACTGCTTACAGACCGAAACCTTAATACAA	6151			
Query 601	CATCTTTGACCTTGCAGGAGGAGGGATCCAATCCTCTACCAACACCTG 650				
Sbjct 6152	CATCTTTGACCTTGCAGGAGGAGGGATCCAATCCTCTACCAACACCTG 6201				

Figure 22. Sequence alignment analysis of *COI* and *16s rRNA* from OFT. Amplified *COI* and *16s rRNA* were analyzed by automated DNA sequencing. Both regions were perfectly matched with *P. olivaceus* mitochondrial DNA.

COI and *16s rRNA* fragments exhibited 100% identity with *P. olivaceus* sequences registered in GenBank (Figure 22).

3. Karyotype analysis

Representative metaphase chromosome spreads from OFT and OFO cells are presented in Figure 23A, showing the typical diploid chromosome number ($2n = 48$). The 63 metaphase spread pictures were analyzed for number of OFT chromosome sets. The percentage of karyotypically normal cells was calculated to be 48% for OFT (Figure 23B).

4. Sex identification analysis

Given that *P. olivaceus* can undergo environmental sex reversal, it was necessary to verify the original sex of the OFT cell line. For this purpose, SNP markers (5227A/T, 8483C/T, and 5512C/T) developed by NIFS were utilized. All three markers were detected in genomic DNA from male *P. olivaceus* (Figure 24), and the same pattern was observed in the OFT cells, confirming their male origin. This result demonstrated that the original sex of OFT cell line is male.

5. Transfection and efficiency analysis

To introduce exogenous genes, electroporation was selected as the transfection method for this study. OFT cells were transfected with the pEGFP-C1

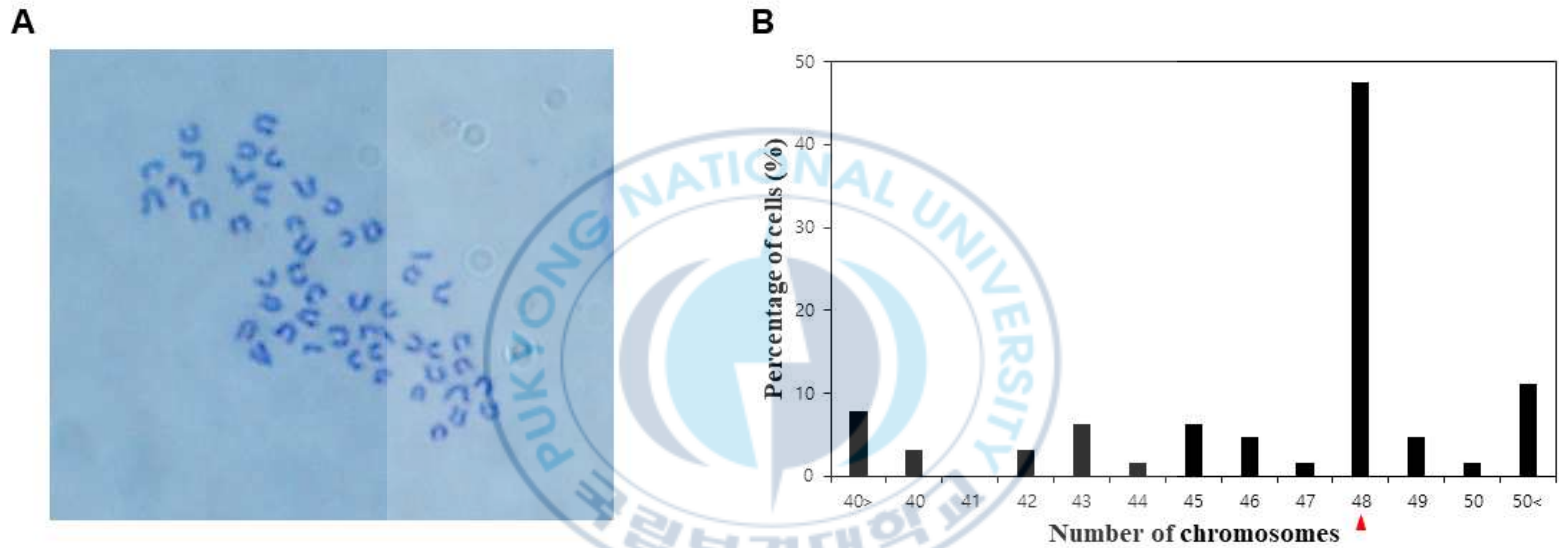


Figure 23. Karyotype analysis from OFT. At passage 30, karyotype analysis were performed from OFT. 63 of karyotype pictures were taken, and they were counted for normality test. (A) The representative picture of karyotype from OFT. (B) The result of normality test ($2n = 48$) from OFT. The red arrowhead indicate the number of diploid *P. olivaceus* chromosome set.

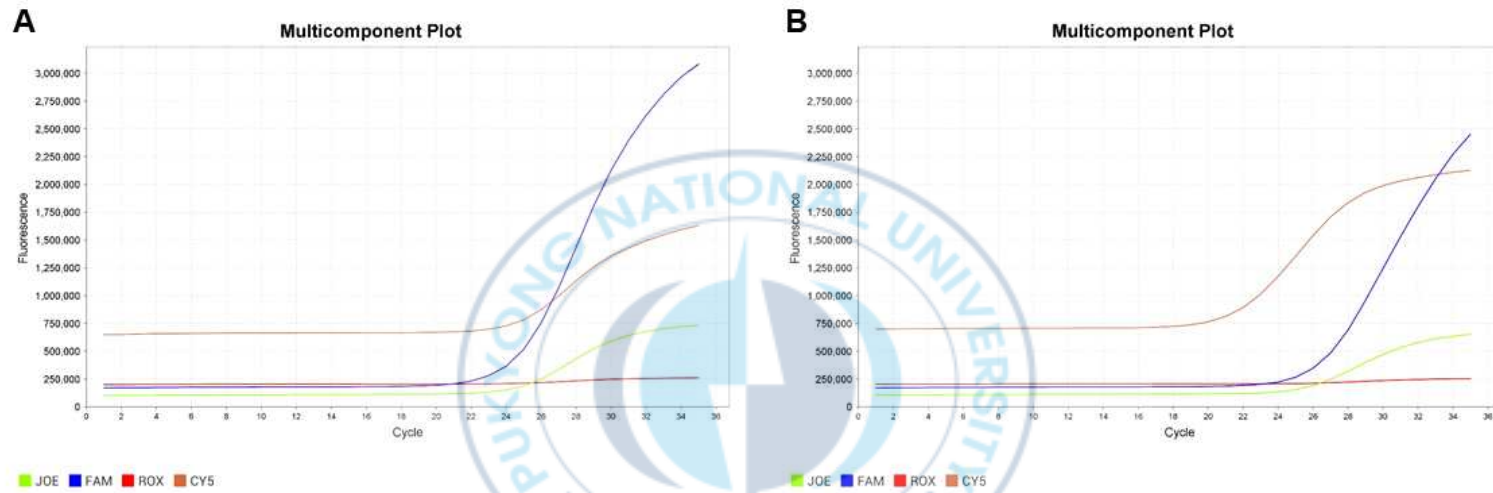


Figure 24. Validation of genetical sex from OFT. At passage 30, genomic DNA was isolated from OFT, and investigation of genetical sex were performed. The genetical sex of OFT was determined by SNP markers (5512T, 5227A, 8483C). For positive control, genomic DNA derived from *P. olivaceus* fin tissue was isolated. (A) The SNP result from male wild type *P. olivaceus*. (B) The SNP result from OFT. Three different SNP markers were detected from male wild type *P. olivaceus* and OFT.

vector and analyzed for transfection efficiency and GFP expression. At 48 hours post-electroporation, strong green fluorescence signals were observed in both cell types (Figure 25). The transfection efficiency was 35.63% for OFT. These results highlight the potential of OFT line for applications requiring exogenous gene expression, including basic research and biotechnological development.

6. Effects of sex hormones, growth factors, and OFT on the culture of 3D co-cultured aggregates

6.1. Evaluation of the effects of sex hormones, growth factors, and OFT on the morphology of 3D co-cultured aggregates

To evaluate the effects of sex hormones, growth factors, and OFT on aggregate morphology, four groups were cultured in ULA plates: Group 1: 1×10^6 primary testicular cells without treatment, Group 2: 1×10^6 primary testicular cells treated with sex hormones and growth factors, Group 3: 5×10^5 primary testicular cells co-cultured with 5×10^5 OFT cells without treatment, and Group 4: 5×10^5 primary testicular cells co-cultured with 5×10^5 OFT cells treated with sex hormones and growth factors. As the results, no aggregate formation was observed in either Group 1 or Group 2 on day 1 of culture, regardless of treatment with sex hormones and growth factors (Figure 26A). In contrast, aggregate formations were observed in Group 3 and Group 4 on day 1 of culture, regardless of treatment with sex

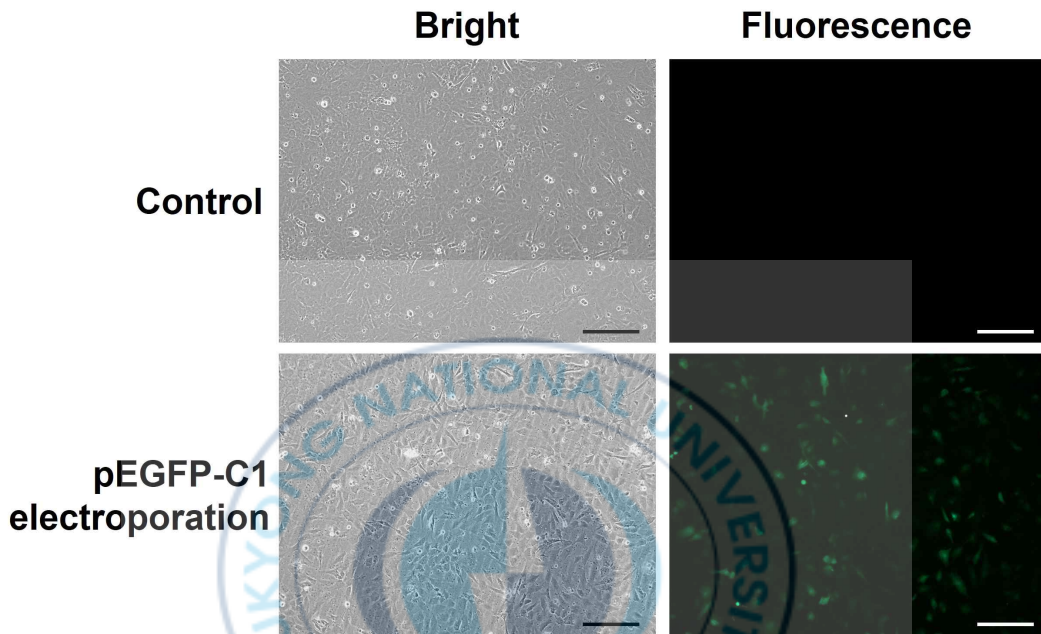


Figure 25. Electroporation of green fluorescent protein expression vector into OFT. The OFT cell line was electroporated with green fluorescent protein expression vector (pEGFP-C1). Subsequently, the OFT cells were cultured for 48 hours and observed using fluorescent microscope. Scale bar = 200 μ m.

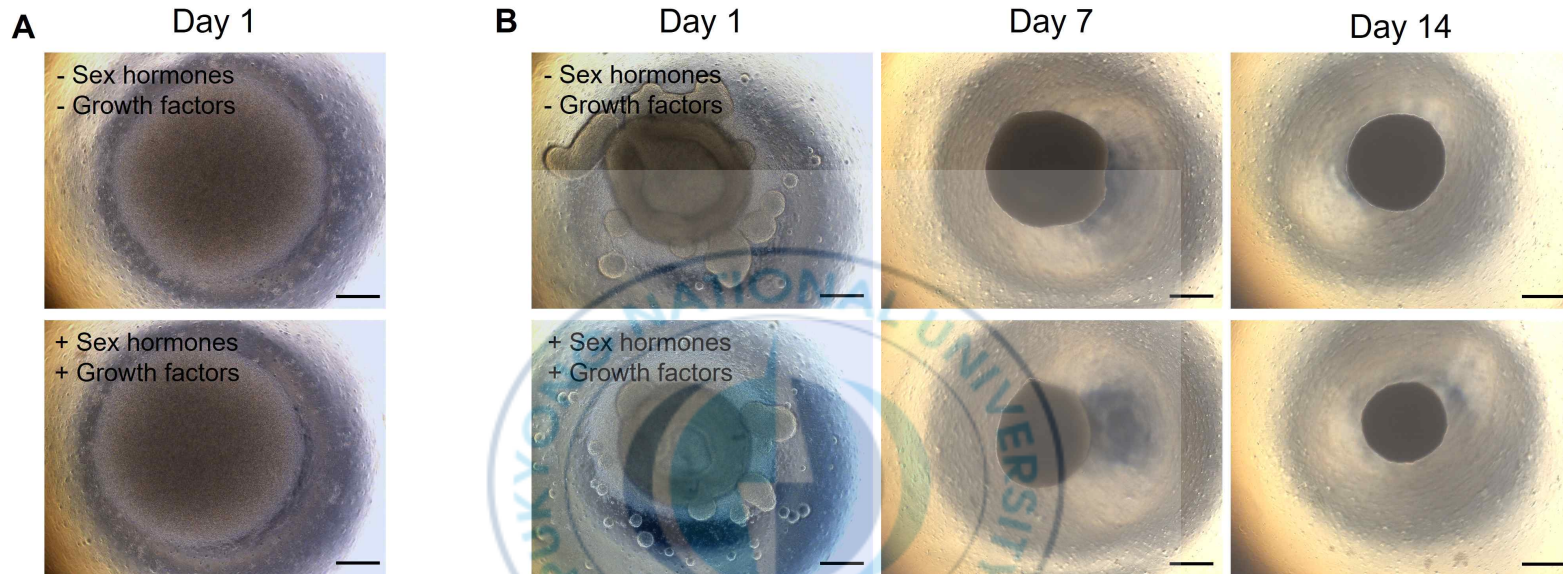


Figure 26. Effects of sex hormones and growth factors, and inclusion with OFT on testicular aggregate formation in *P. olivaceus*. Total 1×10^6 testicular cells were cultured in ULA for 14 days. For inclusion of OFT, 5×10^5 OFT cells and same number of primary testicular cells were seeded in ULA. (A) Representative images of testicular cells cultured in ULA with or without reproductive hormones and growth factors on day 1. Treatments included 11-ketotestosterone (11-KT), 17β -estradiol (E_2), 17α , 20β -dihydroxy-4-pregnen-3-one (DHP), human chorionic gonadotropin (hCG), epidermal growth factor (EGF), and insulin-like growth factor-1 (IGF-1). (B) Representative images of testicular cells co-cultured with OFT under the same treatment conditions in (A). Aggregate formation began to be observed at day 1. Significant difference was not observed, regardless of hormones and growth factors treatment. Scale bar = 400 μ m.

hormones and growth factors (Figure 26B). At day 1, multiple aggregations, which were dramatically aggregated, were observed, regardless treatment. The longer culture period, a single round and compact type of aggregate was observed, regardless of treatment (Figure 26B). From this result suggest that although sex hormones and growth factors are not critical for the formation of aggregate, OFT cell line was enhance the formation of aggregate. For further studies, Group 3 and Group 4 were used.

6.2. Evaluation of the effects of sex hormones and growth factors on the viability of 3D co-cultured aggregates

To evaluate the effects of sex hormones and growth factors on viability, 3D co-cultured aggregates (Group 3 and Group 4) were stained with Live/Dead Viability/Cytotoxicity Kit (Molecular Probes) and trypan blue (Gibco). As shown in Figure 27A, most cells, regardless of treatments of sex hormones and growth factors, were viable demonstrating green fluorescence. Also, comparing with negative control, cells showing red fluorescence were not observed from 3D co-cultured aggregates. Indeed, trypan blue staining confirmed high viability in both conditions, with no significant difference (Figure 27B; 91 ± 0.40 in mESM2 vs 93 ± 1.65 in mESM2 supplemented with sex hormones and growth factors). These results demonstrated that sex hormones and growth factors are not affected in the cell viability.

6.3. Evaluation of the effects of sex hormones and growth factors on the viability of 3D co-cultured aggregates

To evaluate functional differences depending on treatment of sex hormones and growth factors, 3D co-cultured aggregates were analyzed by qRT-PCR for the expression levels of *plzf* (spermatogonial stem cell marker) and *scp3* (mid-meiotic germ cell marker). As the result, when 3D co-cultured aggregates were cultured with mESM2 supplemented with sex hormones and growth factors, significantly higher expression levels of *plzf* and *scp3* were detected, with 2.15 ± 0.69 and 2.34 ± 0.79 fold increases, respectively (Figure 28). These results demonstrated that sex hormones and growth factors are critical for enhancement of spermatogonial stem cell maintenance and differentiation within the 3D co-cultured aggregates.

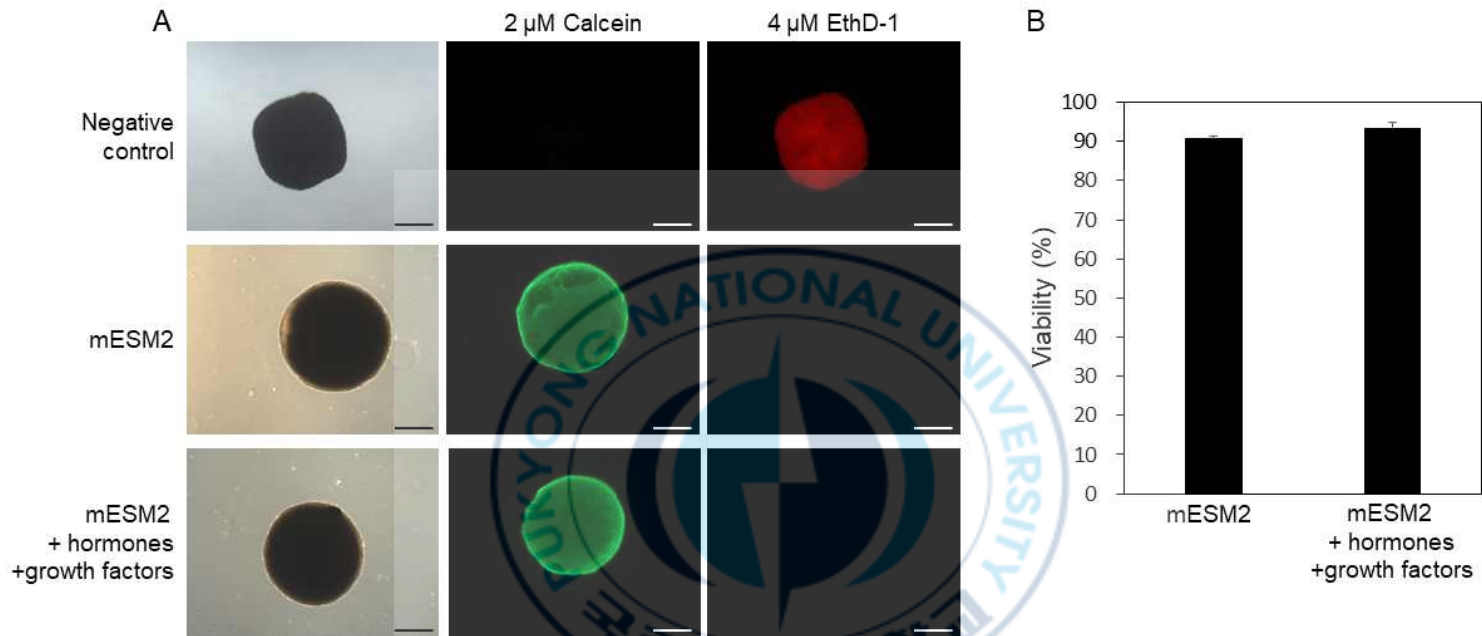


Figure 27. Evaluation of sex hormones and growth factors on the viability of the cells composing 3D co-cultured testicular aggregates. Ovarian aggregates were cultured in ULA containing mESM2 supplemented with or without hormones and growth factors. Subsequently, their viabilities were compared by live/dead cell staining and trypan blue staining (A) Pictures taken after live/dead cells staining. Live cells were stained by 2 μ M calcein and dead cells were stained by 4 μ M EthD-1. Negative control were immersed in 70% ethanol for 1 hour before live/dead cell staining. Scale bar = 400 μ m (B) Comparison of the viability of cells composing ovarian aggregates cultured in each medium. The viabilities were determined by trypan blue staining. All values are expressed as mean \pm standard deviation of three independent experiments at least.

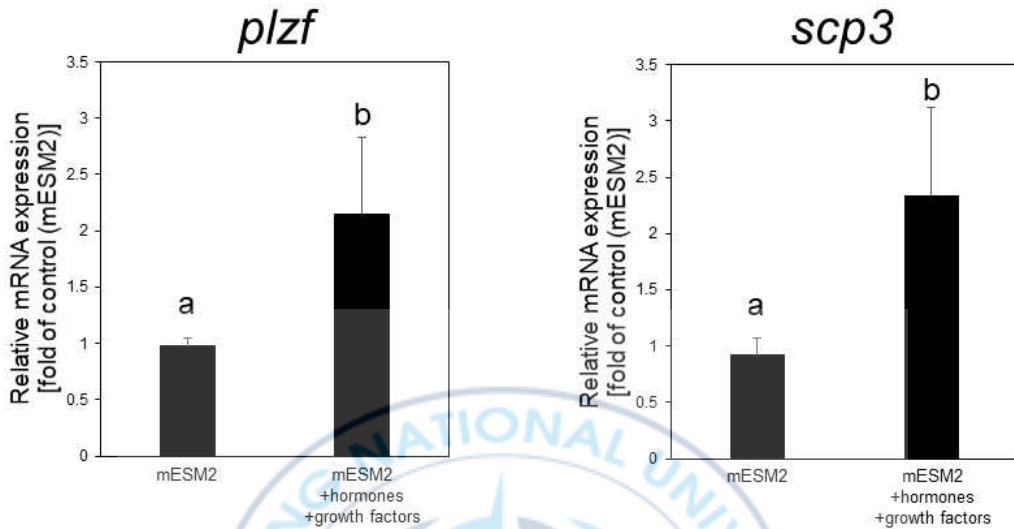


Figure 28. Evaluation of sex hormones and growth factors on the gene expression levels from 3D co-cultured testicular aggregates. Testicular aggregates cultured in each medium were analyzed by qRT-PCR analysis to compare two germ cell specific genes expression levels. (A) Relative mRNA expression of *plzf* (spermatogonia marker). (B) Relative mRNA expression of *scp3* (meiosis marker). Both gene expressions were significantly increased, when testicular aggregates were cultured in mESM2 supplemented with reproductive hormones and growth factors. All values are expressed as mean \pm standard deviation of three independent experiments at least. ^{ab}Different letters indicate significant differences ($p < 0.05$).

IV. Discussion

In this study, olive flounder (*Paralichthys olivaceus*) testicular cell (OFT) line was successfully established, and OFT cell line was used for the formation of *P. olivaceus* 3D co-cultured testicular aggregates. Also, treatments of sex hormones and growth factors were evaluated on the culture of 3D co-cultured testicular aggregates.

At early passages, OFT cell line exhibited fibroblast-like and epithelial-like morphologies, while later passages included cobblestone-like cells, indicating cellular heterogeneity and adaptation during prolonged culture. These patterns are consistent with previous findings in which early passage *Paralichthys olivaceus* Sertoli cell lines presented a mix of fibroblast- and epithelial-like morphologies (Peng et al., 2016). In the context of gonadal cultures, these cell types are often implicated in forming feeder layers that support germ cell maintenance (Kawasaki et al., 2012). RT-PCR analysis confirmed the expression of gonadal somatic cell markers such as *wt1* and *fgl2* in OFT cell line. As *wt1* is a well-established marker for Sertoli cells, its prominent expression in OFT suggests Sertoli cell origin (Higaki et al., 2013). Moreover, OFT cell line expressed *fgl2*, a factor known to promote the self-renewal of spermatogonial stem cells (SSCs; Morimoto et al., 2023), and typically found in Sertoli cells (Gómez et al., 2012)

To confirm the species origin, mitochondrial *COI* and *16s rRNA* gene regions were amplified and sequenced. The resulting sequences were identical to *P. olivaceus*, verifying that OFT cell line originated from this

species. This approach is commonly employed to ensure species origin in established fish cell lines (Peng et al., 2016; Ahmed et al., 2017; Xu et al., 2022).

Chromosomal analysis revealed that approximately 47.6% of OFT cells maintained the normal *P. olivaceus* karyotype ($2n = 48$; Zheng et al., 2015; Kim et al., 2020). Although deviations from the standard chromosome number were observed, these mostly ranged within ± 3 of the diploid number, suggesting minor chromosomal aberrations rather than severe genomic instability (Swaminathan et al., 2010). This chromosomal normality result is comparable to previously reported *P. olivaceus* Sertoli cell lines (Peng et al., 2016) and supports the cytogenetic stability of the established lines during *in vitro* maintenance.

Given the potential for environmental sex reversal in female teleosts, including *P. olivaceus* (Sun et al., 2022; Wang et al., 2017), As pseudo-male gonad cell lines express Sertoli cell markers (Sun et al., 2015), SNP markers developed by National Institute of Fisheries Science were used to clearly determine genetic sex. These developed SNP markers were previously used to determine genetic sex from *P. olivaceus* (Kim et al., 2017). Finally, the SNP analysis result demonstrated that OFT cell line were derived from genetically male (XY).

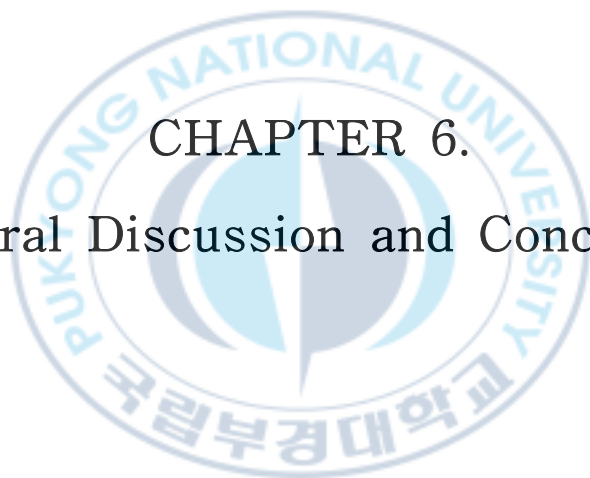
The introduction of exogenous genes was evaluated using electroporation with a GFP expression vector. While previous studies using chemical transfection agents reported low efficiencies in various fish cell lines (Lee et al., 2019), including SIMH and SIGE lines (Parameswaran et al., 2007), electroporation yielded relatively higher transfection rates in the OFT cell line. Although variables such as plasmid type and concentration differ, our

findings suggest that electroporation is a more suitable method for gene delivery in the OFT cell line, enhancing its utility for functional studies and biotechnological applications.

Previously, testicular organoids were self-assembled in 24 hours when testicular cells, which isolated from 5 dpp and 12 dpp male mice, were cultured in nonadherent micro wells (Edmonds and Woodruff, 2020). However, testicular cells isolated from adult mice (8 - 16 weeks) were not self-assembled at the same condition. Instead, when adult testicular cells were co-cultured with immature murine testicular cells, they were rescued the self-aggregation. From this result, Edmonds and Woodruff hypothesized that Sertoli cells are critical for the formation of testicular organoid. Similarly, Alves-Lopes et al. suggested that the abundance of Sertoli cells in immature testes may play a key role in the formation of testicular organoids (Alves-Lopes et al., 2017). Indeed, when isolated testicular cells were co-cultured with OFT cell line in ULA, aggregation was observed within 24 hours, whereas no aggregation was observed within 24 hours when only isolated testicular cells were cultured in ULA. Similarly with the previous studies, the result in this study demonstrated that OFT cell line is critical for the formation of aggregation.

Subsequently, in the evaluation of sex hormones and growth factors, the results demonstrated that those treatments did not affect on the cell viability. However, treatments of sex hormones and growth factors induced significantly increase in *plzf* and *scp3* expression. In this study, sex hormones including 11-ketotestosterone (11-KT), 17 β -estradiol (E₂), 20 β -dihydroxy-4-pregnen-3-one (DHP), and human chorionic gonadotropin (hCG) and growth factors including epidermal growth factor (EGF), and

insulin-like growth factor 1 (IGF-1) were used for culturing 3D co-cultured aggregates. In tilapia, 11-KT was confirmed that it is essential for inducing the initiation of meiosis, while IGF-1 and hCG induced SSCs proliferation (Tokalov and Gutzeit, 2005). Also, in the orange-spotted grouper SSC line, 11-KT treatment induced high expression of meiotic genes including *rec8*, *scp3*, *dmcl* and produced sperm-like cells (Zhong et al., 2022). In the previous studies, there have been reports that E₂ can stimulate early germ cell proliferation. For example, in cryptorchid mice, high dose E₂ treatment significantly increased SSCs proliferation (Li et al., 2007). On the other hands, in the Japanese eel, injection of E₂ promoted SSCs proliferation (Miura et al., 1999). Also, Miura et al. demonstrated in Japanese eel that DHP and DHP receptor are present in early spermatogenesis, and DHP induces meiotic entry (Miura et al., 2006). EGF is a mitogenic growth factor used in mammalian including rat (Wahab-Wahlgren et al., 2003), mouse (Azizi et al., 2017), and human (Medrano et al., 2016) SSC cultures. Taken together, the significant increase of *plzf* expression level from 3D co-cultured testicular aggregates was resulted from the E₂, hCG, IGF-1, and EGF, in contrast, the significant increase of *scp3* expression level was resulted from the 11-KT and DHP. To accurately assess the effects of each sex hormone and growth factor on germ cells within the 3D aggregates, additional studies evaluating each factor individually will be necessary.



CHAPTER 6.

General Discussion and Conclusion

This study aimed to establish a three-dimensional (3D) culture system for gonadal germ cells in fish using both a biological model species, marine medaka (*Oryzias dancena*), and an economically important aquaculture species, olive flounder (*Paralichthys olivaceus*). Through three major experimental phases, I developed and evaluated *in vitro* aggregate systems for testicular and ovarian germ cells, as well as a co-culture model incorporating somatic support cells, providing a foundation for future applications in reproductive biology and germ cell engineering in fish.

In the first part of the study, I optimized a 3D testicular aggregate culture system using *O. dancena* testicular cells. Among the three methods evaluated including Matrigel suspension, 3-layer gradient system, and ultra-low attachment (ULA) plates, the ULA method demonstrated superior aggregate formation and structural stability. Furthermore, modified ESM2 (mESM2) medium influenced type of aggregates and expression of germ cell and somatic markers. Notably, sperm derived from cultured testicular aggregates exhibited fertilization capability, highlighting the potential of the system to support functional spermatogenesis *in vitro*.

The second part focused on the development of ovarian cell aggregates using *O. dancena*. Two distinct ovarian cell populations, separated by Percoll density gradient centrifugation, were evaluated for their ability to form aggregates and maintain germ cell characteristics under ULA conditions. Specific factors, including bFGF, FS, and EE, significantly enhanced the expression of *scp3*, a marker for meiotic germ cells, while bFGF and GDNF increased *nanos2* expression. Interestingly, GDNF alone suppressed *scp3* expression, suggesting stage-specific effects of growth factors. Regardless of hFSH treatment, the ovarian aggregates maintained

oocyte-like cells and continued E₂ production within 22 days, indicating the long-term functional maintenance of female germ cells *in vitro*.

In the final part, olive flounder testis-derived somatic cell line (OFT) was established and evaluated its potential to support germ cell aggregation through co-culture. The OFT cell line displayed characteristics of Sertoli cells and was capable of initiating aggregate formation within 24 hours. While hormone and growth factor treatments did not significantly influence to aggregate viability, they did enhance the expression of germ cell markers, *plzf* and *scp3*, indicating their involvement in germ cell maintenance and differentiation.

Together, these studies present a comprehensive strategy for developing 3D germ cell culture systems in fish. The testis and ovary aggregate models in *O. dancena* demonstrated the feasibility of stage-specific germ cell modulation through developed culture system, while the *P. olivaceus* co-culture system provided a platform to evaluate the functional role of somatic support cells in germline development.

Nevertheless, several limitations must be acknowledged. While gonadal aggregates were successfully generated and maintained, their long-term genomic stability, epigenetic integrity, and *in vivo* functionality remain unverified. Future studies should investigate whether germline stem cells cultured by gonadal aggregates can be transplanted into recipient gonads and undergo complete gametogenesis. Furthermore, although various growth factors were tested, detailed analyses of their dependent effects and the signaling pathways are still needed. In addition, the present systems were optimized only for *O. dancena* and *P. olivaceus*, and thus its general applicability to other species remains to be investigated. Future research

should expand the system to include a wider range of aquaculture species, and explore the integration of automated and scalable culture technologies to facilitate industrial level applications. By addressing these aspects, the 3D germ cell culture system developed here could evolve into a robust platform for both fundamental research and practical application in fish reproductive engineering.



References

- Aflatoonian B, Ruban L, Jones M, Aflatoonian R, Fazeli A, Moore HD (2009) *In vitro* post-meiotic germ cell development from human embryonic stem cells. Hum. Reprod. 24, 3150 - 3159.
- Ahmed I, Huebner H, Mamoori Y, Buchholz R (2017) Identification of newly established *Spodoptera littoralis* cell lines by two DNA barcoding markers. In Vitro Cell. Dev. Biol. Anim. 53, 288 - 292.
- Alves-Lopes JP, Söder O, Stukenborg JB (2017) Testicular organoid generation by a novel *in vitro* three-layer gradient system. Biomaterials. 130, 76 - 89.
- Azizi H, Skutella T, Shahverdi A (2017) Generation of mouse spermatogonial stem-cell-colonies in a non-adherent culture. Cell J. 19, 238-249.
- Bradley A, Evans M, Kaufman MH, Robertson E (1984) Formation of germ line chimaeras from embryo-derived teratocarcinoma cell lines. Nature. 309, 255-256.
- Brito IR, Lima IM, Xu M, Shea LD, Woodruff TK, Figueiredo JR (2014) Three-dimensional systems for *in vitro* follicular culture: overview of alginate-based matrices. Reprod. Fertil. Dev. 26, 915-930.
- Bui-Marinos MP, Todd LA, Douglas AJ, Katzenback BA (2022) So, you want to create a frog cell line? A guide to establishing frog skin cell lines from tissue explants. MethodsX. 9, 101693.
- Burger M, Hess MW, Cottier H (1980) Role of 2-mercaptoethanol in the stimulation of spleen cell culture: Increased uptake of cysteine into the

- TCA-soluble pool. *Immun. Lett.* 4, 193 - 197.
- Cao Z, Mao X, Luo L (2019) Germline stem cells drive ovary regeneration in zebrafish. *Cell. Rep.* 26, 1709-1717.
- Cavaco JE, Bogerd J, Goos H, Schulz RW (2001) Testosterone inhibits 11-ketotestosterone-induced spermatogenesis in African catfish (*Clarias gariepinus*). *Biol. Reprod.* 65, 1807 - 1812.
- Celiz RH, Brito DCC, Novaes MAS, Sa NAR, Naupas LVS, Mbemya TG, Palomino GYQ, Gomes FDR, Fernandes CCL, Silva CVO, Assis Neto AC, Figueiredo JR, Rodrigues APR (2023) Two- three-dimensional system in agarose matrix for *in vitro* culture of testicular fragments of adult sheep. *Small Rumin. Res.* 224.
- Cham TC, Ibtisham F, Fayaz MA, Honaramooz A (2021) Generation of a highly biomimetic organoid, including vasculature, resembling the native immature testis tissue. *Cells.* 10, 1696.
- Chen S, Ye H, Sha Z, Hong Y (2003) Derivation of a pluripotent embryonic cell line from red sea bream blastulas. *J. Fish Biol.* 63, 795 - 805.
- Chen X, Kan Y, Zhong Y, Jawad M, Wei W, Gu K, Gui L, Li M (2022) Generation of a long-term-cultured Chinese hook snout carp spermatogonial stem cell line capable of sperm production *in vitro*. *Biology.* 11, 1069.
- Cho S, Kim K, Choi I, Jeon G, Kim D (2012) Compensatory growth of grower olive flounder (*Paralichthys olivaceus*) with different feeding regime at sub-optimal temperature. *Asian-Australas. J. Anim. Sci.* 25, 272.
- Choi JH, Gong SP (2018) Effects of temperatures and basal media on primary culture of blastomeres derived from embryos at blastula stage in marine medaka *Oryzias dancena*. *J. Embryo Transf.* 33, 343 - 348.

- Choi JH, Kim EJ, Park CJ, Nam YK, Gong SP (2020) Evaluation of veliger-stage larvae for preparing metaphase spreads in Pacific abalone (*Haliotis discus hannai*). J. Anim. Reprod. Biotechnol. 35, 223 - 231.
- Choi JH, Ryu JH, Gong SP (2023) Establishment and optimization of an aggregate culture system of testicular cells from marine medaka, *Oryzias dancena*. J. Mar. Sci. Eng. 11, 2077.
- Cortez J, Levia B, Torres CG, Parraguez VH, de los Reyes M, Carrasco A, Peralta OA (2022) Generation and characterization of bovine testicular organoids derived from primary somatic cell populations. Animals. 12, 2283.
- Costoya JA, Hobbs RM, Barna M, Cattoretti G, Manova K, Sukhwani M, Orwig KE, Wolgemuth DJ, Pandolfi PP (2004) Essential role of Plzf in maintenance of spermatogonial stem cells. Nat. Genet. 36, 653 - 659.
- de Barros FR, Worst RA, Saurin GC, Mendes CM, Assumpção ME, Visintin JA (2012) α -6 integrin expression in bovine spermatogonial cells purified by discontinuous Percoll density gradient. Reprod. Domest. Anim. 47, 887 - 890.
- Dettin L, Ravindranath N, Hofmann MC, Dym M (2003) Morphological characterization of the spermatogonial subtypes in the neonatal mouse testis. Biol. Reprod. 69, 1565 - 1571.
- Dias GC, Batlouni SR, Cassel M, Chehade C, de Jesus LW, Branco GS, Camargo MP, Borella MI (2020) Isolation, *in vitro* study, and stem-cell markers for type A spermatogonia in a Characiformes species. Mol. Reprod. Dev. 87, 783 - 799.
- Dong S, Kang M, Wu X, Ye T (2014) Development of a promising fish model (*Oryzias melastigma*) for assessing multiple responses to

- stresses in the marine environment. *Biomed. Res. Int.* 2014, 563131.
- Edmonds ME, Woodruff TK (2020) Testicular organoid formation is a property of immature somatic cells that self-assemble and exhibit long-term hormone-responsive endocrine function. *Biofabrication.* 12, 045002.
- Fan N, Raatz L, Chon SH, Quaas A, Bruns C, Zhao Y (2022) Subculture and cryopreservation of esophageal adenocarcinoma organoids: pros and cons for single cell digestion. *J. Vis. Exp.* <https://doi.org/10.3791/63281>.
- Fan Z, Liu L, Huang X, Zhao Y, Zhou L, Wang D, Wei J (2017) Establishment and growth responses of Nile tilapia embryonic stem-like cell lines under feeder-free conditions. *Dev. Growth Differ.* 59, 83 - 93.
- Gautier A, Bosseboeuf A, Auvray P, Sourdain P (2014) Maintenance of potential spermatogonial stem cells *in vitro* by GDNF treatment in a chondrichthyan model (*Scyliorhinus canicula*). *Biol. Reprod.* 91, 91.
- Ge W, Chen C, De Felici M, Shen W (2015) *In vitro* differentiation of germ cells from stem cells: comparison between primordial germ cells and *in vitro*-derived primordial germ cell-like cells. *Cell Death Dis.* 6, e1906.
- Goel S, Sugimoto M, Minami N, Yamada M, Kume S, Imai H (2007) Identification, isolation and *in vitro* culture of porcine gonocytes. *Biol. Reprod.* 77, 127 - 137.
- Gómez M, Manzano A, Figueras A, Viñals F, Ventura F, Rosa JL, Bartrons R, Navarro-Sabaté À (2012) Sertoli-secreted FGF-2 induces PFKFB4 expression in mouse spermatogenic cells via MEK/ERK/CREB. *Am. J. Physiol. Endocrinol. Metab.* 303, E695 - E707.

- Graziano MU, Graziano KU, Pinto FM, Bruna CQ, de Souza RQ, Lascala CA (2013) Effectiveness of disinfection with 70% alcohol of contaminated surfaces not previously cleaned. *Rev. Lat. Am. Enfermagem* 21, 618 - 623.
- Guo Y, Hai Y, Yao C, Chen Z, Hou J, Li Z, He Z (2015) Long-term culture and significant expansion of human Sertoli cells while maintaining stable phenotype. *Cell Commun. Signal.* 13, 20.
- Hamidabadi HG, Bojnordi MN (2018) Co-culture of mouse spermatogonial stem cells with sertoli cell as a feeder layer, stimulates the proliferation and spermatogonial stemness profile. *Middle East Fertility Soc. J.* 23, 107-111.
- Hayashi K, Ogushi S, Kurimoto K, Shimamoto S, Ohta H, Saitou M (2012) Offspring from oocytes derived from *in vitro* primordial germ cell-like cells in mice. *Science.* 338, 971-975.
- Heidari B, Gifani M, Shirazi A, Zarnani AH, Baradaran B, Naderi MM, Behzadi B, Borjian-Boroujeni S, Sarvari A, Lakpour N, Akhondi MM (2014) Enrichment of undifferentiated type A spermatogonia from goat testis using Percoll gradient and differential plating. *J. Med. Biotechnol.* 6, 94 - 103.
- Hewlett G, Opitz GH, Schlumberger HG, Lemke H (1977) Growth regulation of a murine lymphoma cell line by 2-mercaptoethanol or a macrophage-activated serum factor. *Eur. J. Immunol.* 7, 781 - 785.
- Higaki S, Koyama Y, Shirai E, Yokota T, Fujioka Y, Sakai N, Takada T (2013) Establishment of testicular and ovarian cell lines from Honmoroko (*Gnathopogon caeruleus*). *Fish Physiol. Biochem.* 39, 701 - 711.

- Higaki S, Shimada M, Kawamoto K, Todo T, Kawasaki T, Tooyama I, Fujioka Y, Sakai N, Takada T (2017) *In vitro* differentiation of fertile sperm from cryopreserved spermatogonia of the endangered cyprinid honmoroko. *Sci. Rep.* 7, 42852.
- Ho SY, Goh CW, Gan JY, Lee YS, Lam MK, Hong N, Hong Y, Chan WK, Shu-Chien AC (2014) Derivation and long-term culture of an embryonic stem-like cell line from zebrafish blastomeres under feeder-free conditions. *Zebrafish.* 11, 407 - 420.
- Hong Y, Liu T, Zhao H, Xu H, Wang W, Liu R, Chen T, Deng J, Gui JF (2004) Establishment of a normal medaka fish spermatogonial stem cell line capable of sperm production *in vitro*. *Proc. Natl. Acad. Sci. USA.* 101, 8011 - 8016.
- Hong Y, Scharl M (1996) Establishment and growth responses of early medaka fish (*Oryzias latipes*) embryonic cells in feeder-free culture. *Mol. Mar. Biol. Biotechnol.* 5, 93 - 104.
- Huleihel M, Nourashrafeddin S, Plant TM (2015) Application of three-dimensional culture systems to study mammalian spermatogenesis, with an emphasis on the rhesus monkey (*Macaca mulatta*). *Asian J. Androl.* 17, 972.
- Hwa JC, Sum R (1994) Triploidy induction in olive flounder (*Paralichthys olivaceus*). *J. Aquac.* 7, 55 - 61.
- Ibtisham F, Honaramoo A (2020) Spermatogonial stem cells for *in vitro* spermatogenesis and *in vivo* restoration of fertility. *Cells.* 9, 745.
- Iwanami Y, Kobayashi T, Kato M, Hirabayashi M, Hochi S (2006) Characteristics of rat round spermatids differentiated from spermatogonial cells during co-culture with Sertoli cells.

- Theriogenology. 65, 288 - 298.
- Iwasaki-Takahashi Y, Shikina S, Watanabe M, Banba A, Yagisawa M, Takahashi K, Fujihara R, Okabe T, Valdez DM Jr, Yamauchi A, Yoshizaki G (2020) Production of functional eggs and sperm from *in vitro*-expanded type A spermatogonia in rainbow trout. Commun. Biol. 3, 308.
- Jabari A, Gilani MAS, Koruji M, Gholami K, Mohsenzadeh M, Khadivi F, Gashti NG, Nikmahzar A, Mojaverrostami S, Talebi A, Movassagh SA, Rezaie MJ, Abbasi M (2020) Three-dimensional co-culture of human spermatogonial stem cells with Sertoli cells in soft agar culture system supplemented by growth factors and laminin. Acta. Histochem. 122, 151572.
- Jeong Y, Ryu JH, Nam YK, Gong SP, Kang SM (2018) Enhanced adhesion of fish ovarian germline stem cells on solid surfaces by mussel-inspired polymer coating. Mar. Drugs. 17, 11.
- Jenc JC (2011) Somatic gonadal cells: the supporting cast for the germline. Genesis. 49, 753 - 775.
- Kanatsu-Shinohara M, Ogonuki N, Inoue K, Miki H, Ogura A, Toyokuni S, Shinohara T (2003) Long-term proliferation and germline transmission of mouse male germline stem cells in culture. Biol. Reprod. 69, 612 - 616.
- Kanatsu-Shinohara M, Muneto T, Lee J, Takenaka M, Chuma S, Nakatsuji N, Horiuchi T, Shinohara T (2008) Long-term culture of male germline stem cells from hamster testes. Biol. Reprod. 78, 611 - 617.
- Kang JH, Ryu JH, Nam YK, Gong SP (2019) Effectiveness of a medaka whole-testis organ-culture system using an agarose gel stand for

- germ-cell proliferation and differentiation. *J. Biomater. Tissue Eng.* 9, 206 - 212.
- Kawasaki T, Saito K, Sakai C, Shinya M, Sakai N (2012) Production of zebrafish offspring from cultured spermatogonial stem cells. *Genes Cells.* 17, 316 - 325.
- Kim J, Cho JY, Kim JW, Kim HC, Noh JK, Kim YO, Hwang HK, Kim WJ, Yeo SY, An CM (2019) CRISPR/Cas9-mediated myostatin disruption enhances muscle mass in olive flounder. *Aquaculture.* 512, 734336.
- Kim WS, Jang MS, Kim JO, Kim DW, Jung SJ, Kim SR, Park MA, Oh MJ (2009) Effect of storage conditions of olive flounder *Paralichthys olivaceus* serum on enzyme-linked immunosorbent assay. *J. Fish Pathol.* 22, 167-172.
- Kim WJ, Nam BH, An CM, Kim HC, Kong HJ, Kim YO, Kim KK (2017) Genetic marker and method for identifying the sex in olive flounder. KR Patent 101770966B1, 31 Dec 2017.
- Kitano T, Takenaka T, Takagi H, Yoshiura Y, Kazeto Y, Hirai T, Mukai K, Nozu R (2022) Roles of gonadotropin receptors in sexual development of medaka. *Cells.* 11, 387.
- Kleppe L, Crespo D, Guralp HK, Lareyre JJ, Skaftnesmo KO, Ayllon F, Fraser TWK, Fjelldal PG, Hansen TJ (2025) Production of donor-derived atlantic salmon progeny using allogeneic surrogate broodstock technology. *Aquaculture.* 608, 742752.
- Knaut H, Pelegri F, Bohmann K, Schwarz H, Nusslein-Volhard C (2000) Zebrafish vasa RNA but not its protein is a component of the germ plasm and segregates asymmetrically before germline specification. *J.*

- Cell Biol. 149, 875–888.
- Ko MG, Jung HS, Lee HB, Kim DS (2016) Cytogenetic analysis of all-female triploid olive flounder for ploidy verification. Korean J. Fish. Aquat. Sci. 49, 671 - 674.
- Kubota H, Avarbock MR, Brinster RL (2004) Growth factors essential for self-renewal and expansion of mouse spermatogonial stem cells. Proc. Natl. Acad. Sci. USA. 101, 16489 - 16494.
- Kumar S, Singla SK, Manik R, Palta P, Chauhan MS (2020) Effect of basic fibroblast growth factor on cumulus-cell expansion, embryo production and gene expression in buffalo. Reprod. Biol. 20, 501 - 511.
- Lacerda S, Batlouni S, Assis L, Resende F, Campos-Silva S, Campos-Silva R, Campos-Silva T, Segatelli T, França L (2008) Germ-cell transplantation in tilapia (*Oreochromis niloticus*). Cybium. 32, 115 - 118.
- Lacerda SM, Costa GM, de França LR (2014) Biology and identity of fish spermatogonial stem cell. Gen. Comp. Endocrinol. 207, 56 - 65.
- Lacerda S, Martinez ERM, Mura I, Doretto LB, Costa GM, Silva M, Digmayer M, Nóbrega R, França L (2019) Duration of spermatogenesis and identification of stem-cell markers in the catfish jundiá. Gen. Comp. Endocrinol. 273, 249 - 259.
- Leal MC, de Waal PP, García-López A, Chen SX, Bogerd J, Schulz RW (2009) Zebrafish primary testis-tissue culture: An *ex-vivo* approach to study testis function. Gen. Comp. Endocrinol. 162, 134 - 138.
- Lee D, Ryu JH, Lee ST, Nam YK, Kim DS, Gong SP (2015) Embryonic stem-cell activities in an embryonic cell line derived from marine medaka. Fish Physiol. Biochem. 41, 1569 - 1576.
- Lee JH, Kim HJ, Kim H, Lee SJ, Gye MC (2006) *In vitro* spermatogenesis

- in a three-dimensional rat testicular-cell culture within collagen gel. *Biomaterials*. 27, 2845 - 2853.
- Lee JH, Lee ST, Nam YK, Gong SP (2019) Gene delivery into Siberian sturgeon cell lines using commercial transfection reagents. *In Vitro Cell. Dev. Biol. Anim.* 55, 76 - 81.
- Lee JH, Choi JH, Choi JK, Gong SP (2021) Improved conditions for whole-testis organ culture to enhance spermatogonial proliferation in marine medaka. *In Vitro Cell. Dev. Biol. Anim.* 57, 808 - 816.
- Lee Y, Lee M, Lee SW, Choi NY, Ham S, Lee HJ, Ko K, Ko K (2019) Reprogramming of spermatogonial stem cells into pluripotent stem cells in the spheroidal state. *Anim. Cells Syst.* 23, 392-398.
- Lenhart KF, DiNardo S (2015) Somatic-cell encystment promotes abscission in germline stem cells after a regulated block in cytokinesis. *Dev. Cell*. 34, 192 - 205.
- Lim MJ, Kim SJ, Jo A, Kim SW (2025) Enhanced application potential of alveolar organoids through epithelial and niche cell interactions. *Sci. Rep.* 15, 17538.
- Linhartová Z, Rodina M, Guralp H, Gazo I, Saito T, Pšenička M (2014) Isolation and cryopreservation of early germ-cell stages in tench (*Tinca tinca*). *Czech J. Anim. Sci.* 59, 381 - 390.
- Livak KJ, Schmittgen TD (2001) Analysis of relative gene-expression data using real-time quantitative PCR and the $2[-\Delta\Delta CT]$ method. *Methods*. 25, 402 - 408.
- Li X, Zheng M, Xu B, Li D, Shen Y, Nie Y, Ma L, Wu J (2021) Offspring-producing 3D ovarian organoids from female germline stem cells for toxicology testing. *Biomaterials*. 279, 121213.

- Li ZE, Li XD, Zhang QS, Wang YC, Zhang MX, Lu YJ, Duan CM, Yang XZ, Feng LX (2007) 17 beta-estradiol stimulates proliferation of spermatogonia in experimental cryptorchid mice. *Asian J. Pharmacol.* 9, 659-667.
- Li Z, Li M, Hong N, Yi M, Hong Y (2014) Formation and cultivation of medaka primordial germ cells. *Cell Tissue Res.* 357, 71-81.
- Luo H, Li X, Tian GG, Li D, Hou C, Ding X, Hou L, Lyu Q, Yang Y, Cooney AJ, Xie W, Xiong J, Wang H, Zhao X, Wu J (2021) Offspring production of ovarian organoids derived from spermatogonial stem cells via defined factors with chromatin reorganization. *J. Adv. Res.* 33, 81 - 98.
- Lubzens E, Young G, Bobe J, Cerdà J (2010) Oogenesis in teleosts: how fish eggs are formed. *Gen. Comp. Endocrinol.* 165, 367 - 389.
- Maru Y, Tanaka N, Itami M, Hippo Y (2019) Efficient use of patient-derived organoids as a preclinical model for gynecologic tumours. *Gynecol. Oncol.* 154, 189 - 198.
- Masaki K, Sakai M, Kuroki S, Jo JI, Hoshina K, Fujimori Y, Oka K, Amano T, Yamanaka T, Tachibana M, Tabata Y, Shiozawa T, Ishizuk O, Hochi S, Takashima S (2018) FGF2 has distinct molecular functions from GDNF in the mouse germline niche. *Stem Cell Rep.* 10, 1782 - 1792.
- Matsuoka S, Gupta S, Suzuki E, Hiromi Y, Asaoka M (2014) Gone early, a novel germline factor, ensures the proper size of the stem cell precursor pool in the *Drosophila* ovary. *PLoS ONE.* 9, e113423.
- Medrano JV, Rombaut C, Simon C, Pellicer A, Goossens E (2016) Human spermatogonial stem cells display limited proliferation *in vitro* under mouse spermatogonial stem cell culture conditions. *Fertil Steril.* 106,

1539-1549.

- Meng X, Lindahl M, Hyvönen ME, Parvinen M, de Rooij DG, Hess MW, Raatikainen-Ahokas A, Sainio K, Rauvala H, Lakso M, Pichel JG, Westphal H, Saarma M, Sariola H (2000) Regulation of undifferentiated spermatogonia fate by GDNF. *Science*. 287, 1489 - 1493.
- Miura C, Miura T (2011) Analysis of spermatogenesis using an eel model. *Aqua-BioSci. Monogr.* 4, 105 - 129.
- Miura T, Higuchi M, Ozaki Y, Ohta T, Miura C (2006) Progesterin is an essential factor for the initiation of the meiosis in spermatogenic cells of the eel. *Proc. Natl. Acad. Sci.* 103, 7333-7338.
- Miura T, Miura C, Ohta T, Nader MR, Todo T, Yamauchi K (1999) Estradiol-17 β stimulates the renewal of spermatogonial stem cells in males. *Biochem. Biophys. Res. Commun.* 144, 5504-5510.
- Mizapour T, Movahedin M, Tengku Ibrahim TA, Koruji M, Haron AW, Nowroozi MR, Rafieian SH (2012) Effects of basic fibroblast growth factor and LIF on proliferation of human spermatogonial stem cells. *Andrologia.* 44, 41 - 55.
- Mohapatra S, Liu Z, Zhou L, Zhang Y, Wang D (2011) Molecular cloning of *wtl1a* and *wtl1b* and their possible role in fish sex determination. *Indian J. Sci. Technol.* 4, 85 - 86.
- Morimoto H, Kanatsu-Shinohara M, Shinohara T (2023) WIN18,446 enhances spermatogonial stem-cell homing and fertility after transplantation by increasing blood-testis-barrier permeability. *J. Reprod. Dev.* 69, 347 - 355.
- Nakamura S, Watakabe I, Nishimura T, Toyoda A, Taniguchi Y, Tanaka M (2012) Analysis of medaka *sox9* orthologue reveals a conserved role in germ-cell maintenance. *PLoS ONE.* 7, e29982.

- Nanki Y, Chiyoda T, Hirasawa A, Ookubo A, Itoh M, Ueno M, Akahane T, Kameyama K, Yamagami W, Kataoka F, Aoki D (2020) Patient-derived ovarian cancer organoids capture the genomic profiles of primary tumours applicable for drug sensitivity and resistance testing. *Sci. Rep.* 10, 12581.
- Nie M, Zou C, Peng L, Wu Z, You F (2023) Establishment and application of four long-term culture cell lines of the olive flounder *Paralichthys olivaceus* blastocysts. *Com. Biochem. Physiol. C Toxicol, Pharmacol.* 265, 109536.
- Nóbrega RH, Morais RDVS, Crespo D, de Waal PP, de França LR, Schulz RW, Bogerd J (2015) FSH stimulates spermatogonial proliferation and differentiation in zebrafish via Igf3. *Endocrinology.* 156, 3804 - 3817.
- Ogiwara K, Fujimori C, Rajapakse S, Takahashi T (2013) Luteinizing hormone and receptor characterization and role in ovulation of medaka. *PLoS ONE.* 8, e54482.
- Okita K, Ichisaka T, Yamanaka S (2007) Generation of germline-competent induced pluripotent stem cells. *Nature.* 448, 313-317.
- Okutsu T, Yano A, Nagasawa K, Shikina S, Kobayashi T, Takeuchi Y, Yoshizaki G (2006) Manipulation of fish germ cells: visualization, cryopreservation and transplantation. *J. Reprod. Dev.* 52, 685 - 693.
- Panda RP, Barman HK, Mohapatra C (2011) Isolation of enriched carp spermatogonial stem cells from *Labeo rohita* testis for *in vitro* propagation. *Theriogenology.* 76, 241 - 251.
- Parameswaran V, Ishaq Ahmed V, Shukla R, Bhonde R, Sahul-Hameed A (2007) Development of two new fish cell lines for virus isolation. *Mar. Biotechnol.* 9, 281 - 291.

- Park JW, Lee DI, Jung HS, Kim J, Yang HR, Lee JH (2021) Estimation of genetic parameters and improvement of growth traits in selected olive flounder. Korean J. Fish. Aquat. Sci. 54, 974 - 981.
- Peng L, Zheng Y, You F, Wu Z, Zou Y, Zhang P (2016) Establishment of a testicular Sertoli-cell line from olive flounder. Chin. J. Oceanol. Limnol. 34, 1054 - 1063.
- Peng L, Zhou Y, Xu W, Jiang M, Li H, Long M, Liu W, Liu J, Zhao X, Xiao Y (2019) Generation of stable induced pluripotent stem-like cells from adult zebrafish fibroblast. Int. J. Biol. Sci. 15, 2340-2349.
- Ren Y, Tao Y, Sun Z, Wang Y, Li W, He Z, Wang G, Yang Y, Hou J (2024) Female-recipient infertility and donor-spermatogonial purification for germ-cell transplantation in olive flounder. Animals. 14, 2887.
- Reuter K, Ehmcke J, Stukenborg JB, Simoni M, Damm OS, Redmann K, Schlatt S, Wistuba J (2014) Reassembly of somatic cells and testicular organogenesis *in vitro*. Tissue Cell. 46, 86 - 96.
- Richer G, Baert Y, Goossens E (2019) *In vitro* spermatogenesis through testis modelling: toward testicular organoids. Andrology. 8, 879 - 891.
- Roselló RA, Chen CC, Dai R, Howard JT, Hochgeschwender U, Jarvis ED (2013) Mammalian genes induce partially reprogrammed pluripotent stem cells in non-mammalian vertebrate and invertebrate species. eLife. 2, e00036.
- Ryu JH, Gong SP (2017) Effects of developmental stage of donor embryos on culture of marine medaka embryonic stem-like cells. Korean J. Fish. Aquat. Sci. 50, 160 - 168.
- Ryu JH, Gong SP (2020) Effects of feeder cells on the primary culture of

- ovarian cell populations from adult Japanese medaka (*Oryzias latipes*).
J. Anim. Reprod. Biotechnol. 35, 65–72.
- Ryu JH, Gong SP (2020) Enhanced enrichment of medaka ovarian germline stem cells via density-gradient centrifugation and differential plating. Biomolecules. 10, 1477.
- Sadri-Ardekani H, Mizrak SC, van Daalen SK, Korver CM, Roepers-Gajadien HL, Koruji M, Hovingh S, de Reijke TM, de la Rosette JJ, van der Veen F, de Rooij DG, Repping S, van Pelt AM. (2009) Propagation of human spermatogonial stem cells *in vitro*. J. Am. Med. Assoc. 302, 2127 - 2134.
- Sakib S, Yu Y, Voigt A, Ungrin M, Dobrinski I (2019) Generation of porcine testicular organoids with testis specific architecture using microwell culture. J. Vis. Exp. e60387.
- Sato T, Tatagiri K, Gohbara A, Inoue K, Ogonuki N, Ogura A, Kubota Y, Ogawa T (2011) *In vitro* production of functional sperm in cultured neonatal mouse testes. Nature. 471, 504 - 507.
- Shang M, Su B, Perera DA, Alsaqufi A, Lipke EA, Cek S, Dunn DA, Qin Z, Peatman E, Dunham RA (2018) Germ-line cell identification, isolation and transplantation in two North-American catfish species. Fish Physiol. Biochem. 44, 717 - 733.
- Shivdasani AA, Ingham PW (2003) TGF- β signalling regulates stem-cell maintenance and transit-amplifying cell proliferation in *Drosophila* spermatogenesis. Curr. Biol. 13, 2065 - 2072.
- Son MJ, Gong SP (2022) Feeder-cell-dependent primary culture of single blastula-derived embryonic cell lines from marine medaka. In Vitro Cell. Dev. Biol. Anim. 9, 840 - 850.

- Spradling A, Fuller MT, Braun RE, Yoshida S (2011) Germline stem cells. Cold Spring Harb. Perspect. Biol. 3, a002642.
- Stukenborg JB, Wistuba J, Luetjens CM, Elhija MA, Huleihel M, Lunenfeld E, Gromoll J, Nieschlag E, Schlatt S (2008) Co-culture of spermatogonia with somatic cells in a 3D soft-agar system. J. Androl. 29, 312 - 329.
- Strange DP, Zarandi ZP, Trivedi G, Atala A, Bishop CE, Sadri-Ardekani H, Verma S (2018) Human testicular organoid system as a tool to study Zika-virus pathogenesis. Emerg. Microbes Infect. 7, 82.
- Suarez-Martinez E, Suazo-Sanchez I, Celis-Romero M, Carnero A (2022) 3D and organoid culture in research: Physiology, hereditary genetic diseases and cancer. Cell Biosci. 12, 39.
- Sun A, Wang T, Wang N, Liu X, Sha Z, Chen S (2015) Establishment of an ovarian cell line from half-smooth tongue sole. J. Fish Biol. 86, 46 - 59.
- Sun X, Tao B, Wang Y, Hu W, Sun Y (2022) Isolation and characterization of germline stem cells in the hermaphroditic fish *Monopterus albus*. Int. J. Mol. Sci. 23, 5861.
- Swaminathan TR, Lakra WS, Gopalakrishnan A, Basheer V, Khushwaha B, Sajeela K (2010) Development of a new epithelial cell line from green chromide fin. In Vitro Cell. Dev. Biol. Anim. 46, 647 - 656.
- Tan L, Liu Q, He Y, Zhang J, Hou J, Ren Y, Ma W, Wang Q, Shao C (2023) Establishment of a spermatogonial stem-cell line from tiger puffer fish. Animals. 13, 2959.
- Tokalov SV, Gutzeit HO (2005) Spermatogenesis in testis primary cell cultures of the tilapia (*Oreochromis niloticus*). Dev. Dyn. 223, 1238-1247.
- Topraggaleh TR, Valojerdi MR, Montazeri L, Baharvand H (2019) A testis-derived macroporous 3D scaffold for generation of mouse

- testicular organoids. *Biomater. Sci.* 7, 1422 - 1436.
- Wahab-Wahlgren A, Martinelle N, Holst M, Jahnukainen K, Parvinen M, Soder O (2003) EGF stimulates rat spermatogonial DNA synthesis in seminiferous tube segments *in vitro*. *Mol. Cell Endocrinol.* 201, 39-46.
- Walsh CJ, Rhody N, Main KL, Restivo J, Tarnecki AM (2024) Advances in development of long-term embryonic stem cell-like cultures from a marine fish, *Sciaenops ocellatus*. *Curr. Res. Food Sci.* 9, 100841.
- Wang D, Hildorf S, Ntemou E, Mamsen LS, Dong L, Pors SE, Fedder J, Clasen-Linde E, Cortes D, Thorup J, Andersen CY (2022) Organotypic culture of testicular tissue from infant boys with cryptorchidism. *Int. J. Mol. Sci.* 23, 7975.
- Wang X, Liu Q, Xiao Y, Yang Y, Wang Y, Song Z, You F, An H, Li J (2017) High temperature causes masculinization of genetically female olive flounder with PGC proliferation arrest. *Aquaculture.* 479, 808 - 816.
- Wong TT, Tesfamichael A, Collodi P (2013) Production of zebrafish offspring from cultured female germline stem cells. *PLoS ONE.* 8, e62660.
- Wu J, Kang K, Liu S, Ma Y, Yu M, Zhao X (2023) Recent progress of *in vitro* 3D culture of male germ stem cells. *J. Funct. Biomater.* 14, 543.
- Wu Z, Falciatori I, Molyneux LA, Richardson TE, Chapman KM, Hamra FK (2009) Spermatogonial culture medium: an efficient nutrient mixture for rat spermatogonial stem cells. *Biol. Reprod.* 81, 77 - 86.
- Xie X, Nóbrega R, Pšenička M (2020) Spermatogonial stem cells in fish: characterization, isolation and *in vitro* culture systems. *Biomolecules.* 10, 644.
- Xu Y, Shrestha N, Pr at V, Beloqui A (2021) *In vitro*, *ex vivo* and *in vivo*

- models for studying drug transport across intestinal barriers. *Adv. Drug Deliv. Rev.* 175, 113795.
- Xu Y, Zhong Z, Zhang Z, Feng Y, Zhao L, Jiang Y, Wang Y (2021) Establishment of gonadal cell lines from large yellow croaker for gene-expression studies. *Aquaculture.* 546, 737300.
- Yang H, Tiersch TR (2009) Sperm-motility initiation and duration in medaka. *Theriogenology.* 72, 386 - 392.
- Yi M, Hong N, Hong Y (2010) Derivation and characterization of haploid embryonic stem-cell cultures in medaka fish. *Nat. Protoc.* 5, 1418 - 1430.
- Yom-Din S, Hollander-Cohen L, Aizen J, Boehm B, Shpilman M, Golan M, Hurvitz A, Degani G, Levavi-Sivan B (2016) Gonadotropins in Russian sturgeon: their role in steroid secretion. *PLoS ONE.* 11, e0162344.
- Yoshizaki G, Yazawa R (2019) Application of surrogate broodstock technology in aquaculture. *Fish Sci.* 85, 429 - 437.
- Zeng W, Dong H, Chen X, Bergmann SM, Yang Y, Wei X, Tong G, Li H, Yu H, Chen Y (2022) Establishment of a permanent heart cell line from largemouth bass for virology and immunology. *Aquaculture.* 547, 737427.
- Zhang H, Zhang WW, Mo CY, Dong MD, Jia KT, Liu W, Yi MS (2022) Production of functional sperm from *in vitro*-cultured pre-meiotic spermatogonia in a marine fish. *Zool. Res.* 43, 537 - 551.
- Zheng Y, Peng L, You F, Zou Y, Zhang P, Chen S (2015) Establishment of a fish-cell line from the brain of Japanese flounder. *J. Fish Biol.* 87, 115 - 122.
- Zhong C, Tao Y, Liu M, Wu X, Yang Y, Wang T, Meng Z, Xu H, Liu X

(2022) Establishment of a spermatogonial stem-cell line with potential of meiosis in a hermaphroditic fish, *Epinephelus coioides*. Cells. 11, 2868.



감사의 글

감사의 글 페이지는 가장 채우기 쉬울 것 같아 늘 미뤘지만, 역시 막상 쓰려니, 가장 어려운 페이지가 되어있습니다. 아마 많은 분들께 진심을 전달하고 싶은 욕심이 벽차올라서 그럴지도 모르겠습니다.

가장 먼저, 학문의 여정을 이끌어주시고 연구자로서의 시야를 넓혀주신 공승표 교수님께 깊은 감사를 드립니다. 교수님의 따뜻한 격려와 세심한 지도는 제가 다시 일어설 수 있는 버팀목이 되어 주었습니다. 부족한 저를 끝까지 믿고 기다려주신 점, 평생 잊지 않겠습니다.

‘출탁동시’ 프로그램을 시작했을 때부터, 바깥에서 열심히 껌질을 깨주신 남윤권 교수님, 항상 웃음으로 맞이해주시고 재밌는 연구 주제를 던져주신 김찬희 교수님! 바쁘신 시간을 내어 심사해주셔서 감사합니다. 늘 웃음과 열정 넘치시는 최윤희 교수님! 첫 번식생리 수업하셨을 때가 기억이 납니다. 덕분에 생식선줄기세포 연구에 도움이 되었습니다. 감사합니다. 그리고 제 고민, 걱정을 편견없이 묵묵히 들어주시고 해학적으로 풀어주신 김종명 교수님! 정말 감사드립니다.

학부부터 박사과정까지 긴 생활동안, 잘 안되는 실험은 밤새 토론하고, 같이 웃기도, 울기도 한 김여름, “친구로서” 사랑한다고 고생했다고 말을 전하고 싶습니다. 우리 세포공학 실험실 실장 한단희, 같이 실험실 생활을 해서 행운이라고 생각합니다. 곧 박사과정에 들어갈 정은수, 처음 들어왔을 때보다 많이 성장한 모습이 보여서 앞으로 잘 해낼거라고 생각합니다. 실험실 막내 강채완, 정신없을 때 만나서 많이 챙겨주지 못한 것 같아 미안합니다. 그치만 잘 할거라 믿습니다. 곧 좋은 소식을 전해줄 이지훈 박사님, 강지혜 후배님! 진심으로 축하드리고 힘든 일이 있을 때, 같이 걱정해줘서 감사합니다. 학위과정에서 제 도토리 창고 같았던 김종명 교수님방 동료분들, 변준환 박사님, 유채은, 전유정! 여러분들과 같이 함께할 수 있어서 진심으로 감사드립니다.

12학번 황금기수에서 왕언니 김은정 정말정말 고생많았다고 전해주고 싶습니다. 그리고 곧 좋은 소식을 맞이할 김하함, 정말 부럽습니다. 늘 좋은 일이 있기를 기원합니다. 같은 일을 하고 있는 서준혁 형, 다음으로 미뤄졌지만 더 멋진 연구로 마무리하실거라 믿습니다. 서로 힘들 때, 술잔을 기울인 김경영, 류재영, 이도훈! 덕분에 힘든 것을 잊고 학위 과정을 마무리 할 수 있었습니다. 감사합니다.

국립수산과학원에 들어오면서 많은 좋은 분들을 만나서 행운이었습니다. 먼저, 이정용 부장님, 진심어린 충고 덕분에 제가 박사학위를 마칠 수 있었습니다. 감사합니다. 강정하 과장님과 임재현 연구관님, 바쁘신 시간을 내어 심사를 해주셔서 감사합니다. 따듯하고 따끔한 조언으로 정신 번쩍 차리고 마무리할 수 있었습니다. 감사합니다. 제가 관사에서 잘 못먹을까봐 걱정해주시고 눈 마주치면 말없이 끄덕여주신 황인준 연구관님, AI 전문가 김형수 연구사님, 가끔 음료수를 건내주시며 장난기 어린 눈으로 봐주신 노은수 박사님, 힘든일 있으면 언제든지 물어보라고 말씀해주신 정효선 박사님, 유전자가위 유전적 다양성을 분석해주신 이다인 박사님, 업무화면이 영화에서 보던 해킹파일 같은 프로그램을 돌리시던 박정욱 박사님, 재치가 넘치시고 속이 정말 깊으신 김영삼 박사님, 그리고 힘들 때 귀신같이 알아차리시고 밥먹자고 해주시는 누나같은 이민정 박사님, 여러분 모두 진심으로 감사드립니다. 그리고 지금은 다른 기관에 계신 김영옥 소장님, 공희정 센터장님, 김주원 박사님께도 감사드립니다. 그리고, 저를 믿고 실험재료를 제공해주신 원경미 연구관님, 도용현 박사님, 신민규 박사님 감사합니다. 멋진 결과를 가져오도록 노력하겠습니다. 그리고 늘 고민을 들어주시고 웃음으로 맞이해주신 김형수 박사님, 김혜성 박사님 그리고 김효원 박사님께도 감사드립니다. 마지막으로 저를 믿고 응원해주신 LMO팀, 조자영 선생님, 이주연 선생님, 전아영 선생님, 박경미 선생님, 김현태 선생님, 딱딱한 회사생활에서 숨통이 트일 수 있었습니다. 감사합니다.

멀리서 응원해주신 류준형 박사님, 얼른 만나서 멋진 연구 같이하기를 소망해봅니다. 친형이 있다면 이런 느낌일까 생각이 들게한 정연우 박사님, 힘들 때나 기쁠 때 진심으로 대해주셔서 정말 감사합니다.

이경택, 박용준, 황제일! 내 강릉 친구들, 아마 내 박사학위 논문을 전달한다면
라면 받침으로 사용하겠지...? 그래도 너희가 있어서 큰 힘이 된다. 표현은 못 했지만.

멋지게 일을 마무리하신 아버지, 늘 열정과 근면 성실의 어머니, 작은 것에도 행복을
아는 효주, 뭐든지 물어보면 꿰뚫고 있는 만물박사 지우, 참 길었던 학위 생활에서 늘
멋지다고 제가 작아지지 않게 손을 내어주어서 진심으로 감사하고 사랑합니다.

많은 시간이 흐르고 계절이 바뀌는 동안, 이 연구는 조용히, 그리고 묵묵히 제
삶의 중심이 되어있었습니다. 어느덧 원고를 정리하며 지난 시간을 되돌아보니,
수많은 고민과 시행착오의 순간들이 떠오릅니다. 때로는 확신 없이 나아가야 했고,
때로는 길을 잃기도, 그리고 때로는 고독하게 멈춰서 절망만 하기도 했습니다.
그러니, 혹시 저와 비슷한 상황에서, 실낱같은 해답을 찾고자 이 원고를 펼친 선배님들,
후배님들, 동료분들 혹은 미래의 나에게 말해주고 싶습니다. “우리는 잘하고 있어요.
깨진 틈이 있는 창문에서 밝은 빛이 더 잘들고, 진정 사랑해 본 사람이 가장 깊은 이별의
아픔을 알고 있듯이, 수 많은 실험과 데이터 앞에 서 있는 우리는, 성공을 위해서 그저 많은
실패를 맞이할 뿐이에요. 그러니, 우리 웃으면서 실패를 맞이해요. 그리고 같이 생각해봐요,
기다릴게요.”